

WRDC-TR-89-3093

PROBABILISTIC DAMAGE TOLERANCE METHOD
FOR METALLIC AEROSPACE STRUCTURE

Margery E. Artley
Structural Integrity Branch
Structural Division

September 1989

Final Report for Period July 1984 - February 1989

Approved for Public Release; Distribution Unlimited



AD-A215 402

DTIC
ELECTE
NOV 29 1989
S E D

FLIGHT DYNAMICS LABORATORY
WRIGHT RESEARCH AND DEVELOPMENT CENTER
AIR FORCE SYSTEMS COMMAND
WRIGHT-PATTERSON AIR FORCE BASE, OHIO 45433-6553

NOTICE

When Government drawings, specifications, or other data are used for any purpose other than in connection with a definitely Government-related procurement, the United States Government incurs no responsibility or any obligation whatsoever. The fact that the government may have formulated or in any way supplied the said drawings, specifications, or other data, is not to be regarded by implication, or otherwise in any manner construed, as licensing the holder, or any other person or corporation; or as conveying any rights or permission to manufacture, use, or sell any patented invention that may in any way be related thereto.

This report is releasable to the National Technical Information Service (NTIS). At NTIS, it will be available to the general public, including foreign nations.

This technical report has been reviewed and is approved for publication.

Joseph G. Burns
for MARGERY E. ARTLEY
Project Engineer

George P. Sendeckyj
GEORGE P. SENDECKYJ, Actg Tech Mgr
Fatigue, Fracture & Reliability Gp
Structural Integrity Branch

FOR THE COMMANDER

James L. Rudd
JAMES L. RUDD, Chief
Structural Integrity Branch
Structures Division

If your address has changed, if you wish to be removed from our mailing list, or if the addressee is no longer employed by your organization please notify WRDC/FIBEC, WPAFB, OH 45433-6553 to help us maintain a current mailing list.

Copies of this report should not be returned unless return is required by security considerations, contractual obligations, or notice on a specific document.

Unclassified

SECURITY CLASSIFICATION OF THIS PAGE

REPORT DOCUMENTATION PAGE

Form Approved
GMB No 0704-0188

1a. REPORT SECURITY CLASSIFICATION
Unclassified

1b. RESTRICTIVE MARKINGS

2a. SECURITY CLASSIFICATION AUTHORITY

2b. DECLASSIFICATION/DOWNGRADING SCHEDULE

3. DISTRIBUTION/AVAILABILITY OF REPORT
Approved for Public Release, Unlimited Distribution

4. PERFORMING ORGANIZATION REPORT NUMBER(S)
WRDC-TR-89-3093

5. MONITORING ORGANIZATION REPORT NUMBER(S)

6a. NAME OF PERFORMING ORGANIZATION
Fatigue, Fracture & Reliability
Gp; Flight Dynamics Laboratory

6b. OFFICE SYMBOL (if applicable)
WRDC/FIBEC

7a. NAME OF MONITORING ORGANIZATION

6c. ADDRESS (City, State, and ZIP Code)
WRDC/FIBEC
Wright-Patterson AFB OH 45433-6553

7b. ADDRESS (City, State, and ZIP Code)

8a. NAME OF FUNDING/SPONSORING ORGANIZATION

8b. OFFICE SYMBOL (if applicable)

9. PROCUREMENT INSTRUMENT IDENTIFICATION NUMBER

8c. ADDRESS (City, State, and ZIP Code)

10. SOURCE OF FUNDING NUMBERS

PROGRAM ELEMENT NO	PROJECT NO.	TASK NO	WORK UNIT ACCESSION NO
61102F	2307	N1	24

11. TITLE (Include Security Classification)
Probabilistic Damage Tolerance Methods for Metallic Aerospace Structures

12. PERSONAL AUTHOR(S)
Margery E. Artley

13a. TYPE OF REPORT
Final

13b. TIME COVERED
FROM Jul 84 TO Feb 89

14. DATE OF REPORT (Year, Month, Day)
1989 September

15. PAGE COUNT
134

16. SUPPLEMENTARY NOTATION

17. COSATI CODES

FIELD	GROUP	SUB-GROUP
13	13	
12	03	

18. SUBJECT TERMS (Continue on reverse if necessary and identify by block number)
Probabilistic Methods, Damage Tolerance, Metallic Structures

19. ABSTRACT (Continue on reverse if necessary and identify by block number)

ABSTRACT

Damage tolerance analysis, based on fracture mechanics, is an important tool for ensuring the safety of flight of airframes. Traditionally, these analyses are deterministic in nature, but probabilistic methods have been applied to damage tolerance analysis in limited cases. The purpose of this dissertation is to formulate probabilistic damage tolerance analyses for metallic structural components, based on U.S. Air Force damage tolerance philosophy for slow crack growth and fail safe components. A survey of the literature was conducted on probabilistic durability and damage tolerance methods. The important elements of the methods are covered; including the initial fatigue quality, the variability in crack growth rate, and the probability of crack detection.

(Continued)

20. DISTRIBUTION/AVAILABILITY OF ABSTRACT
 UNCLASSIFIED/UNLIMITED SAME AS RPT DTIC USERS

21. ABSTRACT SECURITY CLASSIFICATION
Unclassified

22a. NAME OF RESPONSIBLE INDIVIDUAL
Joseph G Burns

22b. TELEPHONE (Include Area Code)
(513) 255-6104

22c. OFFICE SYMBOL

19. Continued

A probabilistic damage tolerance analysis was performed with a deterministic crack growth rate and then a stochastic crack growth rate, based on a probabilistic durability method. Examples of slow crack growth and fail safe structures are presented. As an example of a slow crack growth component, a lug from an aircraft subjected to an 80-flight fighter/trainer wing lower surface spectrum was selected. A stiffened panel from a lower wing skin of a tanker was selected as an example of a fail-safe component. Crack arrest in the panel, followed by catastrophic failure of the stiffener was considered as the failure mechanism.

The model formulated here can be used to decide on the frequency and quality of the inspection of a component needed to keep the probability of failure at acceptable levels. Results of this study can serve as bases for decision making for inspection maintenance and fleet management.

Accession For	
NTIS GRA&I	<input checked="" type="checkbox"/>
DTIC TAB	<input type="checkbox"/>
Unannounced	<input type="checkbox"/>
Justification	
By _____	
Distribution/	
Availability Codes	
Dist	Avail and/or Special
A-1	

PROBABILISTIC DAMAGE TOLERANCE METHODS FOR
METALLIC AEROSPACE STRUCTURES

By

Margery E. Artley

B.S.C.E. 1975, Purdue University,
West Lafayette, IN 47907
M.S.C.E. 1976, Purdue University
West Lafayette, IN 47907

A Dissertation submitted to

The Faculty of

The School of Engineering and Applied Science of
The George Washington University in partial
satisfaction of the requirements for
the degree of Doctor of Science

February 20, 1989

Dissertation directed by

Jann-Nan Yang, Sc.D.

Professor of Engineering and Applied Science

Dedicated to
My Parents, Tom and Eleanor

ACKNOWLEDGEMENT

The author wishes to express her great appreciation to Professor J.N. Yang, dissertation research director, for his valuable guidance, insightful suggestions, and needed encouragement.

The author is sincerely grateful to Dr. Frank D. Adams of the Air Force Wright Aeronautical Laboratories for his constant encouragement and gentle prodding. Thanks also to Dr. George P. Sendeckyj, AFWAL/FIBEC, for his helpful suggestions and invaluable discussion.

The author is also grateful to the faculty of the School of Engineering and Applied Science of the George Washington University for providing the fundamental engineering and mathematical tools necessary to perform this study.

And finally, the author is indebted to the U.S. Air Force Wright Aeronautical Laboratories, Flight Dynamics Laboratory, Wright-Patterson AFB, OH, for funding this program of study under the Long-Term, Full-Time Training program and the structural integrity in-house work unit No. 2307N124.

TABLE OF CONTENTS

	Page
ABSTRACT	ii
ACKNOWLEDGEMENTS	v
LIST OF TABLES	ix
LIST OF FIGURES	x
Chapter	
I INTRODUCTION	
1.1 Objectives and Scope	1-1
1.2 Overview of Damage Tolerance Philosophy	1-1
II BACKGROUND	
2.1 Initial Fatigue Quality	2-1
2.1.1 The Equivalent Initial Flaw Size Distribution	2-1
2.1.2 Time-to-Crack-Initiation Distribution	2-3
2.2 Stochastic Crack Growth Model	2-5
2.3 Probability of Detection	2-11
2.4 Probabilistic Life Prediction	2-13
III ANALYTICAL FORMULATION OF PROBABILISTIC APPROACH TO LIFE PREDICTION	
3.1 Deterministic Crack Growth Approach	3-1
3.1.1 Analytical Crack Growth Approach	3-1
3.1.1.1 No Inspection	3-3
3.1.1.2 One or Multiple Inspections.	3-4
3.1.2 Master Curve Approach	3-9
3.1.2.1 No Inspection	3-12

3.1.2.2	One or Multiple Inspections.	3-12
3.2	Stochastic Crack Growth Approach	3-18
3.2.1	Analytical Crack Growth Approach	3-19
3.2.1.1	No Inspection	3-20
3.2.1.2	One or Multiple Inspections.	3-22
IV	EXAMPLES OF STOCHASTIC LIFE PREDICTION	
4.0	Introduction	4-1
4.1	Lug Example	4-1
4.1.1	Deterministic Crack Growth Approach	4-9
4.1.2	Stochastic Crack Growth Approach	4-10
4.2	Stiffened Panel Example	4-20
4.2.1	Slow Crack Growth Approach	4-36
4.2.1.1	Deterministic Crack Growth Approach	4-36
4.2.1.2	Stochastic Crack Growth Approach	4-42
4.2.2	Crack Arrest Approach	4-47
4.2.2.1	Deterministic Crack Growth Approach	4-48
4.2.2.1.1	General Master Curve Approach	4-48
4.2.2.1.2	Special Case, $\beta(a)=1$	4-48
4.2.2.2	Stochastic Crack Growth Approach	4-53
4.2.2.2.1	General Master Curve Approach	4-53
4.2.2.2.2	Special Case, $\beta(a)=1$	4-55

	4.3	Conclusions	4-59
V		CONCLUSIONS AND RECOMMENDATIONS	
	5.1	Summary	5-1
	5.2	Conclusions	5-4
	5.3	Recommendations for Future Research	5-5
VI		REFERENCES	6-1
AI		Appendix	A-1

LIST OF TABLES

Table	Page
4.1 Parameters for the Aluminum Lug Example with a Straight Shank without Bushings or Bearings . . .	4-3
4.2 The Average Percentage of Repair for the Lug Example using Deterministic Crack Growth Analysis for NDI Systems #1 and #2	4-13
4.3 The Average Percentage of Repair for the Lug Example using Stochastic Crack Growth Analysis for NDI Systems #1 and #2	4-21
4.4 Fail-Safe Structure Requirements for Air Force Damage Tolerance [from Ref. 1]	4-25
4.5 Values of Crack Length, Beta, and Residual Strength for an 8 inch Stiffener Spacing	4-29
4.6 Parameters for the Stiffened Panel Example . . .	4-39
4.7 Average Percentage of Repair for the Stiffened Panel Example using Deterministic Crack Growth, Visual and NDI System #1 Inspections, Critical Crack Size = 6.061 inches	4-43
4.8 Average Percentage of Repair for the Stiffened Panel Example using Stochastic Crack Growth, Visual and NDI System #1 Inspections, Critical Crack Size = 6.061 inches	4-46
4.9 Average Percentage of Repair for the Stiffened Panel Example using Deterministic Crack Growth, Visual Inspections, Critical Crack Size = 8.142 inches	4-54
4.10 Average Percentage of Repair for the Stiffened Panel Example using Stochastic Crack Growth, Visual and NDI System #1 Inspections, Critical Crack Size = 8.142 inches	4-58

LIST OF FIGURES

Figure		Page
2.1	Compatibility between TDCI and EIFS	2-4
2.2	Crack Length Versus Cycles for Constant Amplitude Data (from Ref. 20)	2-8
2.3	Predicted Crack Length Versus Cycles for Constant Amplitude Data (from Ref. 20)	2-9
3.1	The "Log-Odds" Function for Probability of Detection	3-5
3.2	Calculation of $y_G(t)$	3-13
3.3	Utilization of the Master Curve	3-15
3.4	Calculation of $y(x,kt)$	3 17
4.1	Geometry of the Lug	4-4
4.2	Sample Crack Growth Rate versus Crack Length of a Lug (Sample S3-A-3 from Ref. 73)	4-5
4.3	Critical Crack Sizes for 35 Service Failed Lugs (after Ref. 72).	4-7
4.4	Probability of Detection Curves for Two NDI Inspection Systems	4-8
4.5	The Cumulative Probability of Failure for the Lug Example, with Deterministic Crack Growth Method, NDI System #1, 8000 Flights and 0-3 Inspections	4-11
4.6	The Cumulative Probability of Failure for the Lug Example, with Deterministic Crack Growth Method, NDI System #2, 8000 Flights and 0-3 Inspections	4-12
4.7	The Cumulative Probability of Failure for the Lug Example, with Stochastic Crack Growth Method, NDI System #1, 4000 Flights and 0-4 Inspections	4-15
4.8	The Cumulative Probability of Failure for the Lug Example, with Stochastic Crack Growth Method, NDI System #2, 4000 Flights and 0-4 Inspections	4-16

4.9	The Cumulative Probability of Failure for the Lug Example, with Stochastic Crack Growth Method, NDI System #1, 2000 Flights and 0-4 Inspections	4-18
4.10	The Cumulative Probability of Failure for the Lug Example, with Stochastic Crack Growth Method, NDI System #2, 2000 Flights, and 0-4 Inspections	4-19
4.11a	Residual-Strength Requirements for Air Force Damage Tolerance (After Ref. 1)	4-23
4.11b	Damage-Growth Requirements for Air Force Damage Tolerance (After Ref. 1)	4-24
4.12	Geometry of the Stiffened Panel	4-27
4.13	Residual Strength of a Plate as a Function of Crack Length for a Center Cracked Panel with Broken Center Stiffener	4-30
4.14	Residual strength of a stiffener and a plate as a function of crack length for a center cracked panel; stiffener spacing = 8 inches, $K_c=120$ ksi $\sqrt{\text{in.}}$, $F_{tu}=82$ ksi	4-31
4.15	The Stress Exceedance Curve for a Lower Aft Panel and Stiffener	4-35
4.16	The Probability of Detection Curve for a Visual Inspection	4-37
4.17	Residual Strength as a Function of Crack Length for an Unstiffened Panel, $K_c=120$ ksi $\sqrt{\text{in.}}$	4-38
4.18	The Cumulative Probability of Failure for an Unstiffened Panel, with $a_{xx}=6.061$ inches, the Deterministic Crack Growth Method and 0, 4 and 5 Visual Inspections	4-41
4.19	The Cumulative Probability of Failure for an Unstiffened Panel, with $a_{xx}=6.061$ inches, the Stochastic Crack Growth Method and 0 and 5 Visual Inspections	4-44
4.20	The Cumulative Probability of Failure for an Unstiffened Panel, with $a_{xx}=6.061$ inches, the Stochastic Crack Growth Method, 0-5 Inspections with NDI System #1	4-45
4.21	Two Master Curves, One with Crack Arrest, the Other Without	4-49

4.22	The Crack Growth Model Showing the Crack Growth of the Median Initial Flaw Size, the Tenth Percentile, and the 90th Percentile Initial Flaws	4-51
4.23	The Cumulative Probability of Failure for a Stiffened Panel, with a _{xx} =8.142 inches, the Deterministic Crack Growth Method, and 0-3 Visual Inspections	4-52
4.24	The Cumulative Probability of Failure for a Stiffened Panel, with a _{xx} =8.142 inches, the Stochastic Crack Growth Method, and 0 and 5 Visual Inspections	4-56
4.25	The Cumulative Probability of Failure for a Stiffened Panel, with a _{xx} =8.142 inches, the Stochastic Crack Growth Method, and 0-5 Inspections using NDI System #1	4-57
4.26	The Cumulative Probability of Failure for a Stiffened Panel, with a _{xx} =8.142 inches, the Stochastic Crack Growth Method, 0 and 5 Visual and NDI System #1 Inspections.	4-60

CHAPTER I

INTRODUCTION

1.1 Objectives and Scope

The purpose of this dissertation is to formulate a probabilistic damage tolerance analysis for metal structural components, which takes into account the statistical nature of the initial fatigue quality of the component, the variability in crack growth rates, the residual strength of the fail-safe structure, and the reliability and frequency of the inspection. The goal of this research is to develop a probabilistic methodology which can be used to set rational inspection and maintenance schedules for airframes.

This model will be useful to engineers in designing airframes which will meet Air Force damage tolerance design requirements to ensure safety and reliability during the design service lifetime. The model can also be used by maintenance managers in selecting levels of inspection and inspection frequency in life extension programs. Examples of slow crack growth and fail-safe components are presented.

1.2 Background: Overview of the Damage Tolerance Philosophy

Ensuring that metal airframes are damage tolerant is a primary concern of airframe designers and owners. In particular, military leaders have a need to ensure that current and future weapon systems are damage tolerant. Damage tolerance is an issue of safety of flight. There are

approximately 20 to 200 damage tolerant critical components per airframe. One of the most important problems in the design and analysis of aircraft structures is the prediction of fatigue crack growth in fracture critical components. The Air Force damage tolerance design philosophy dictates that assumed damage in the structure must not reach critical crack size during two design lives.

Military specifications exist which address damage tolerance for U.S. Air Force metallic airframes [1,2]. The governing military standard dealing with structural integrity is MIL-STD 1520A [3]. Extensive guidelines with examples on how to perform a damage tolerant analysis deterministically are given in [4].

The damage tolerance requirements address two distinct types of design philosophies for structures, slow crack growth and fail-safe. These requirements include both analytical and experimental parts, and they are functions of design concept and the degree of inspectability. Initial flaw sizes are specified for primary damage for non-inspectable and depot or base level inspectable structure for both slow crack growth and fail safe structures. Subsequent crack growth and residual strength requirements are specified which must be met in the presence of this assumed initial damage. The requirements depend on the degree of inspectability designed into the component. The USAF design philosophy dictates that the assumed damage in the structure must not reach critical crack size during

one-half of the structure's design life for slow crack growth structure that can be inspected at depot or base level. If the component is non-inspectable, then the damage must not reach critical crack size during two design lifetimes.

A parallel set of requirements exist for fail-safe structures, with an addition of the residual strength requirement. The damaged structure must be able to sustain the expected maximum load which will occur in five lifetimes, but the residual strength does not need to be greater than 1.2 times the expected maximum load which will occur in one lifetime. For the non-inspectable structure, the residual strength must be greater than the expected maximum load which will occur in twenty lifetimes. The residual strength must be at least equal to the design limit load, but need not be greater than 1.2 times the expected maximum load which will occur in one lifetime. The residual strength for the intact structure must be at least as great as the design limit load but need not be greater than 1.2 times the maximum load expected to occur in one lifetime. Beyond that requirement, the intact structure must resist a load equal to the design limit load or 1.15 times the residual strength, at the instant of load-path failure or crack arrest. The 1.15 is a factor which accounts for dynamic effects.

A fail safe design can be classified as either

containing multiple load-path or crack-arrest features. A structure designed with multiple load-paths is a redundant structure. When one of the elements fails, the remaining elements are designed to carry the load for a specific period of time which may be the time required to get it repaired.

A structure containing crack arrest features is designed so that a rapidly growing crack is stopped at a stiffener or other crack arrest feature before complete failure. The remaining uncracked structure, with assumed continuing damage, should be able to carry the load until the cracked section is repaired.

There are similar requirements for fail safe and multiple load path dependent structures. The initial damage consists of primary and continuing assumptions. This initial damage must not result in failure of the intact structure within one fourth of the design service life. The intact structure must be able to sustain the maximum load expected in five lifetimes. This load must be equal to or greater than the design limit load, but not greater than 1.2 times the maximum load expected in one lifetime. At the instant of load-path failure, the structure must be able to sustain a maximum load of 1.25 times the maximum load expected to occur in five lifetimes. The residual strength need not exceed 1.38 times the maximum load expected to occur in one lifetime. The initial damage assumed in the remaining structure is the failed load path plus the

continuing damage assumed in the adjacent load path structure in addition to the amount of the crack growth that occurs before load-path failure. This initial damage must not result in failure of the remaining structure within one half of the design service life. The intact structure must be able to sustain the maximum load expected to occur five lifetimes. This maximum load must be equal or greater than the design limit load but need not exceed 1.2 times the maximum load expected in one lifetime.

To date, no airframe in the USAF inventory has been designed or qualified as a fail safe (multiple load path or crack arrest) structure. Selected components of three aircraft, however, are being managed as fail safe structures as a result of durability and damage tolerant assessments.

As the above discussion implies, the current damage tolerant requirements are presented in a deterministic format; however, fatigue crack growth is a highly variable phenomena which depends on the initial quality of the component, the statistical characteristics of the fatigue crack growth rate, and the random nature of the stress history. An equally important factor is the reliability of the inspection, which has to be regarded as another random variable. Assessment of the quality of the structure at any point in time is the basis of a fracture mechanics-based design and life management program. A probabilistic analysis can greatly improve the ability of the designer to

ensure safety of flight of a damage tolerant critical component.

In Chapter II, a review of the literature is presented which describes a general deterministic damage tolerance analysis for structures designed for slow crack growth or for fail safety. Next, the probabilistic methods which have been developed for durability analysis are presented, and finally, the probabilistic method which have been performed for damage tolerance life prediction are presented.

In Chapter III, two methods for calculating the probability of failure and probability of repair are presented for slow crack growth and fail safe components. One takes into account crack arrest, and the other does not.

In Chapter IV, an example of a structure designed to withstand slow crack growth is presented in the form of a lug attachment fitting. An example of a component designed to be fail safe by arresting the crack is presented in the form of a lower wing panel of a tanker aircraft. It is shown that the probability of failure decreases as the inspection and repair frequency increases. The improvement depends on the quality of the inspection. Two different levels of inspection are shown for the lug example. A visual inspection and one level of nondestructive inspection are shown for the lower wing panel example.

In Chapter V, the summary and conclusions are stated and topics for future research are presented.

CHAPTER II

BACKGROUND

The key to assessing the reliability of a structure is to realistically describe (1) the initial fatigue quality of the component, (2) the variability in the crack growth rate, and (3) the reliability of the inspection. In this chapter, some of the literature which addresses these three areas is presented. The assumptions used in this methodology are cited. This chapter concludes with a section on probabilistic life analysis methodologies.

2.1 Initial Fatigue Quality

The initial fatigue quality can be described statistically by (1) the equivalent initial flaw size (EIFS) distribution or (2) the distribution of time-to-crack-initiation. Both concepts are useful design tools for making life predictions.

2.1.1 The Equivalent Initial Flaw Size Distribution

The direct determination of the initial flaw size of the inherent flaws is not possible because the initial flaws of a high quality structure are not detectable. Furthermore, not all flaws are propagated from an initial defect. For these reasons, the equivalent initial flaw size concept was introduced by Gray and Rudd [5,6] and developed

by Yang and Manning [e.g. 7-11] as an analysis technique to be used to represent the initial fatigue quality of structural details in the durability analysis.

The EIFS is defined by Manning and Yang [e.g. 10] as an artificial crack size which results in an actual crack size at an actual point in time when the initial flaw is grown forward. It is determined by back-extrapolating fractographic results.

The general procedure for defining the initial fatigue quality is summarized in the Air Force Durability Handbook [12]. The Weibull compatible distribution function proposed by Yang and Manning [8,9] is reasonable for representing the EIFS cumulative distribution.

$$F_{a(0)}(x) = \exp \left\{ - \left[\frac{\ln(x_u/x)}{\phi} \right]^\alpha \right\} \quad ; \quad 0 < x < x_u \quad (2.1)$$
$$= 1.0 \quad ; \quad x \geq x_u$$

in which $F_{a(0)}(x) = P[a(0) < x]$, $a(0) = \text{EIFS} = \text{crack size at time } \tau = 0$, $x_u = \text{EIFS upper bound limit}$, and α and ϕ are empirical parameters. The Weibull compatible distribution is a derived distribution in the crack length domain. The Weibull compatible distribution was selected to characterize the initial fatigue quality for the method developed here because of its success in reflecting initial fatigue quality in similar situations [8-12].

2.1.2 The Time-to-Crack-Initiation Distribution

The time-to-crack-initiation (TTCI) is another quantity for assessing a material's resistance to cracking under service load environments. A reference crack size is selected, and the time it takes for a crack to develop and grow to the reference crack size is recorded for a sample of fatigue specimens. The time to crack initiation was proposed in [17] as a random variable with an extreme value distribution, such as a two-parameter Weibull distribution, having a given characteristic life and a defined shape parameter. Yang et al. [8] and Shinozuka [13] have demonstrated the existence of compatibility between the EIFSD function and the TTCI distribution function for the Weibull and lognormal distributions, as illustrated in Figure 2.1. Figure 2.1 illustrates the time-to-crack-initiation (TTCI) distribution as a Weibull distribution with time as the independent random variable. A power law was then used to reflect the crack growth law which transforms the distribution back to the y axis at time zero. The resulting derived distribution is termed a Weibull compatible distribution and the independent random variable is crack length. The model developed and presented here started with the assumption of the Weibull compatible distribution. Since the distribution of TTCI depends on the service loading condition, it can not be used to

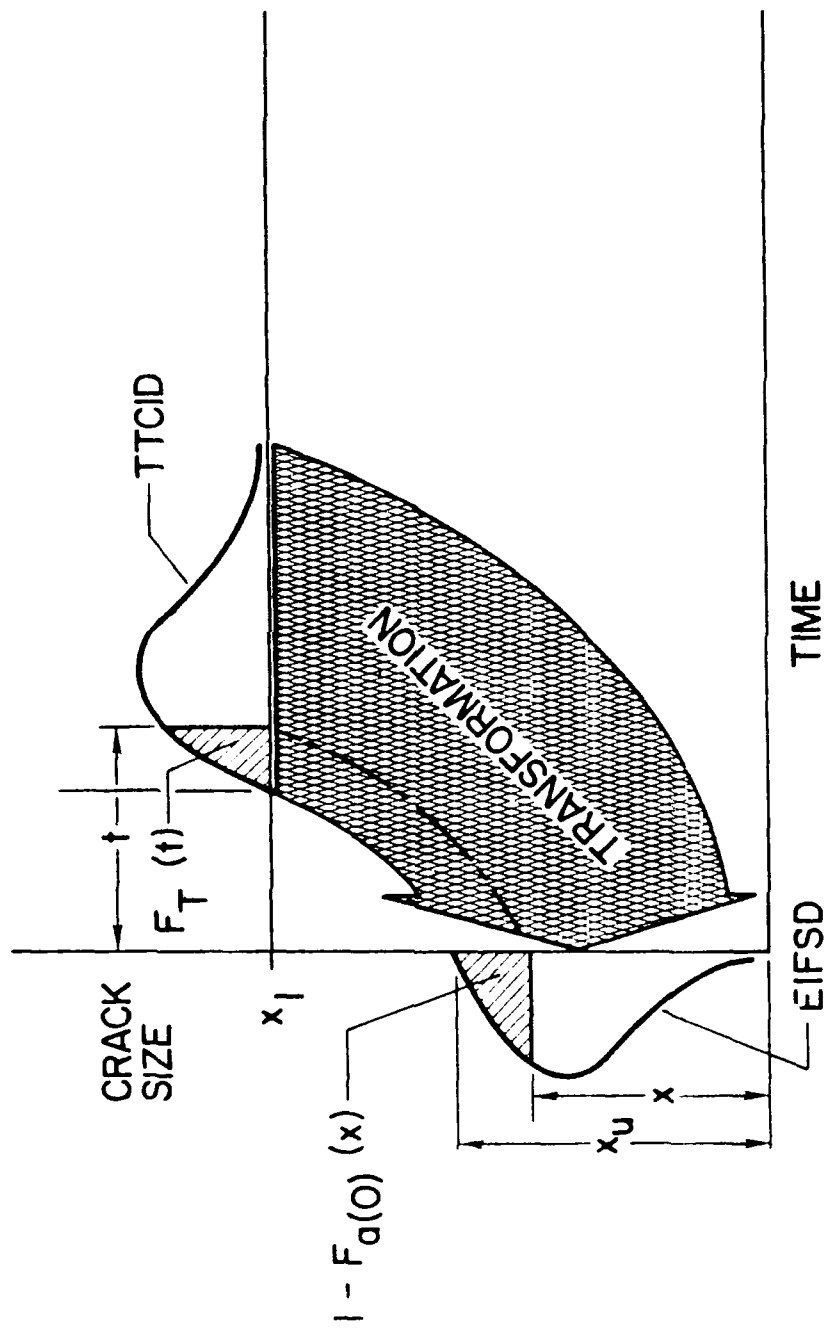


Figure 2.1 Compatibility between TTCI and EIFS

characterize the initial fatigue quality as that of the equivalent initial flaw size.

2.2 Stochastic Crack Growth Model

The second component in life prediction is the crack growth damage computation. The crack growth rate involves statistical variabilities. The variability in crack growth is due to a number of factors; 1) the random error in measuring crack length, a , in the test, 2) the systematic errors in the measurement of a , and 3) the inherent statistical variation in the material crack growth resistance, service loads, etc. The crack growth rate calculation method used in data reduction affects the amount of variability. Several studies have been conducted to characterize the variability of the crack growth rate. They are cited below.

Clark and Hudak [18] reported on an extensive interlaboratory program which was conducted to assess the variability and bias associated with fatigue crack growth rate testing. The results of the study showed that the primary source of variability in fatigue crack growth rate testing is the experimental procedure used to obtain the raw test data. The data processing technique used to evaluate the raw test data also affected the reported variability. The polynomial techniques produced da/dN data with substantially lower variability than that produced by the

secant methods. No indication of bias was present for any specific data processing technique. It was concluded that the data processing technique was not found to be an important source of variability. They found that the crack growth process could be accurately characterized by a lognormal distribution.

Weibull, et al. [19] further investigated the role of the experimental procedure in producing variability in the a vs. N data. Specifically, they looked at the effect of measurement precision on the variability in fatigue crack growth rate data. Variability in the derived crack growth rate data was found to depend strongly on the magnitude of the measurement interval relative to the measurement precision. It was pointed out that it may be incorrect to assume that the observed scatter in the da/dN data is a result primarily of the variation in the material properties.

Virkler, et al. [20] considered six distributions to describe the variability in da/dN . Tests were performed on center-cracked panels of 2024-T34 aluminum under constant amplitude loading. The three-parameter lognormal distribution fit the variability in cycle count data the best. They then repredicted the crack growth data using a Monte Carlo simulation method of choosing crack growth rate increments. This method is analogous to assuming that the underlying process is composed of white noise. This approach assumes that the crack growth data were spatially

uncorrelated. The mean of the life was predicted quite well, but the variability was greatly underestimated, as can be observed by comparing the actual data in Figure 2.2 to the predicted data in Figure 2.3. These results highlight that crack growth rate is not independent in the space domain.

Artley et al. [21] directly evaluated the variability in crack growth rate by applying a constant stress intensity factor, K , flight-by-flight load history to a center-cracked panel of 7075-T6 aluminum. The coefficient of variation of the crack growth rates calculated by the secant method of differentiation stabilized at approximately twelve percent, while the seven-point polynomial method stabilized at six percent. The polynomial methods smooth data by selecting the best curve through the data and calculating the slope.

Yang et al. [22] showed that the scatter in da/dN could be described by the lognormal distribution for engine materials. Variability in crack growth rate for engine materials is further investigated in references [23,24,25].

Bogdanoff and Kozin [e.g. 26,27] have taken the statistical variability of fatigue crack growth into account by proposing account by proposing that the crack size $a(t)$ is a discrete Markov chain. Their model is based on crack size rather than crack growth rate, so it has only limited appeal.

Lin and Yang [28,30] and Yang [e.g.22,31,32,33,34], took the statistical variability of the crack growth rate into account by randomizing the crack growth rate equation,

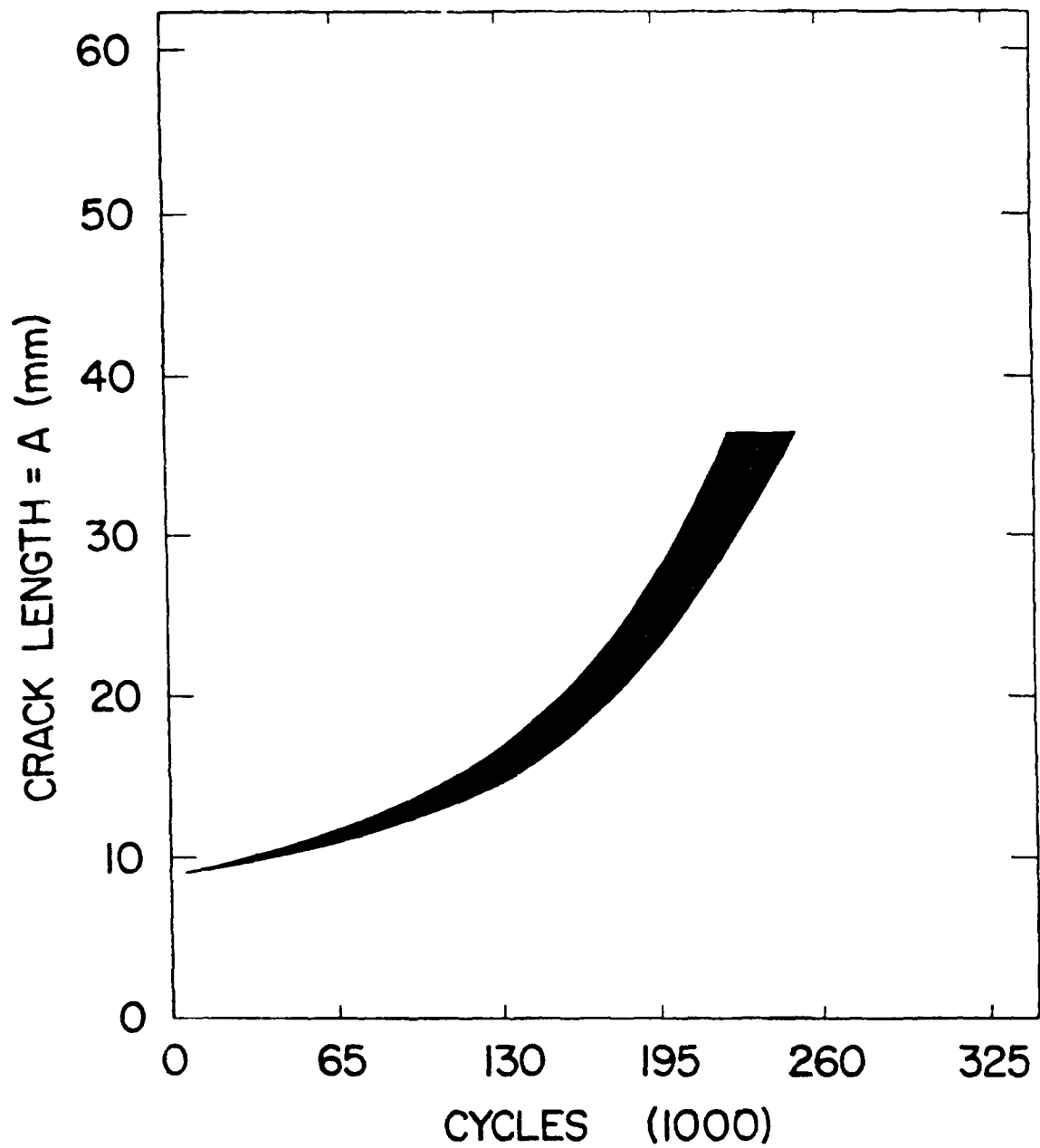


Figure 2.2 Crack Length Versus Cycles for Constant Amplitude Data (from Ref. 20)

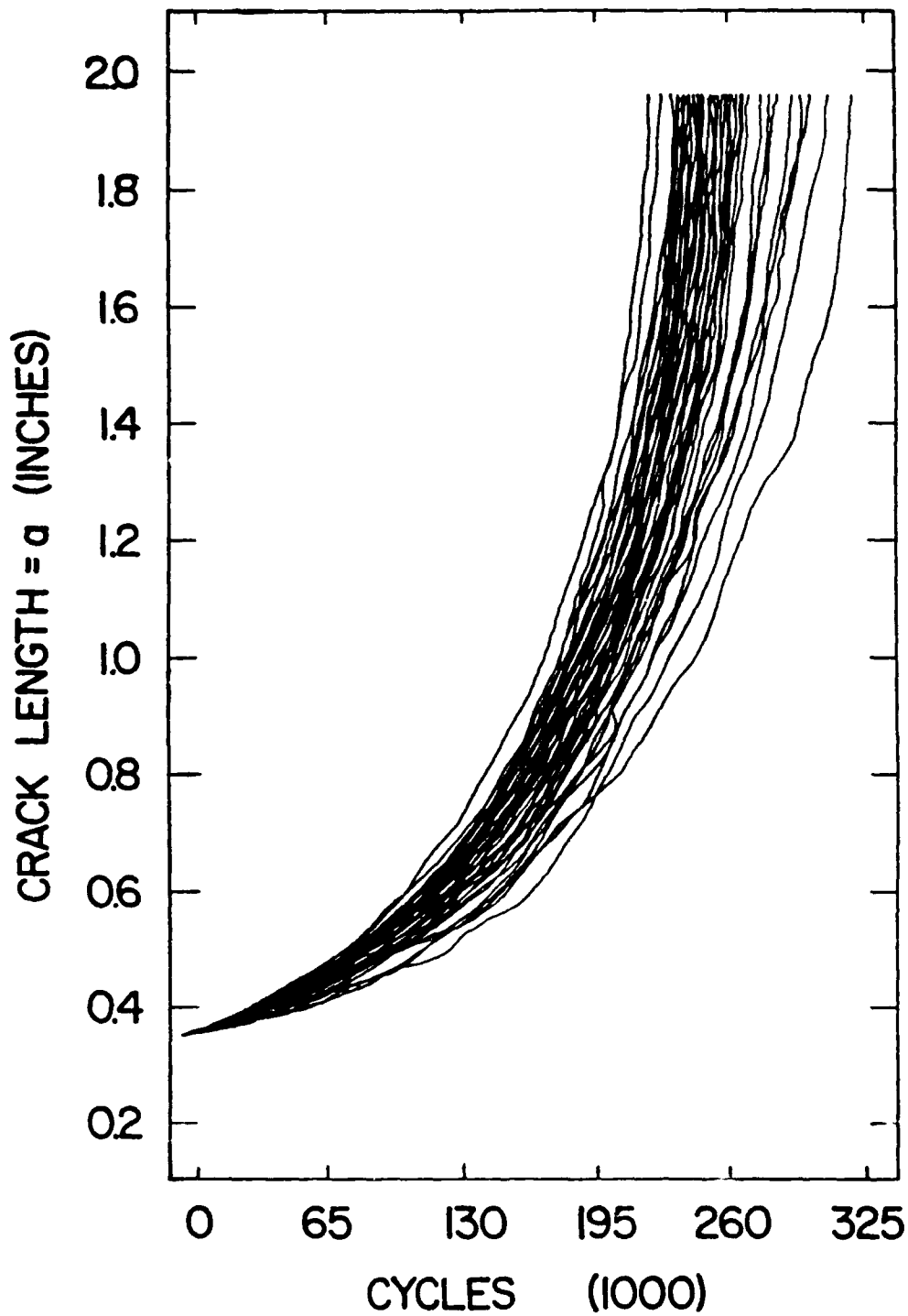


Figure 2.3 Predicted Crack Length Versus Cycles for Constant Amplitude Data (from Ref.20)

$$\frac{da(t)}{dt} = X(t)Qa(t)^b \quad (2.2)$$

where "a" is crack length, "t" is time in flight hours or hours, da/dt is the crack growth rate, Q and b are constants which depend on the material and spectrum loading conditions, and X(t) is a non-negative stationary stochastic process with a median value equal to unity. They proposed that X(t) followed a general lognormal random process model. As a special case of the lognormal random process model, Yang et al. [e.g.31-39] considered that X(t)=X, where X is a lognormal random variable. The approximation has been found to be extremely effective for representing crack growth from fastener hole specimens under spectrum loadings. For this reason it was used in the model developed here. A deterministic crack growth rate model was also considered.

Various approaches have been suggested to solve the general lognormal random process model including the method of Monte Carlo simulation by Yang et al. [31,32], the Poisson pulse process by Lin and Yang [28-29], the cumulant closure technique by Lin and Yang [30], the second moment approximation by Yang et al. [31,32], the finite strip method by Spencer et al. [40,41], etc. Finally, the random process X(t) in time has also been considered as a random process X(K) in stress intensity factor K by Ortiz [42,43].

Yang et al. [22,25,44,45] has developed probabilistic crack growth models for engine components. The lognormal crack growth rate model was proposed for crack propagation of engine components subjected to either constant amplitude

load histories or block type spectrum loadings. The hyperbolic sine (SINH) crack growth rate function developed at Pratt and Whitney [46] was used for engine components.

2.3 Probability of Detection

The third element to be considered in developing a probabilistic model to assess the current quality of the airframe is the reliability of the inspection. Almost all NDI data from aerospace components consists of indications of whether flaws are present or not. The indication of the presence of a flaw does not necessarily mean that a flaw or crack is actually present.

There are four levels of crack indications as noted in the C141 modification program [47]. Their definitions follow. A suspect is a flaw-like condition obtained when using the first primary non-destructive technique. An indication is a rejectable condition for a flaw-like indication which was previously categorized as a suspect when obtained using the first backup NDI technique. If the primary NDI technique is eddy current; this term applies to an indication obtained after repeatedly cleaning the hole. A confirmed indication is a rejectable condition which was previously an indication and has been confirmed by laboratory personnel, but was not determined to be crack-like in nature. And finally, a confirmed crack is a term used to describe a flaw which was previously categorized as a confirmed indication when located by a

laboratory personnel using enhanced visual inspection. The challenge is presented to consider this approach and definitions when devising a representation of the reliability of the inspection.

If the flaw indication is positive, the hole is reamed out at 1/64 inch and the NDI is performed again. If the flaw indication is still positive, then the hole is reamed out 1/64 inch again. This is done three times for a straight hole and four times for a tapered hole. After this procedure, if the flaw indication is still positive, a repair is made according to a standard technical procedure for that location. The data available from this kind of inspection is either positive or negative, pass/fail of the test. Results are presented as pass/fail for a given discrete crack length.

Berens and Hovey [48-52] have offered an analysis method for handling pass/fail data in such a way as to devise maximum likelihood parameters for establishing the probability of detection. This method is not exact because it is difficult to obtain information on the true size or existence of a flaw without the intensive investigation of tear-down inspection results.

Several researchers [e.g.48,49,53-55] have shown that the probability of detection can be represented by a "Log-Odds" function given by

$$F_D(x) = \left\{ 1 + \exp - \left[\frac{\pi}{\sqrt{3}} \left(\frac{\ln(x) - \mu}{\sigma} \right) \right] \right\}^{-1} \quad (2.3)$$

The "Log-Odds" function given in Eq. (2.3) can be reparameterized to provide a linear form in transformed variables

$$F_D(x) = \frac{\exp(\alpha^* + \beta^* \ln x)}{1 + \exp(\alpha^* + \beta^* \ln x)} \quad (2.4)$$

where α^* and β^* are constants derived from maximum likelihood estimators. The parameters μ and σ in Eq. 2.3 and α^* and β^* in Eq. 2.4 are related by; $\mu = -\alpha^*/\beta^*$ and $\sigma = \pi/(\beta^*\sqrt{3})$. This representation of the inspection reliability was selected for the illustration of the model presented here because of its ability to reflect broad banded and narrow banded inspection systems.

The use of multiple inspections to improve crack detection probability is thoroughly investigated by Yang and Donath [56,57] who showed that multiple inspections do not always insure improved inspection reliability. They showed that when the sequential inspections are done conditionally that grave errors can result.

2.4 Probabilistic Life Prediction

Probabilistic life predictions based on fracture mechanics have been developed for aerospace applications over the last twenty years. In particular several researchers have developed stochastic models for life prediction [e.g.32,44,45,58-65].

Manning et al. [e.g.64] have done extensive work in formulating, validating and refining a probabilistic durability analysis for the U.S. Air Force in support of

their military specification for structural integrity of aircraft structures [1].

Palmberg et al. [65] have presented a probabilistic damage tolerance analysis which takes into account the EIFSD, stochastic crack growth rate and the inspection reliability. They use a stochastic process $X(t)$ to account for the variability in crack growth rate following the approach proposed by Lin and Yang [29,30]. In addition to the probabilistic life prediction for structures under scheduled inspection/repair maintenance cited above, the probabilistic life prediction for structures under scheduled proof test maintenance has also been investigated [66,67].

CHAPTER III

ANALYTICAL FORMULATION OF PROBABILISTIC APPROACH TO LIFE PREDICTION

3.1 Deterministic Crack Growth Approach

3.1.1 Analytical Crack Growth Approach

Suppose the crack growth rate can be represented by the Paris type equation

$$da(t)/dt = c (\Delta K)^m \quad (3.1)$$

in which $a(t)$ = crack size at time t , t - flight hours or flights, ΔK = stress intensity range, and c and m are empirical constants. Solutions of ΔK for many geometries are available in the literature. For example, the solution for a center crack in an infinite panel is given by Equation (3.2)

$$\Delta K = \Delta \sigma \sqrt{2\pi a} \quad (3.2)$$

where $\Delta \sigma$ is the amplitude of the applied cyclic stress. For some variable amplitude loadings, as in the case of flight-by-flight load histories, the $\Delta \sigma$ can be replaced by a $\Delta \sigma_{\text{eff}}$ and K can be replaced by K_{eff} for many variable amplitude loadings. This expression is valid within regions of ΔK especially the middle regions.

Substitution of Eq. (3.2) into Eq. (3.1) yields

$$da(t)/dt = Qa^b(t) \quad (3.3)$$

in which $b = m/2$ and $Q = c [\Delta\sigma\sqrt{\pi}]^m$. Q can take on values $Q_1, Q_2, Q_3, \dots, Q_n$, within segments of the crack growth rate curve.

Equation (3.3) is a convenient form of the power law and it has been suggested by Yang and Manning for durability analysis of aircraft structures [8,10,12]. It will be used here for the damage tolerance analysis.

Equation (3.3) can be integrated from t_1 to t_2 to obtain the relationship between $a(t_1)$ and $a(t_2)$,

$$a(t_2) = \frac{a(t_1)}{[1 - a^c(t_1) cQ(t_2 - t_1)]^{1/c}} \quad (3.4)$$

or

$$a(t_1) = \frac{a(t_2)}{[1 + a^c(t_2) cQ(t_2 - t_1)]^{1/c}} \quad (3.5)$$

where

$$c = b - 1 \quad (3.6)$$

For $t_1 = 0$ and $t_2 = t$, Eqs. (3.4) and (3.5) become

$$a(0) = \frac{a(t)}{[1 - a^c(t) cQt]^{1/c}} \quad (3.7)$$

or

$$a(t) = \frac{a(0)}{[1 - a^c(0) cQt]^{1/c}} \quad (3.8)$$

Equations (3.4) - 3.8) will be used in the methodology to transform the distribution of the crack size from one time instant to another in service.

The initial quality of a metallic structure can be represented by the cumulative distribution at equivalent

initial flaw sizes (EIFS), $a(0)$, i.e., the equivalent flaw size at time zero. The Weibull Compatible distribution, proposed by Yang and Manning [8,9] will be used to describe the equivalent initial flaw size distribution and is repeated here:

$$F_{a(0)}(x) = \exp \left\{ - \left[\frac{\ln(x_u/x)}{\phi} \right]^\alpha \right\} \quad (3.9)$$

where x_u is the upper bound on the EIFS, α and ϕ are empirical constants to be determined from the fractographic data. Procedures for the determination of x_u , α and β have been described in details in Refs. [10,12]

3.1.1.1 No Inspection

We now have the two necessary ingredients to estimate the probability of failure for no inspection, or just prior to the first inspection using the cumulative distribution of initial flaws and the deterministic crack growth equation. The probability that the crack size $a(t)$ at any service time will exceed the critical crack size a_c is given by

$$P_f(t) = P [a(t) \geq a_c] \quad (3.10)$$

Substituting Eq. (3.8) into Eq. (3.9), one obtains

$$P_f(t) = P [a(0) \leq y_c(t)] = 1 - F_{a(0)}[y_c(t)] \quad (3.11)$$

in which $F_{a(0)}[y_c(t)]$ is defined in Eq. (3.9) and

$$y_c(t) = \frac{x_c}{[1 - x_c^c c_Q t]^{1/c}} \quad (3.12)$$

in Eq. (3.12), $y_c(t)$ is the value of the initial flaw which will grow to critical flaw size in the given time interval $[0, t]$. The solution for the failure probability given by

Eq. (3.11) is applicable to the first inspection interval, or where no inspection is performed. The probability of failure for the case where one or multiple inspections are performed will be derived the following.

3.1.1.2 One or Multiple Inspections

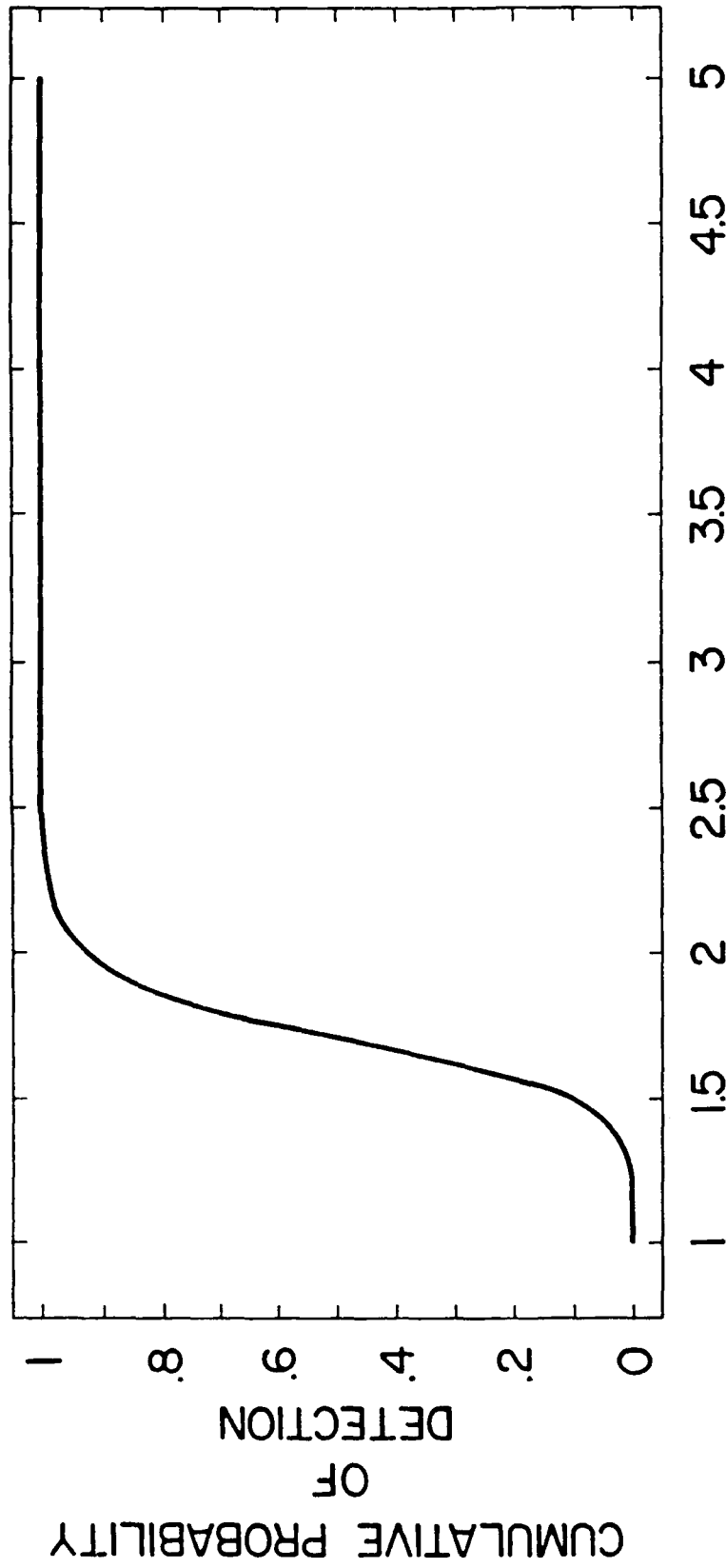
In considering the effect of inspections on the probability of failure, it becomes convenient to use the probability density function to describe the flaw size distribution rather than the cumulative distribution function. The probability of detection, which is introduced in Chapter II, is shown in Equation (3.13):

$$F_D(x) = \frac{\exp(\alpha^* + \beta^* \ln x)}{1 + \exp(\alpha^* + \beta^* \ln x)} \quad (3.13)$$

in which x is the crack size, and α^* and β^* are constants depending on the capability of the inspection system.

Equation (3.13) is illustrated in Figure 3.1. The equation accounts for the fact that nondestructive inspection (NDI) systems are not capable of repeatedly producing correct readings when applied to flaws of the same length.

The distribution of flaw sizes at any point in time prior to any inspection can be found by transforming the density function of flaw sizes, $a(0)$, at time zero to the flaw sizes $a(t)$ at time t . This transformation can be made using the relationship between the crack length at time zero $a(0)$ and the crack length at any other time, $a(t)$, given by Eq. (3.8). The probability density function $f_{a(t)}(x)$ of the crack size $a(t)$ at time t is obtained as



CRACK LENGTH = a (INCHES)

Figure 3.1 The "Log-Odds" Function for Probability of Detection

$$f_{a(t)}(x) = f_{a(0)}[y(x,t)] \left| \frac{dy(x,t)}{dx} \right| \quad (3.14)$$

$$= f_{a(0)}[y(x,t)] J(x,t)$$

in which it follows from Eq. (3.8) that

$$y(x,t) = \frac{x}{(1 - x^c c_Q t)^{1/c}}$$

and

$$J(x,t) = \left[\frac{1}{1 + x^c c_Q t} \right]^{1 + 1/c} \quad (3.15)$$

In Eq. (3.14), $f_{a(0)}(x)$ is the probability density function of EIFS obtained by taking derivative of $F_{a(0)}(x)$ with respect to x ,

$$f_{a(0)}(x) = \frac{\alpha}{\varphi x} \left[\frac{\ln(x_u/x)}{\varphi} \right]^{\alpha-1} \exp \left\{ - \left[\frac{\ln(x_u/x)}{\varphi} \right]^\alpha \right\} \quad (3.16)$$

With the above procedure for transforming the crack sizes from one point in time to another, the expressions for the density functions after several inspections can be formulated. The probability density function of the crack size right before the first inspection at τ is given by Eq. (3.14) with $t = \tau$, i.e.,

$$f_{a(\tau)}(x) = f_{a(0)}[y(x,\tau)] J(x,\tau) \quad (3.17)$$

The probability of failure in the first service interval $[0,\tau]$ is given by

$$p(1) = \int_{a_c}^{\infty} f_{a(\tau)}(x) dx \quad (3.18)$$

and the probability of repair during the first inspection maintenance is given by

$$G(1) = \int_0^{a_c} f_{a(\tau)}(x) F_D(x) dx \quad (3.19)$$

in which $F_D(x)$ is the probability of crack detection given by Eq. (3.13). It can be shown that $p(1)$ given in Eq. (3.18) is identical to $P_f(t)$ in Eq. (3.10) with $t = \tau$. After the first inspection maintenance at τ , the probability density of the crack size $a(\tau^+)$ is modified, because of possible repair,

$$f_{a(\tau^+)}(x) = G(1)f_{a(0)}(x) + F_D^*(x)f_{a(\tau)}(x) ; x < a_c \quad (3.20)$$

in which the first term is contributed by the repaired population and $F_D^*(x)$ is the probability of not detecting (missing) a crack of size x during inspection,

$$F_D^*(x) = 1 - F_D(x) \quad (3.21)$$

The density function of crack lengths after the second service interval at 2τ before inspection is obtained by transforming Eq. (3.20) to the time 2τ as follows

$$f_{a(2\tau)}(x) = G(1)f_{a(\tau)}(x) + F_D^*(x)f_{a(2\tau)}(x) \quad (3.22)$$

in which $f_{a(2\tau)}(x)$ is the probability density function of the crack size $a(2\tau)$ for the population originated at $t = 0$. $f_{a(\tau)}(x)$ is obtained from Eq. (3.17) by setting $t = 2\tau$.

As a result, owing to crack propagation, the crack size and its probability density increase as a function of service time. Meanwhile, the probability density function is subjected to modification during each inspection and repair maintenance. Following a similar procedure described above, the probability density function of the crack size,

$a(n\tau)$, at $n\tau$ right before the n th inspection maintenance, can be obtained in a recurrent form,

$$f_{a(n\tau)}(x) = \left\{ \prod_{m=1}^{n-1} F_D^* [Y(x; m\tau)] \right\} f_{a(0)} [Y(x; n\tau)] J(x; n\tau) + \sum_{k=1}^{n-1} G(n-k) \bar{A}_k \quad ; \quad \text{for } n=2,3 \quad (3.23)$$

in which the first term is contributed by the original population introduced at $t = 0$, and the second summation term is contributed by the repaired populations introduced at n -kth inspection maintenance ($k=1,2,\dots,n-1$).

In Eq. 3.23, $G(n-k)$ is the probability of repair at $(n-k)\tau$, and

$$\bar{A}_k = \left\{ \prod_{m=1}^{k-1} F_D^* [Y(x; m\tau)] \right\} f_{a(0)} [Y(x; k\tau)] J(x; k\tau) \quad (3.24)$$

in which $Y(x; m\tau)$ and $J(x; k\tau)$ are given by Eqs. (3.15) and (3.16), respectively. It should be mentioned that in Eq. 3.24,

$$\prod_{m=1}^{k-1} F_D^* [Y(x; m\tau, z)] = 1 \text{ for } k = 1 \text{ and } F_D^* [Y] = 0 \text{ for } Y > a_c.$$

The probability of failure in the n th service interval $[(n-1)\tau, n\tau]$, denoted by $p(n)$, is obtained as

$$p(n) = \int_{a_c}^{\infty} f_{a(n\tau)}(x) dx \quad ; \quad \text{for } n=2,3,\dots \quad (3.25)$$

and the probability of repair, $G(n)$ during the n th inspection maintenance is given by

$$G(n) = \int_0^{a_c} f_{a(n\tau)}(x) F_D(x) dx \quad ; \quad \text{for } n=2,3,\dots \quad (3.25a)$$

Equations (3.23) - (3.26) are recurrent solutions of $n = 2, 3, \dots$, where the solutions for $n = 1$ are given by Eqs. (3.18) - (3.19).

The probability of failure in each service interval $p(n)$, $n = 1, 2, \dots$ has been derived in Eq. (3.25). The probability of failure within m service intervals, i.e., in the service interval $[0, m\tau]$, denoted by p_m , is obtained as

$$p_m = 1 - \prod_{n=1}^m [1-p(n)] \quad (3.26)$$

3.1.2 Master Curve Approach

In some instances, the crack growth rate equation cannot be expressed analytically. For instance, Eq. (3.1) does not hold for the entire region of crack size. This is particularly true for a redundant structure, where the crack growth rate in a stiffened panel slows down and is arrested as it approaches the stiffener. In this connection, the so-called master curve approach developed by Yang [8] will be used in the following.

Both the crack propagation and residual strength are functions of the crack tip stress intensity factor, K . The effect of stiffeners on the stress intensity factor in redundant, built-up structures can be expressed as:

$$\Delta K = \Delta \sigma \sqrt{\pi a} \beta(a) \quad (3.27)$$

where $\beta(a)$, a function of crack size $a(t)$, is a correction factor to account for the effect of geometry on the crack growth. Substituting Eq. (3.27) into Eq. (3.1), one obtains the growth rate equation as follows

$$\frac{da(t)}{dt} = Qa^b(t) \left[\beta(a) \right]^{2b} \quad (3.28)$$

Unfortunately, the correction factor $\beta(a)$ cannot be expressed analytically as a function of the crack size $a(t)$. Swift [68] has reported discrete values of crack size and $\beta(a)$ for several stiffener spacings and areas. Thus, Eq. (3.28) cannot be integrated to yield an analytical relation for crack size, $a(t)$, as a function of time, t . Consequently, numerical integration should be used to obtain the crack size-time relation.

In addition to the panel-stiffener system described above, there are other situations where the analytical crack size-time relation does not exist and a general computer program, such as the MODGRO developed by the U.S. Air Force [69] should be used. By use of numerical integration procedures, the crack size $a(t_2)$ at t_2 flight hours can be expressed in terms of $a(t_1)$ where $t_2 > t_1$ as follows

$$a(t_2) = a(t_1) + \Sigma \Delta a(t_j) \quad (3.29)$$

in which $\Delta a(t_j)$ is the crack growth increment per flight hour at t_j , where $t_1 \leq t_j \leq t_2$. The crack growth curve, $a(t)$ as a function of service time t thus obtained, is referred to as the "master curve."

Since the design loading spectra consist of many repeated flights and missions, it is reasonable to assume that the relation between $a(t_1)$ and $a(t_2)$ depends on the difference of the service time $t_2 - t_1$. Thus, only one master curve for each maximum stress level is sufficient for the determination of the crack growth damage. For the purpose of mathematical derivation later, the analytical master curve $a(t)$ can be symbolically represented by

$$a(t_1) = W[a(t_2), t_2 - t_1] \quad (3.30)$$

in which W is a general function representing the master curve. It is a monotonically increasing function of $t_2 - t_1$. For instance, for a special case in which Eq. (3.3) is valid, one obtains the function W after integration as $a(t_1) = W[a(t_2), t_2 - t_1] = a(t_2) / [1 + a^c(t_2) c Q(t_2 - t_1)]^{1/c}$.

For the particular case where $t_1 = 0$ and $t_2 = t$, Eq. 3.30 becomes

$$a(0) = W[a(t), t] \quad (3.31)$$

In the present analysis, the master curve can be obtained, starting from an arbitrary crack size that is smaller than the EIFS, by using any crack growth general computer program, such as the MODGRU program [69]. In this dissertation, since the panel-stiffener system is of major concern, Eq. (3.28) will be integrated numerically to obtain the master curve. The procedures using the cubic spline method are described in Appendix A.

The probability of failure of a structural component under scheduled inspection and maintenance using the master

curve approach described above will be derived in the following (after Ref. 8).

3.1.2.1 No Inspection

The probability that a crack $a(t)$ at any service time t will exceed the critical crack size a_c is given by

$$\begin{aligned} p_f(t) &= P [a(t) \geq a_c] \\ &= 1 - P [a(0) \leq y_c(t)] \\ &= 1 - F_{a(0)} [y_c(t)] \end{aligned} \quad (3.32)$$

in which $F_{a(0)} [y_c(t)]$ is distribution function of the equivalent initial flaw size given by Eq. (3.9) and it follows from Eq. (3.31) that

$$Y_c(t) = W[a_c, t] \quad (3.33)$$

In Eq. (3.33), $Y_c(t)$ is the corresponding crack size at $t = 0$ when the crack size at the time t is a_c . With the master curve numerically defined, Eq. (3.31), the value of $Y_c(t)$ in Eqs. (3.32) and (3.33) can be determined easily as shown in Fig. 3.2.

3.1.2.2 One or Multiple Inspections

The probability density function of the crack size $a(\tau)$ right before the first inspection at τ is obtained from that of EIFS through the transformation given by Eq. (3.31) as follows

$$f_{a(\tau)}(x) = f_{a(0)} [Y(x, \tau)] J(x, \tau) \quad (3.34)$$

in which

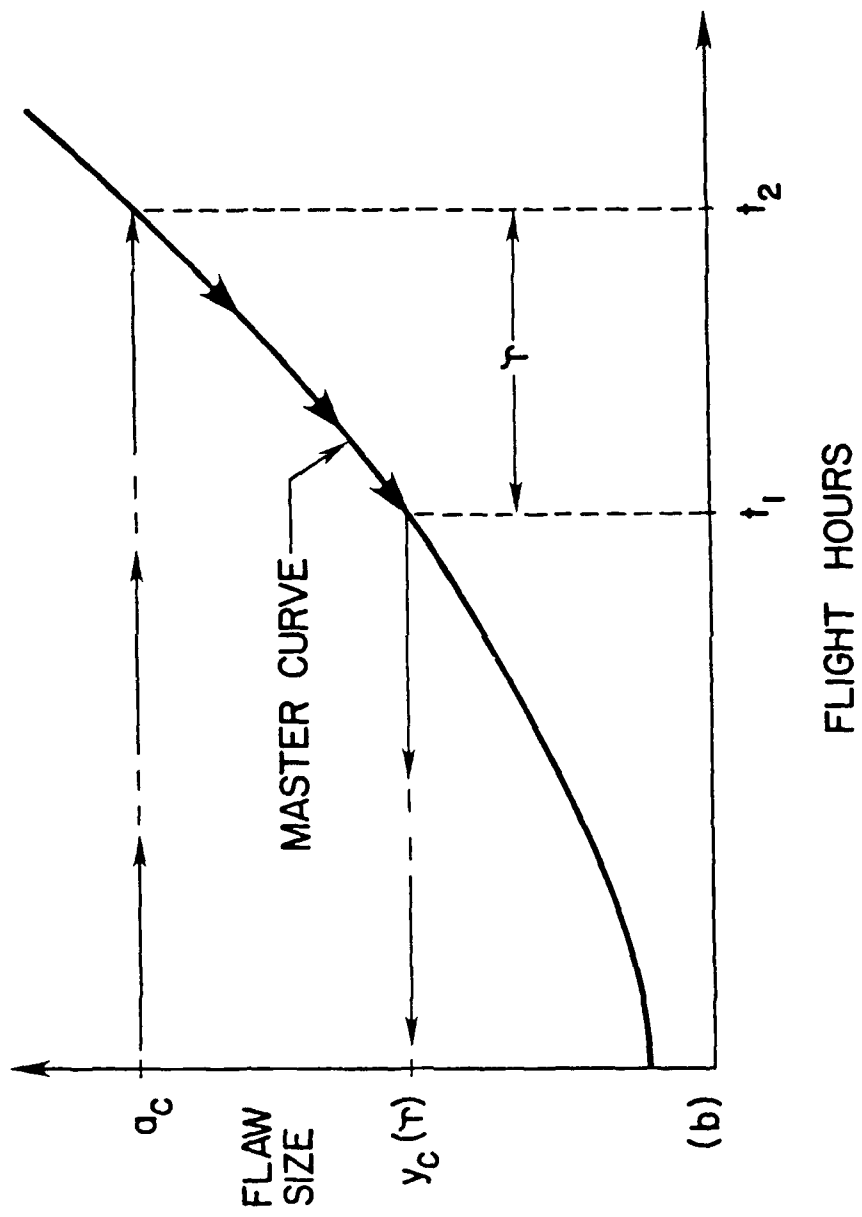


Figure 3.2 Calculation of $Y_c(\tau)$

$$y(x, \tau) = W(x, \tau)$$

$$J(x, \tau) = \frac{dy(x, \tau)}{d\tau} \frac{d\tau}{dx} \quad (3.35)$$

In Eq. (3.35), $y(x, \tau)$ is the corresponding crack size at $t = 0$ when the crack size at τ is equal to x , i.e., $a(\tau) = x$. Furthermore, $y(x, \tau)$ can also be interpreted as the crack size at $t_1 = t_2 - \tau$, i.e., $a(t_1) = y(x, \tau)$, when the corresponding crack size at t_2 is equal to x , i.e., $a(t_2) = x$. With the crack growth master curve being defined numerically, the determination of $y(x, \tau)$, and slopes $dy(x, \tau)/d\tau$ and $d\tau/dx$ can easily be made as shown in Fig. 3.3.

The probability of failure in the first service interval $[0, \tau]$ is obtained as

$$p(1) = \int_{a_c}^{\infty} f_{a(\tau)}(x) dx \quad (3.36)$$

in which $f_{a(\tau)}(x)$ has been derived in Eq. (3.34). The probability of repair during the first inspection maintenance is given by

$$G(1) = \int_0^{a_c} f_{a(\tau)}(x) F_D(x) dx \quad (3.37)$$

In a similar manner, the probability density function of the crack size $a(n\tau)$ at the service time $n\tau$ right before the n th inspection maintenance is obtained [Ref. 31] as

$$f_{a(n\tau)}(x) = A_n + \sum_{k=1}^{n-1} G(n-k) A_k \quad \text{for } n = 2, 3, \dots \quad (3.38)$$

in which A_n is the contribution from the original population that has not been repaired, and the second summation term is contributed by repaired population at each inspection maintenance.

$$A_1 = f_{a(0)}[y(x,\tau)] J(x,\tau)$$

$$A_k = \left\{ \prod_{m=1}^{k-1} F_D^* [y(x,m\tau)] \right\} f_{a(0)}[y(x,k\tau)] J(x,k\tau) \quad k = 2, 3, \dots \quad (3.39)$$

where

$$Y(x,k\tau) = W[x,k\tau]$$

$$J(x,k\tau) = \frac{dy(x,k\tau)}{d\tau} \frac{dx}{d\tau} \quad (3.40)$$

Again, $y(x,k\tau)$ is the crack size at $t_1 = t_2 - k\tau$, i.e., $a(t_2 - k\tau) = y(x,k\tau)$, when the corresponding crack size at t_2 is equal to x , i.e., $a(t_2) = x$. Thus, given the crack growth master curve, the crack size $y(x,k\tau)$, and the slopes $dy(x,k\tau)/d\tau$ and $dx/d\tau$ for $k = 1, 2, \dots$ can be determined as shown in Fig. 3.4.

In Eq. (3.38), $G(j)$ is the probability of detecting (or repairing) a crack of any size during the j th inspection

$$G(j) = \int_0^{a_c} f_{a(j\tau)}(x) F_D(x) dx \quad ; \quad j = 2, 3, \dots \quad (3.41)$$

Thus, the probability of failure in the n th service interval, i.e., $[(n-1)\tau, n\tau]$, is obtained as

$$p(n) = \int_{a_c}^{\infty} f_{a(n\tau)}(x) dx \quad (3.42)$$

The probability of failure in n service intervals, i.e.,

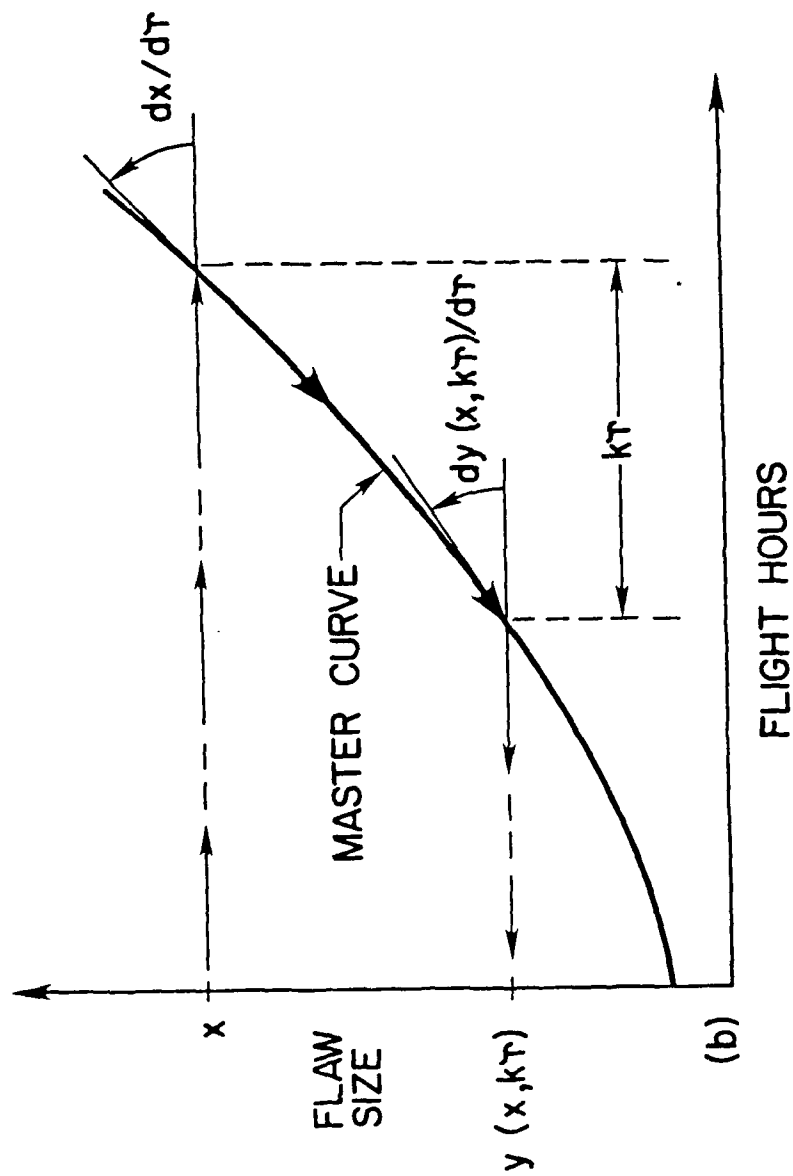


Figure 3.4 Calculation of $y(x, k\tau)$

[0,nt], is given by

$$P_n = 1 - \prod_{j=1}^n [1-p(j)] \quad (3.43)$$

3.2 Stochastic Crack Growth Approach

In the previous section, the crack growth rate variability is not accounted for in the estimation of probability of failure of the structure. This approach is slightly unconservative, since the crack growth rate variability tends to increase the failure probability of the structure in service. It is mentioned that the distribution of the equivalent initial flaw size (EIFS) is established by back-extrapolation of experimental fractographic data to time zero. When the back-extrapolation is conducted using a deterministic crack growth model, the EIFS distribution, Eq. (3.9), is referred to as the deterministic-based EIFS distribution [Ref. 10]. When the back extrapolation is made using a stochastic crack growth model, the EIFS distribution is referred to as the stochastic-based EIFS distribution. For the deterministic-based EIFS distribution, it has been shown that the accuracy for predicting the crack growth damage accumulation in service using the deterministic crack growth approach is quite reasonable, although it is slightly unconservative [Refs. 10,12,36,37]. On the other hand, the stochastic crack growth approach should be used if the stochastic-based EIFS distribution is employed.

3.2.1 Analytical Crack Growth Approach

In this section, the formulation for computing the probability of structural failure will be presented using a stochastic crack growth approach following Ref. 31. Various stochastic crack growth models have been proposed in the literature as described in Chapter II. Of all of the stochastic crack growth models available, the lognormal random variable model proposed by Yang [Refs. 31,32] shown in Eq. (2.20) is the simplest for practical applications. Likewise, such a model always results in a slight conservative prediction for crack growth damage accumulation. Consequently, it will be adopted in the present study.

The lognormal random variable model for crack propagation is repeated in the following

$$\frac{da(t)}{dt} = Z Q[a(t)]^b \quad (3.44)$$

in which Z is a lognormal random variable with a median of 1.0. Z is introduced to account for the crack growth rate variability resulting from various sources [see Refs. 31,32,61,62], such as the variabilities due to material cracking resistance, spectrum loading, crack geometry, crack modeling, etc.

The probability density function of the lognormal random variable Z is given by

$$f_Z(z) = \frac{1}{\sqrt{2\pi} z \sigma_Z} \exp \left\{ -\frac{1}{2} \left[\frac{\ln z}{\sigma_Z} \right]^2 \right\} ; z \geq 0 \quad (3.45)$$

in which σ_Z is the standard deviation of $\ln Z$.

3.2.1.1 No Inspection

Integrating Eq. (3.44) from $t = 0$ to $t = t$, one obtains

$$a(0) = \frac{a(t)}{[1+a^c(t)cQtZ]^{1/c}} \quad (3.46)$$

or

$$a(t) = \frac{a(0)}{[1-a^c(0)cQtZ]^{1/c}} \quad (3.47)$$

Where $c = b-1$ in Eq. (3.47), the crack size at any service time t involved two random variables, $a(0)$ and Z . The conditional distribution function $F_{a(t)}(x|z)$ of the crack size $a(t)$ given Z takes a value z , i.e., $Z=z$, is obtained from the distribution function of $a(0)$, given by Eq. (3.9), through the transformation of Eq. (3.46) as follows

$$F_{a(t)}(x|z) = F_{a(0)} [y(x,t,z)] \quad (3.48)$$

in which it follows from Eq. (3.46) that

$$y(x,t,z) = \frac{x}{[1+x^c cQtz]^{1/c}} \quad (3.49)$$

The unconditional distribution function of $a(0)$ is obtained from the conditional one using the theorem of total probability

$$F_{a(t)}(x) = \int_0^{\infty} F_{a(0)} [y(x,t,z)] f_Z(z) dz \quad (3.50)$$

where $f_Z(z)$ is the probability density function of Z given by Eq. (3.45).

The probability of failure within the time interval $[0,t]$, denoted by $p_f(t)$, is given by

$$\begin{aligned}
p_f(t) &= P[a(t) \geq a_c] & (3.51) \\
&= 1 - P[a(t) < a_c] \\
&= 1 - F_{a(t)}(a_c)
\end{aligned}$$

Substitution of Eq. (3.50) into Eq. (3.51) leads to the following expression for the probability of failure

$$p_f(t) = 1 - \int_0^{\infty} F_{a(0)}[Y(a_c, t, z)] f_z(z) dz \quad (3.52)$$

in which it follows from Eq. (3.49) that

$$Y(a_c, t, z) = \frac{a_c}{[1 + a_c^c c Q z t]^{1/c}} \quad (3.53)$$

The analytical integration for Eq. (3.52) usually is not possible, hence a straight forward numerical integration can be carried out to estimate the probability of failure $p_f(t)$.

3.2.1.2 One or Multiple Inspections

The crack size at the end of the first inspection interval $a(\tau)$ can be obtained in term of the initial flaw size $a(0)$ from Eq. (3.47) by setting $t=\tau$ as follows

$$a(\tau) = \frac{a(0)}{[1 - a^c(0) c Q \tau Z]^{1/c}} \quad (3.54)$$

in which $c = b - 1$. The probability density function, $f_{a(\tau)}(x)$, of $a(\tau)$ is obtained from that of $a(0)$ and Z through the transformation of Eq. (3.54); with the results,

$$f_{a(\tau)}(x) = \int_0^{\infty} f_{a(0)}[Y(x; \tau, z)] J(x; \tau, z) f_z(z) dz \quad (3.55)$$

in which $f_z(z)$ is given by Eq. (3.45), $f_{a(0)}(x)$ is the probability density of $a(0)$ given by Eq. (3.16) and

$$\begin{aligned} y(x; \tau, z) &= x/[1+x^c c_Q \tau z]^{1/c} \\ J(x; \tau, z) &= 1/[1+x^c c_Q \tau z]^{1+1/c} \end{aligned} \quad (3.56)$$

The probability of failure in the first service interval $(0, \tau)$, denoted by $p(1)$, is equal to the probability that $a(\tau)$ is greater than the critical crack size a_c ,

$$p(1) = \int_{a_c}^{\infty} f_{a(\tau)}(x) dx \quad (3.57)$$

The probability of repairing or detecting a crack, during the first inspection maintenance at τ , denoted by $G(1)$, is given by

$$G(1) = \int_0^{a_c} f_{a(\tau)}(x) F_D(x) dx \quad (3.58)$$

in which $F_D(x)$ is the probability of detecting a crack size x given by Eq. (3.13).

After the first inspection maintenance at τ , the probability density of the crack size $a(\tau^+)$ is modified, because of possible repair

$$f_{a(\tau^+)}(x) = G(1)f_{a(0)}(x) + F_D^*(x)f_{a(\tau)}(x) ; x < a_c \quad (3.59)$$

in which the first term is contributed by the renewal population (repaired fastener hole), and $F_D^*(x)$ is the probability of not detecting (missing) a crack of size x during inspection,

$$F_D^*(x) = 1 - F_D(x) \quad (3.60)$$

Following a similar procedure presented in Section 3.1.1, the probability density function of the crack size, $a(n\tau)$, at $n\tau$ right before the n th inspection maintenance, can be obtained in a recurrent form,

$$f_{a(n\tau)}(x) = \int_0^{\infty} f_{a(n\tau)}(x|z) f_z(z) dz \quad (3.61)$$

in which $f_{a(n\tau)}(x|z)$ is the conditional probability density of $a(n\tau)$ under the condition that $Z=z$,

$$f_{a(n\tau)}(x|z) = \left\{ \prod_{m=1}^{n-1} F_D^*[y(x;m\tau, z)] \right\} f_{a(0)}[y(x;n\tau, z)] J(x;n\tau, z) + \sum_{k=1}^{n-1} G(n-k) \bar{A}_k \quad ; \text{ for } n=2, 3, \dots \quad (3.62)$$

in which the first term is contributed by the original population introduced at $t = 0$, and the second summation term is contributed by the renewal populations (repaired locations) introduced at n -kth inspection maintenance ($k=1, 2, \dots, n-1$).

In Eq. (3.62), $G(n-k)$ is the probability of repairing a crack at $(n-k)\tau$, and

$$\bar{A}_k = \left\{ \prod_{m=1}^{k-1} F_D^*[Y(x;m\tau, z)] \right\} f_{a(0)}[y(x;k\tau, z)] J(x;k\tau, z) \quad (3.63)$$

in which $y(x;m\tau, z)$ and $J(x;k\tau, z)$ are given by Eq. (3.56).

It should be mentioned that in Eq. (3.63),

$$\prod_{m=1}^{k-1} F_D^*[Y(x;m\tau, z)] = 1 \text{ for } k = 1 \text{ and } F_D^*[Y] = 0 \text{ for } y > a_c.$$

The probability of failure in the n th service interval $[(n-1)\tau, n\tau]$, denoted by $p(n)$, is obtained as

$$p(n) = \int_{a_c}^{\infty} f_{a(n\tau)}(x) dx \quad ; \text{ for } n=2,3,\dots \quad (3.64)$$

and the probability of repairing a crack, $G(n)$ during the n th inspection maintenance is given by

$$G(n) = \int_0^{\infty} f_{a(n\tau)}(x) F_D(x) dx \quad ; \text{ for } n=2,3,\dots \quad (3.65)$$

Equations (3.61) - (3.65) are the recurrent solutions for $n=2,3,\dots$, where the solutions for $n = 1$ are given by Eqs. (3.55) - (3.58).

The probability of failure of a critical location in n service intervals $(0, n\tau)$, denoted by $P(n\tau)$, is given by

$$p(n\tau) = 1 - \prod_{j=1}^n [1-p(j)] \quad (3.66)$$

CHAPTER IV

EXAMPLES OF STOCHASTIC LIFE PREDICTION

4.0 Introduction

In this chapter, examples of the analysis approaches introduced in Chapter III will be presented. First, a lug problem will be presented in which the probability of repair and the probability of failure will be calculated using both a deterministic crack growth approach and a stochastic crack growth approach. Second, a stiffened panel problem will be presented in which the probability of repair and the probability of failure will also be calculated using a slow crack growth analysis and a fail-safe crack-arrest analysis. Both deterministic and stochastic crack growth approaches will be used.

4.1 Lug Example

A lug attachment fitting was selected as an example of a slow crack growth, damage tolerant critical structural component. It is representative of the category of single load path damage tolerant components [70]. The lug is a highly stressed and nonredundant structural component whose failure can be catastrophic [71].

A computer program was developed to calculate the probability of repair and the probability of failure for both stochastic crack growth and deterministic crack growth approaches from an initial flaw size distribution. The

probability of repair represents the average percentage of lugs in a fleet of aircraft that will contain detectable cracks and require repair. The probability of failure reflects the average percentage of lugs that will fail in a fleet of aircraft.

The parameters used in this example for straight aluminum lugs without bushing or bearings are summarized in Table (4.1) after reference [72]. A discussion of how these parameters were selected follows:

Test data were selected from those tabulated in reference [73], in which the specimen number S3-A-3 represented a straight shank, axially loaded lug with no bushing. The geometry of the lug is illustrated in Figure (4.1). It was subjected to an 80-flight fighter/trainer wing lower surface spectrum. The crack length versus flight data were differentiated to obtain the crack growth rate data, da/df , using the seven point polynomial method in accordance with American Society for Testing and Materials (ASTM) standard E-647 [74]. The da/df versus crack length data are shown in Figure (4.2). A linear regression analysis was performed on the natural logs of the da/df versus "a" data as follows, Eq. 2.1,

$$\frac{da}{df} = Qa^b \quad (4.1)$$

Taking the natural logs of both sides of Eq. (4.1), one obtains

$$\ln(da/df) = \ln(Q) + b \cdot \ln(a) \quad (4.2)$$

Table 4.1

Parameters for the aluminum lug example with a straight shank without bushing or bearings.

Crack Growth Parameters

$$Q = 7.158E-4 \text{ Flight hours}^{-1}$$

$$b = 1.393$$

$$\sigma_z = 0.2158$$

$$a_{cr} = 0.125 \text{ inch}$$

Initial Flaw Size Parameters

$$\alpha = 1.823$$

$$\phi = 1.455$$

$$x_u = 0.03$$

NDI Parameters

System #1

System #2

$$\alpha_*^* = 55.28$$

$$\alpha_*^* = 13.44$$

$$\beta = 16.4$$

$$\beta = 3.95$$

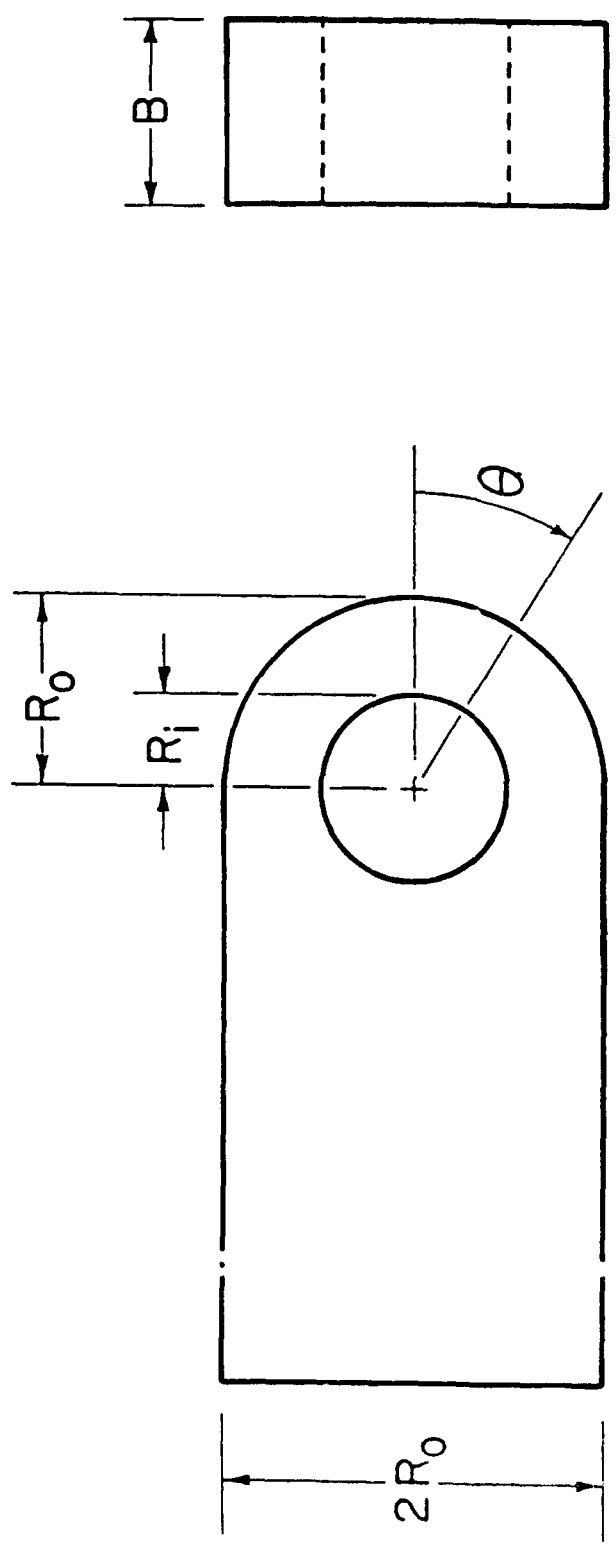


Figure 4.1 Geometry of the Lug

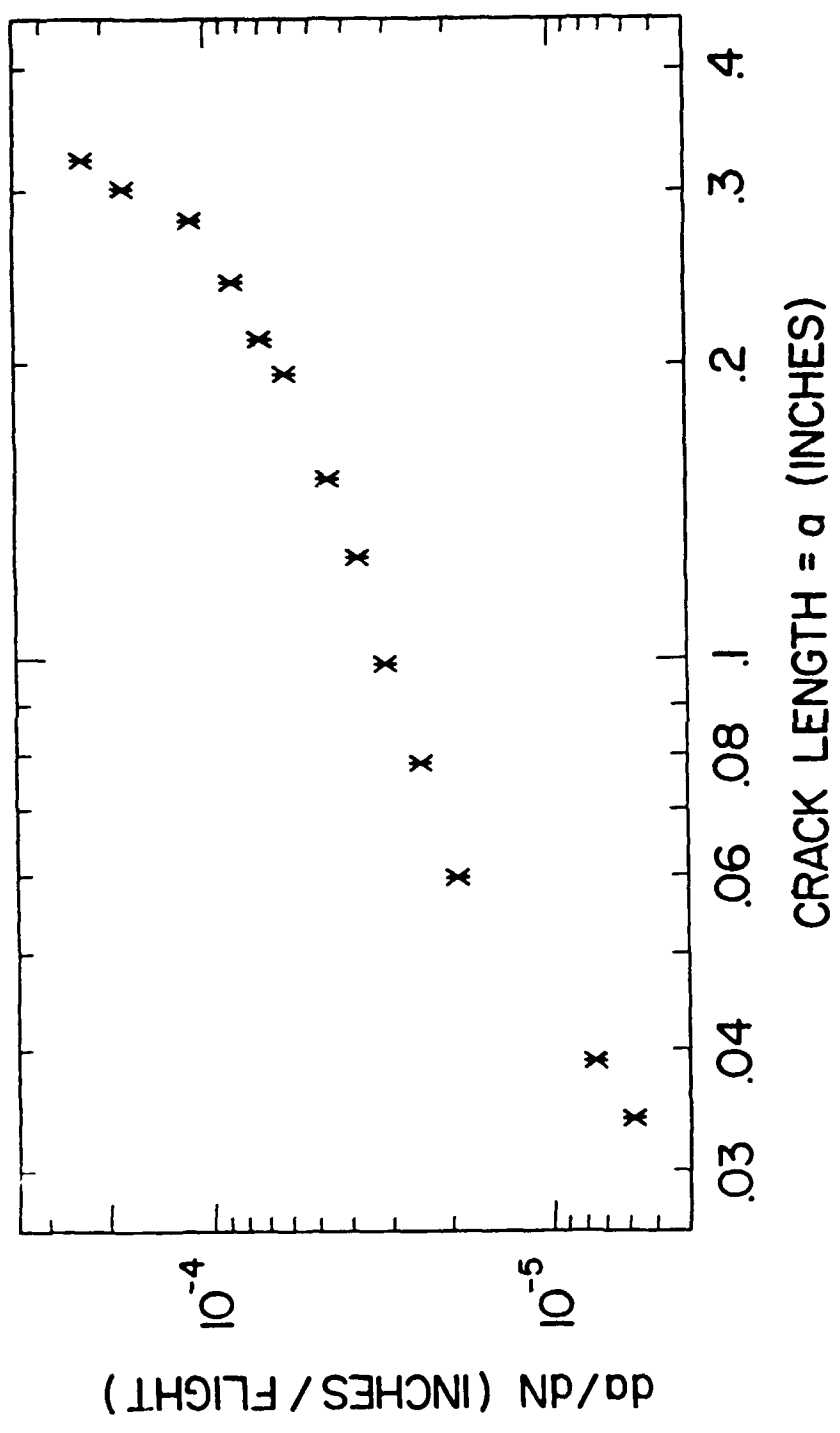


Figure 4.2 Sample Crack Growth Rate versus Crack Length of Lug (Sample S3-A-3 from Ref. 73)

Q and b are the slope and the intercept of the linear equation as plotted on a log-log plot for pooled data sets. Theoretically, Q and b should be estimated from crack growth data of a large sample size. Unfortunately, only the crack growth data for specimen S3-A-3 are available and they are used to determine Q and b using a least squares fit procedure; with the results $Q=7.158(E-4)$, $b=1.393$, and $\sigma_z = 0.2158$. Based on the fiftieth percentile of 35 lugs failed in service (after Ref. 72), the critical flaw size was assumed to be 0.125 inches, see Figure (4.3).

The Weibull-compatible distribution described in Section 3.2 was used to characterize the initial quality. The distribution parameters obtained in the durability analysis for 7000 series aluminum [e.g.35,39] were selected; $\alpha=1.823$, $\phi=1.455$ and $x_u=0.03$. This x_u is a value which might represent the capability of the NDI system. Any flaw large than 0.03 inches would be found through the initial inspection, and the part would be repaired prior to service.

The next assumption involved the levels of inspection. Two levels of NDE systems were considered and the probability of detection parameters, α^* and β^* were used in Equation (2.4). These two levels were taken from reference [39], and are identified in Figure (4.4) as nondestructive inspection (NDI) systems #1 and #2. The respective values for α^* and β^* were 55.28 and 16.4 for #1, and 13.44 and 3.95 for #2. Number 1 is representative of a narrow-banded NDI system which exhibits little statistical uncertainty in flaw

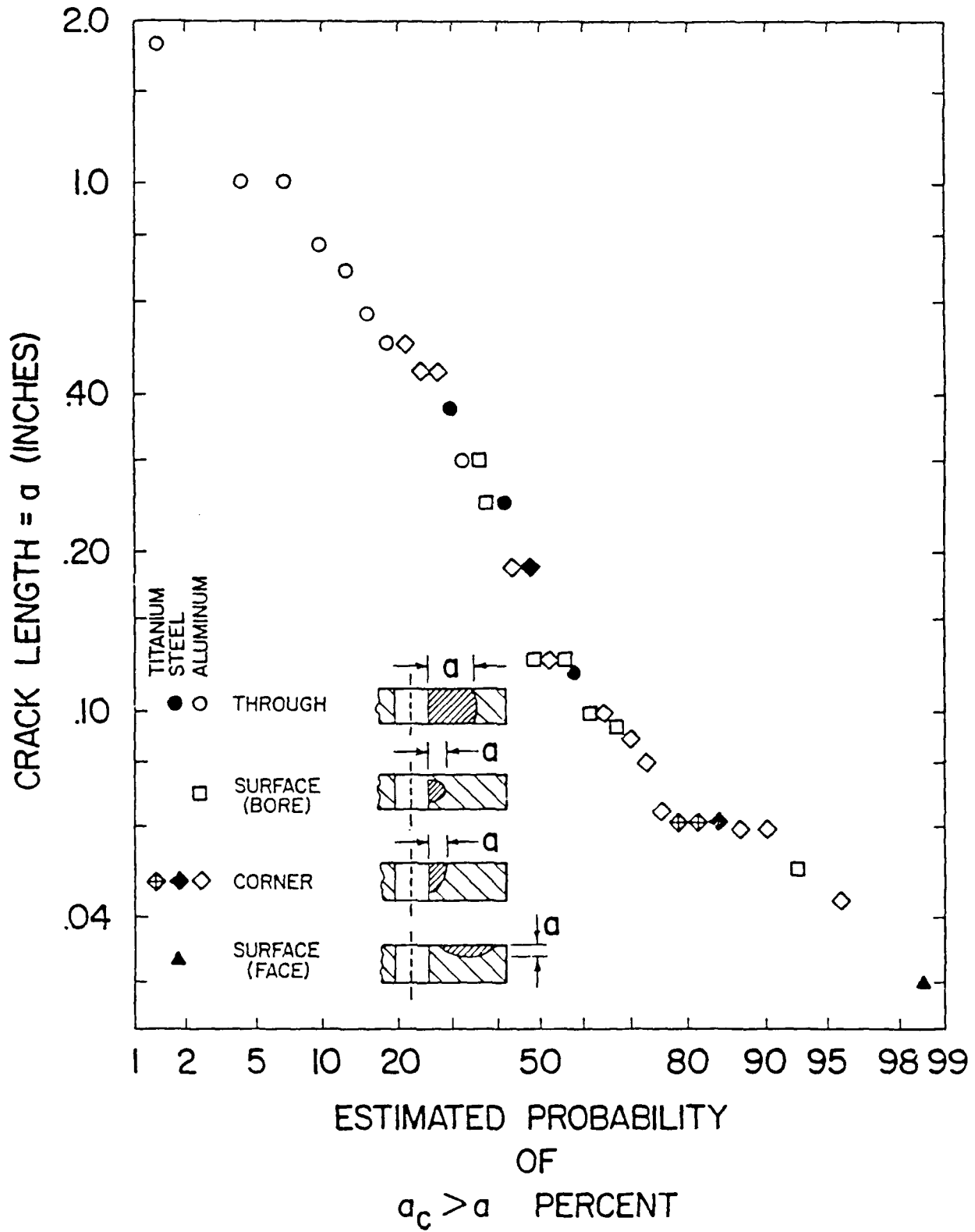


Figure 4.3 Critical Crack Sizes for 35 Service Failed Lugs (after Ref. 72)

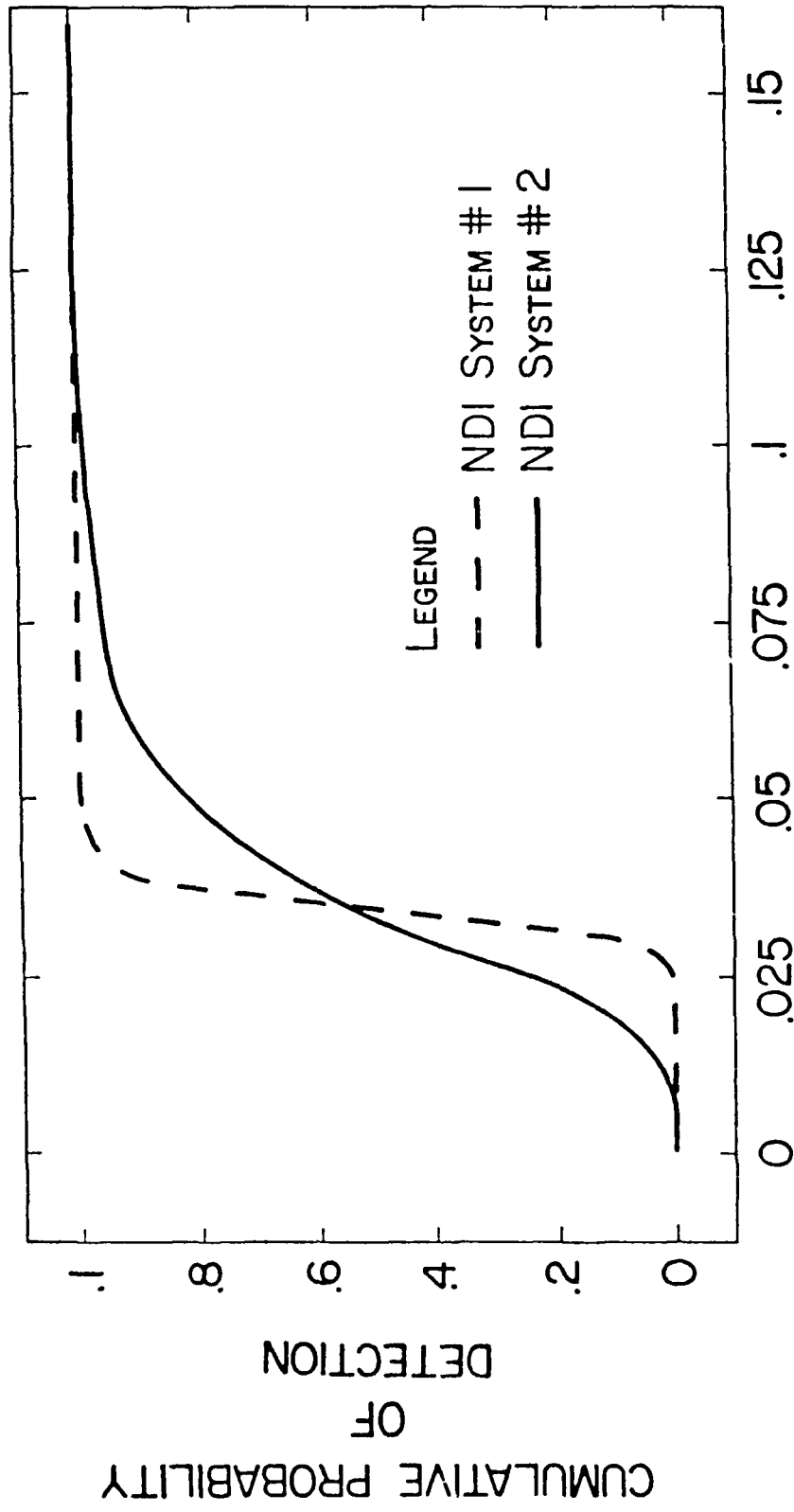


Figure 4.4 Probability of Detection Curves for Two NDI Inspection Systems

detection. This one misses all flaws less than approximately 0.028 inches, and finds all flaws greater than approximately 0.05 inches. NDI system #2 is representative of a wide-banded NDI system, which exhibits significant statistical uncertainty in flaw detection. This one misses all flaws less than approximately 0.01 inch and finds all flaws greater than approximately 0.1 inch. More small flaws, but fewer larger ones are found for #2 than for #1. Results for the probability of failure were investigated using these two NDI systems.

4.1.1 Deterministic Crack Growth Approach

The lug example was analyzed using a deterministic crack growth law, given by equation (4.1). The initial flaw size parameters, the crack growth rate parameters, the NDI system parameters and the critical crack size were identified in the previous section. This analysis is computationally easy, because it involves only one random variable, the initial flaw size, and hence, involves only single integrals for calculating both the probability of repair and the probability of failure.

An inspection interval was desired which resulted in probabilities of failure smaller than 10^{-3} over the service life of the airframe which is approximately 8000 flights. The probability of failure is a function of service flights and inspection reliability.

Figure (4.5) and (4.6) illustrate the probability of failure for no inspection, one, two, and three inspections for NDI systems #1 and #2, respectively. NDI system #1 results in lower probabilities of failure throughout the 8000 flight life, when compared to #2. The probabilities of failure for NDI system #1 are less than 10^{-3} for one inspection, less than 10^{-6} for two inspections, and less than 10^{-9} for three inspections. One inspection at 4000 flights using NDI system #1 would be a possible choice for a force management plan. The probabilities of failure using NDI system #2 are less than 10^{-2} for one inspection and less than 10^{-3} for two and three inspections.

The average number of repairs in a fleet of 100 lugs are shown in Table (4.2) for NDI systems #1 and #2, with one, two, three, and four inspections. NDI system #2 results in finding more flaws than system #1, but the flaws it finds are smaller. It misses some larger ones, leading to higher probabilities of failure.

4.1.2 Stochastic Crack Growth Approach

Next, the variability of crack growth was taken into account in the model. The crack growth model is repeated in the following

$$\frac{da}{df} = Z Q a^b \quad (4.3)$$

where Z is a lognormal random variable with median 1 and standard deviation σ_z . Q and b are the crack growth rate

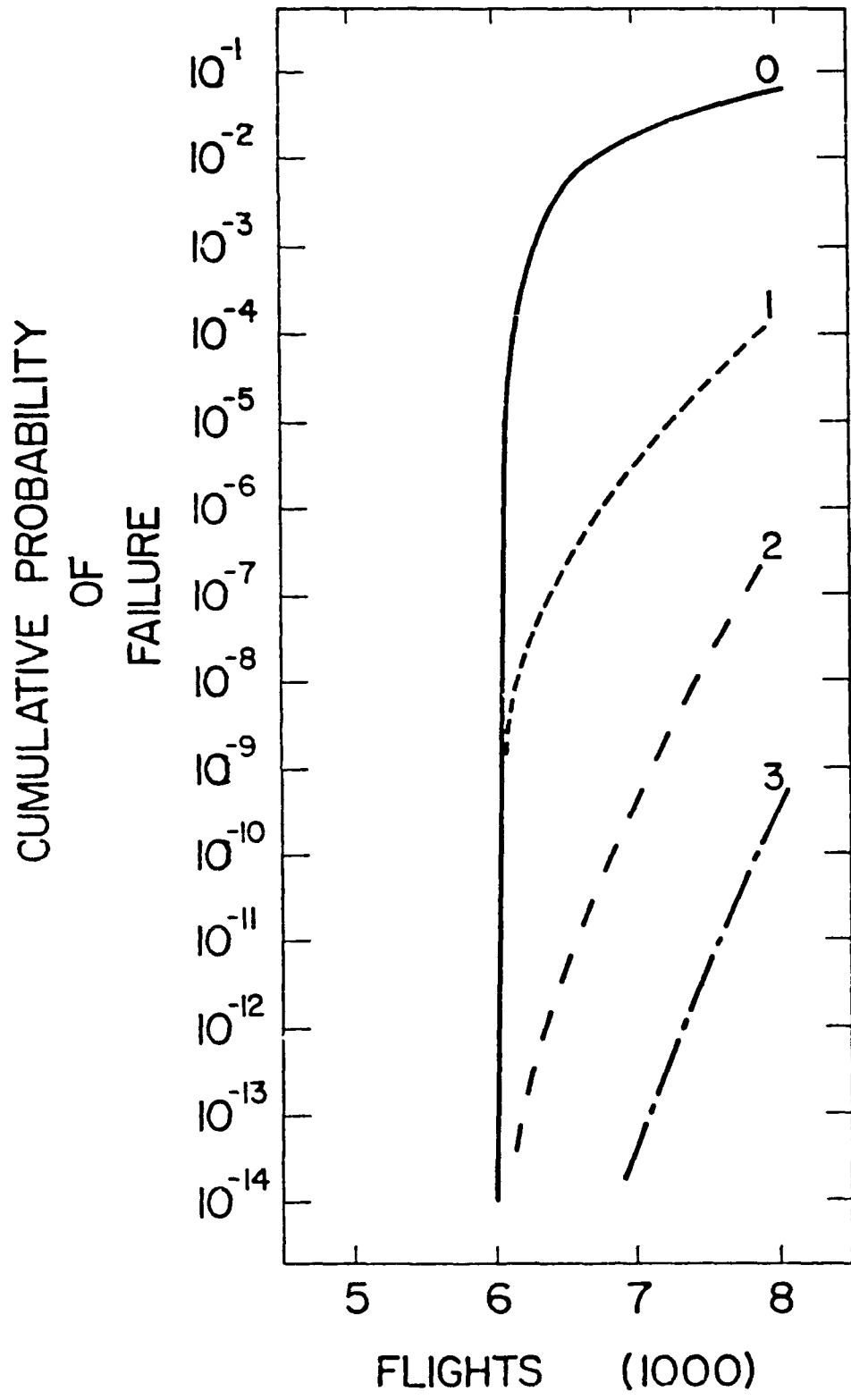


Figure 4.5 The Cumulative Probability of Failure for the Lug Example, with Deterministic Crack Growth Method, NDI System #1, 8000 Flights and 0-3 Inspections

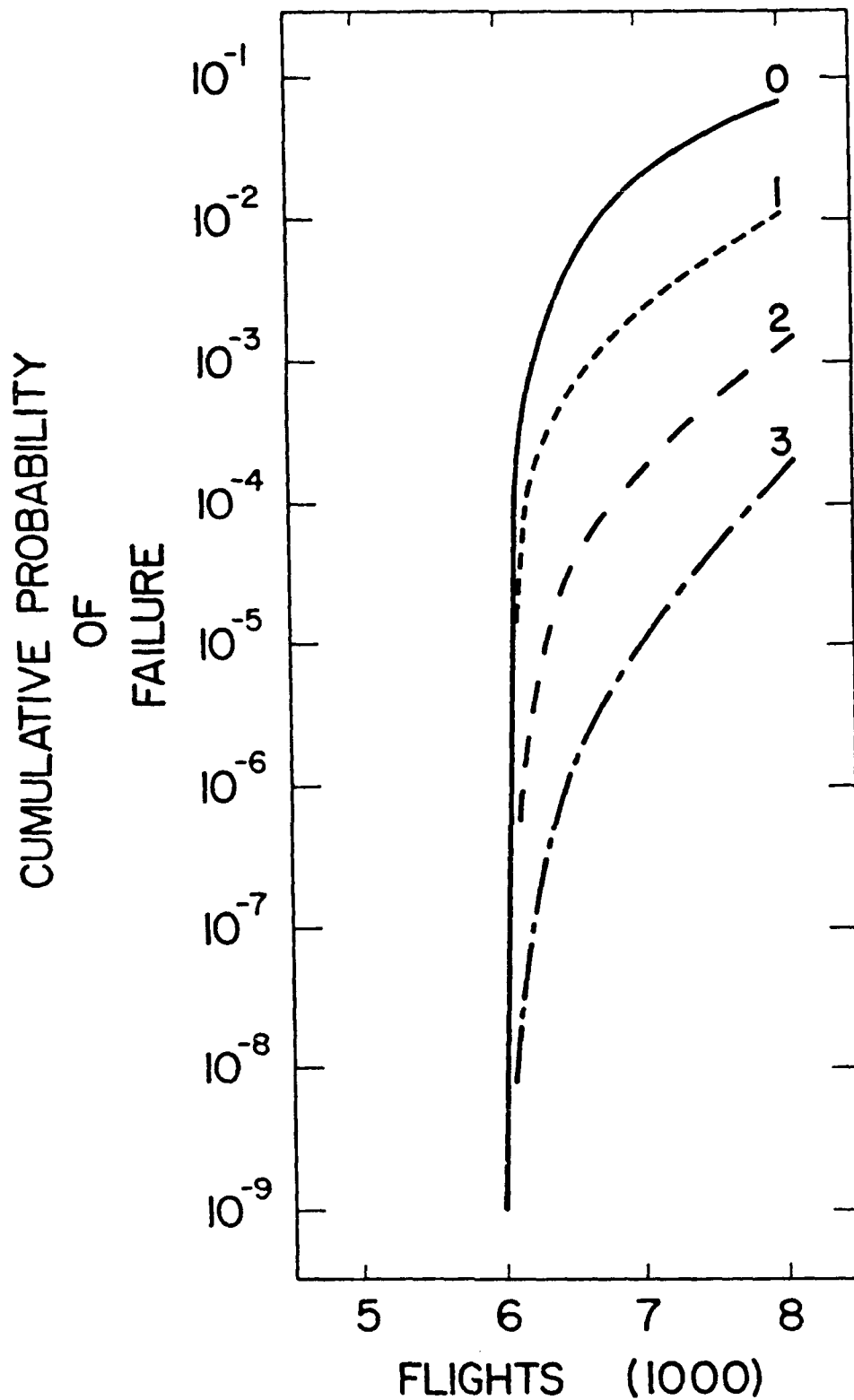


Figure 4.6 The Cumulative Probability of Failure for the Lug Example, with Deterministic Crack Growth Method, NDI System #2, 8000 Flights and 0-3 Inspections

Table 4.2

Average percentage of repair for lug example
using deterministic crack growth analysis

a. NDI System #1

Service Interval	1	2	3	4	Total
4000	14.2				14.2
2667	7.4	14.3			21.7
2000	4.4	10.1	11.2		25.7
1000	2.8	7.4	8.8	9.2	28.2

b. NDI System #2

Service Interval	1	2	3	4	Total
4000	16.4				16.4
2667	10.7	15.2			25.9
2000	8.3	11.5	12.2		32.0
1000	7.0	9.4	10.0	10.1	36.5

parameters as derived from Equation (4.2) and presented in Table (4.1).

A design service life of 4000 flights was selected to represent the life of the lug for reliable performance. The probabilities of failure for no inspection, shown by the solid curve to the left and top, and one, two, three and four inspections, shown by the curves to the right and down, are presented in Figure (4.7) for NDI system #1. The probability of failure rises quickly from 10^{-9} to 10^{-2} as the number of flights increase for no inspection. The probability of failure for one and two inspections is greater than 10^{-3} by the end of the service life. It is less than 10^{-3} for three and four inspections throughout the service life. The increased numbers of isochronal inspections serve to keep the probability of failure from rising as fast as the case of few or no inspections. The corresponding probabilities of failure are presented in Figure (4.8) for NDI system #2. The trend follows NDI system #1; however, inspection and repair serves to lower only slightly the probability of failure at longer lives. The probability of failure is greater than 10^{-3} for one, two and three inspections. It remains less than 10^{-3} for four inspections. For this example, only four or more isochronal inspections will insure adequate levels of safety throughout the expected life.

Next, the required service life was reduced to 2000 flights. The probability of failure with no inspection rose

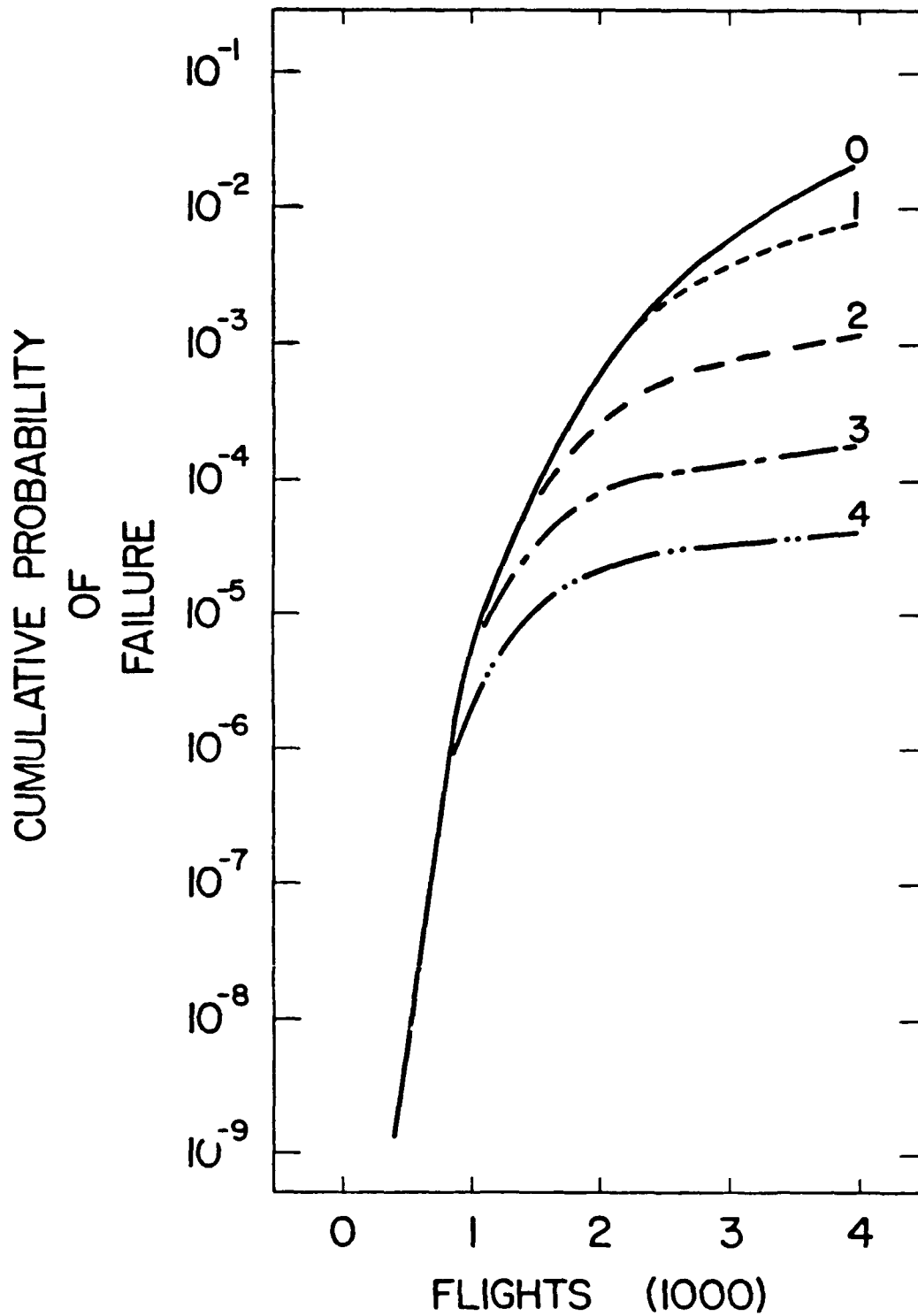


Figure 4.7 The Cumulative Probability of Failure for the Lug Example, with Stochastic Crack Growth Method, NDI System #1, 4000 Flights and 0-4 Inspections

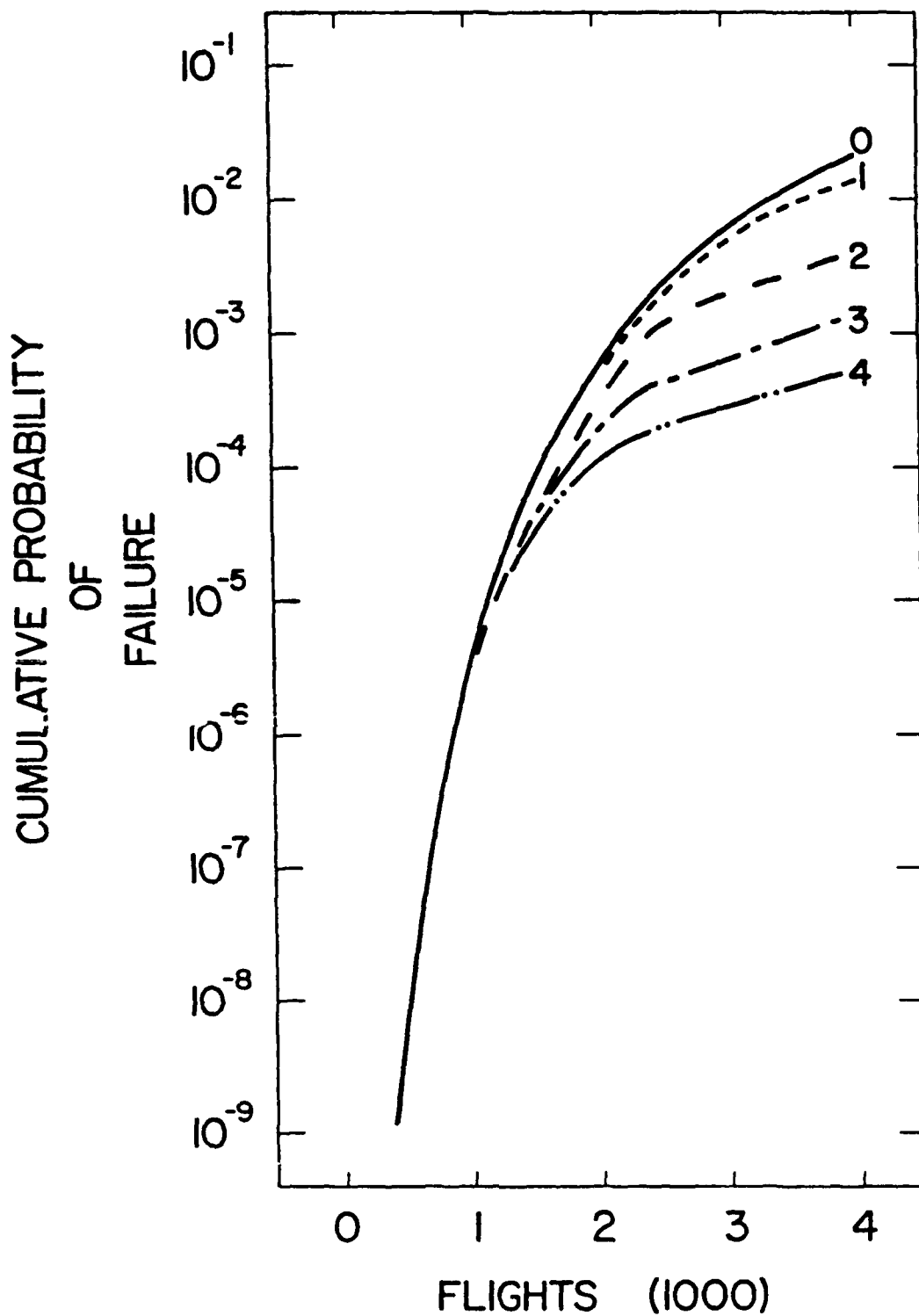


Figure 4.8

The Cumulative Probability of Failure for the Lug Example, with Stochastic Crack Growth Method, NDI System #2, 4000 Flights and 0-4 Inspections

quickly from 10^{-9} to almost 10^{-3} . One possible decision from this result would be to fully replace the part every 2000 flights without inspection. The probabilities of failure were again calculated for the two inspection systems and up to four isochronal inspections. Figures (4.9) and (4.10) illustrate these results for systems #1 and #2, respectively. This time the probabilities of failure for four isochronal inspections remained below 10^{-6} through-out the desired lifetime for NDI system #1, but not for #2. The probabilities of failure for NDI system #1 remain below 10^{-5} for one and two inspections, below 10^{-6} for three inspections and below 10^{-7} for four inspections. The probabilities of failure for NDI system #2 remain below 10^{-3} for one inspection, below 10^{-4} for two and three inspections, and below 10^{-5} for four inspections. Notice, once again, that the probability of failure significantly decreases as the time between inspections decreases.

These results highlight the differences in narrow-banded and wide-banded inspection systems with similar central tendencies. The wide-banded inspection system found more smaller flaws, but missed more larger flaws, leading to a larger probability of failure. The consistency of detection characteristic of the narrow-banded system lead to lower probabilities of failure, compared to the wide-banded system.

The probabilities of repair for these two inspection systems are shown for the four inspection intervals and a

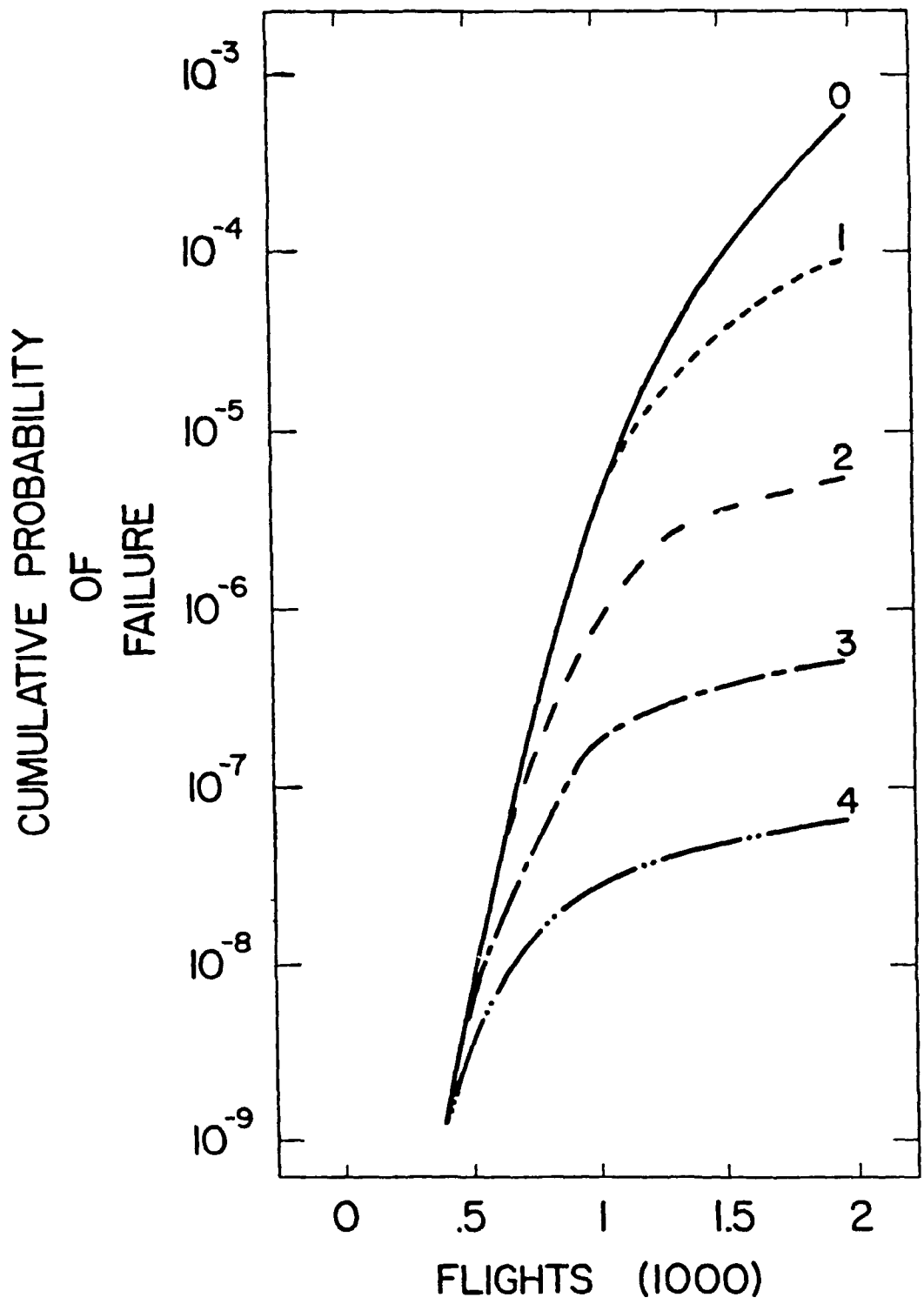


Figure 4.9 The Cumulative Probability of Failure for the Lug Example, with Stochastic Crack Growth Method, NDI System #1, 2000 Flights and 0-4 Inspections

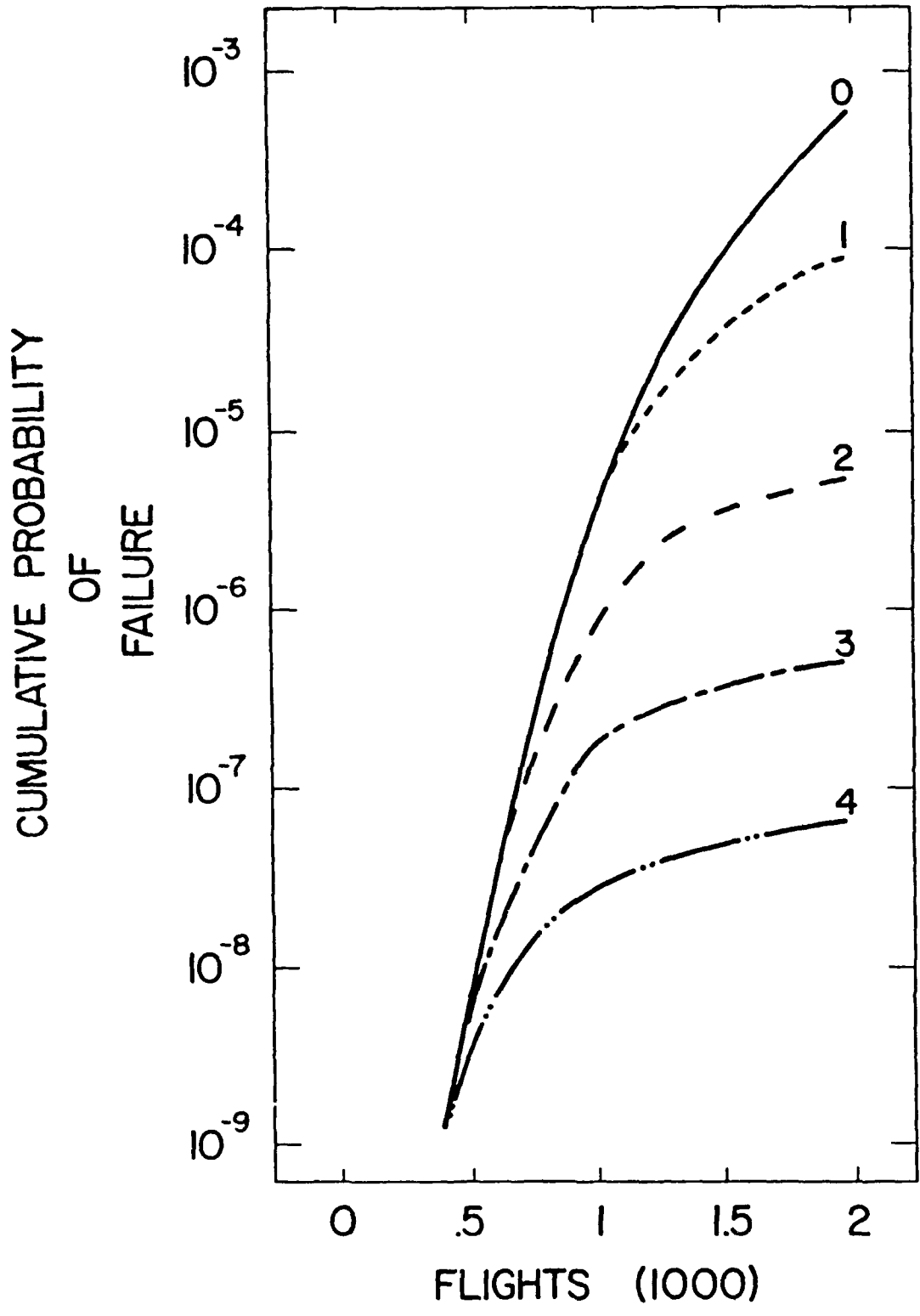


Figure 4.10 The Cumulative Probability of Failure for the Lug Example, with Stochastic Crack Growth Method, NDI Ssystem #2, 2000 Flights, and 0-4 Inspections

life time of 2000 flights in Table (4.3). As can be seen from the table, the use of NDI system #2 results in the detection of more flaws than NDI system #1.

This analysis highlights the significant difference in accounting for a statistical variability of the crack growth rate over a deterministic crack growth rate. It is important to take into account the crack growth rate variability in the life prediction of non-redundant structures.

4.2 Stiffened Panel Example

A stiffened panel is representative of a fail safe structure which is a second category of damage tolerant structures. Structures are defined as fail safe if they contain crack arrest features or they have multiple load paths. Crack arrest structures are designed so that a rapidly growing crack is stopped at a stiffener or other crack arrester before complete failure. The remaining uncracked structure, with assumed continuing damage is designed to carry the load until the cracked section is repaired. A good example of crack arrest structure is the lower part of a transport wing skin or a fuselage. A typical example is a skin-stringer structure, where the primary damage assumed to exist following crack arrest of a rapidly propagating crack is assumed to be two panels of cracked skin plus the broken center stringer [1].

Table 4.3

**Average Percentage of Repair for Lug Example Using
Stochastic Crack Growth**

a. NDI System #1

Service Interval	1	2	3	4	Total
1000	1.55				1.55
667	.62	2.46			3.08
500	.35	1.32	2.46		4.13
400	.24	.81	1.57	2.27	4.89

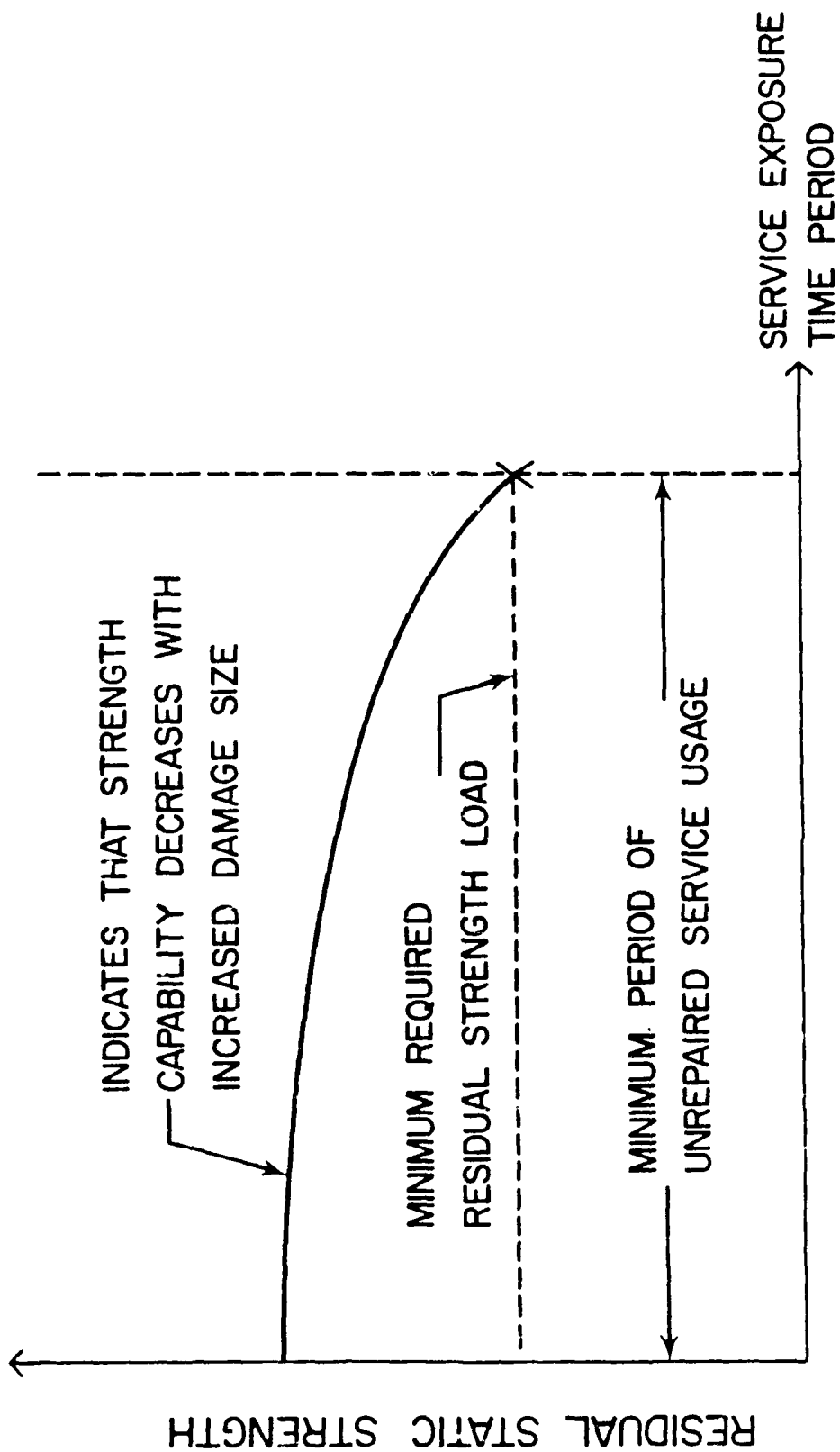
b. NDI System #2

Service Interval	1	2	3	4	Total
1000	6.68				6.68
667	5.30	6.82			12.12
500	4.73	5.57	5.97		16.27
400	4.42	4.92	5.10	5.37	19.81

A multiple load path structure is a redundant structure. When one of the elements fails, the remaining elements carry the load for a specific period of time, such as the time required to have it repaired. Many damage tolerant critical parts are designed with redundancy or with crack arresters, yet few analysts take advantage of this fact when making fatigue life predictions because of the complexity of the analysis. To date, no airframes in the Air Force inventory have been designed or qualified as fail safe structure.

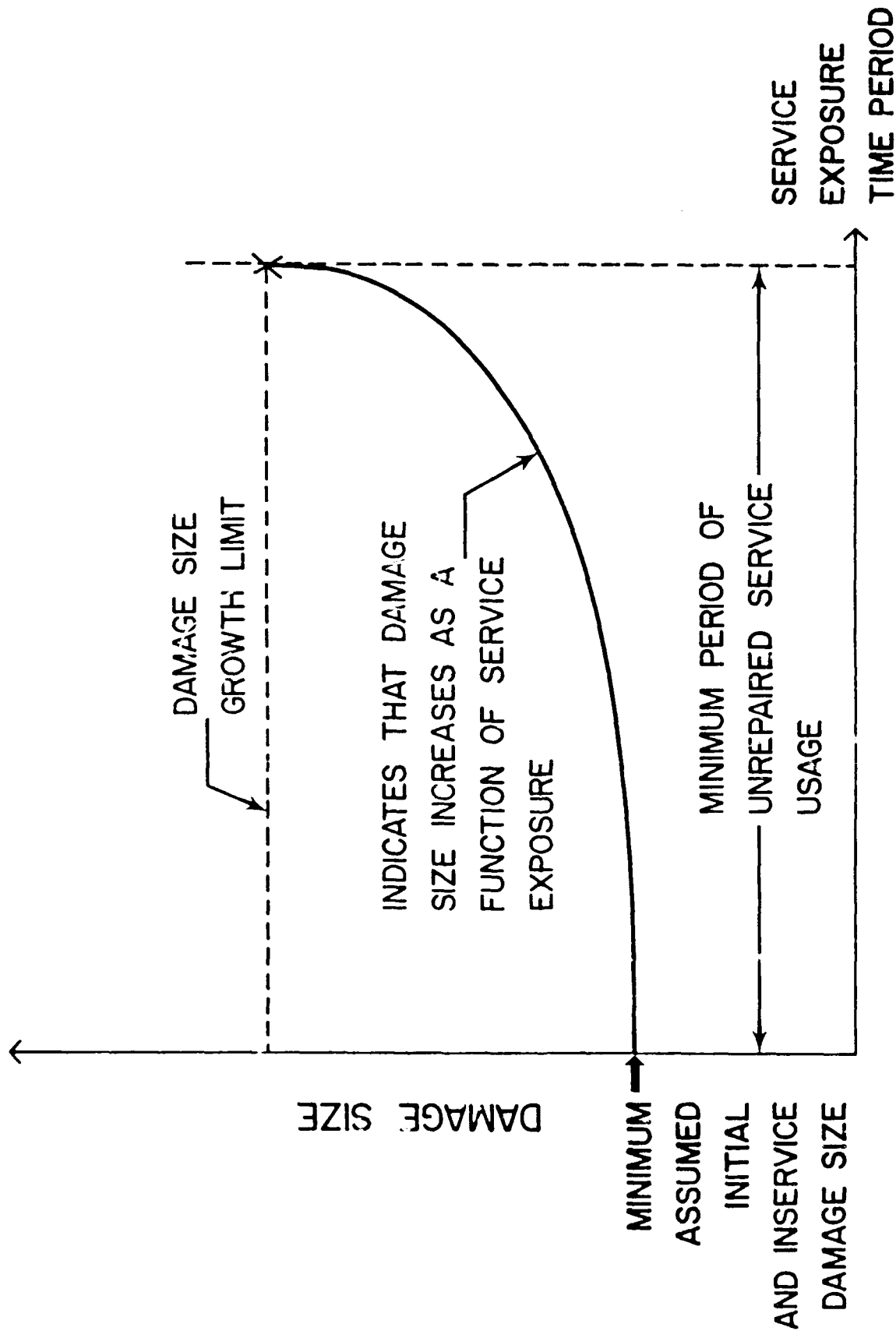
The Air Force damage tolerance requirements [1] state that the safety-of-flight structure must contain the growth of the assumed initial damage for a specified period of service while maintaining a minimum level of residual static strength. This concept is illustrated in Figure (4.11a and 4.11b) [Ref.1]. The safe growth period is also dependent on the scheduled in-service inspection intervals. Safety is assured by assuming the presence of an initial fatigue damage and subsequent growth, and the ability to detect and repair this damage prior to a total loss of the structure throughout a specified service usage interval. The fail-safe requirements are summarized in Table (4.4) for intact and remaining structure, after [Ref.1].

The residual static strength requirement of the remaining structure with depot or base level inspectability is used as the failure criterion for the example presented here. A stiffened panel was selected as representative of a



(a) RESIDUAL STRENGTH DIAGRAM

Figure 4.11a Residual-Strength Requirements for Air Force Damage Tolerance (After Ref. 1)



(b) DAMAGE GROWTH DIAGRAM

Figure 4.11b Damage-Growth Requirements for Air Force Damage Tolerance (After Ref. 1)

Table 4.4

Fail-Safe Structure Requirements from Ref. [1]

INSPECTABILITY	INTACT STRUCTURE		REMAINING STRUCTURE	
	SAFE CRACK GROWTH INTERVAL	RESIDUAL STRENGTH, P _{xx}	SAFE CRACK GROWTH INTERVAL	RESIDUAL STRENGTH, P _{xx}
IN-FLIGHT EVIDENT			RETURN TO BASE	MAXIMUM LOAD IN 100 FLIGHTS
GROUND EVIDENT			ONE FLIGHT	MAXIMUM LOAD IN 100 FLIGHTS
WALK-AROUND VISUAL	ONE LIFETIME	MAXIMUM LOAD IN 20 LIFETIMES	50 FLIGHTS	MAXIMUM LOAD IN 1000 FLIGHTS
SPECIAL VISUAL			2 YEARS	MAXIMUM LOAD IN 50 YEARS
DEPOT OR BASE LEVEL	1/4 LIFETIME	MAXIMUM LOAD IN 5 LIFETIMES	1/2 LIFETIME	MAXIMUM LOAD IN 5 LIFETIMES

• P_{xx} > DESIGN LIMIT LOAD FOR ALL INTACT STRUCTURE & DEPOT OR BASE LEVEL INSPECTABLE REMAINING STRUCTURE

• P_{xx} < 1.2 x MAXIMUM LOAD IN LIFETIME FOR ALL STRUCTURE

• AT TIME OF FAILURE OR ARREST, P_{yy} = 1.15 x P_{xx}

fail-safe structure where analysis was possible. The residual strength, as a function of crack length, was available from the literature for several combinations of stringer spacing and size [68]. An aluminum panel of 0.063 inch thickness, a stringer cross-section area of 0.4113 square inch, a stringer spacing of 8 inches, and a fastener spacing of one inch were selected for study. The stringer was shaped as a Z. This example corresponds in-part to Case 8 in Reference [68], in which the initial damage is represented by a 0.05 inch surface flaw over a broken center stiffener. In this example, the center stiffener is missing. This change in geometry was made so that comparisons of stiffened and unstiffened panels could be made directly. When the broken stiffener is present, it acts to accelerate the crack at the beginning, yielding a much shorter life when compared to a center crack in an unstiffened panel. Without the center stiffener, the beginning growth of the crack is the same for both the stiffened and unstiffened cases, so the advantages of stiffening can be observed. The stiffened panel is illustrated in Figure (4.12).

As explained in Section 3.1, the stress intensity factor, ΔK , in a redundant, built-up structure can be expressed as

$$\Delta K = \Delta \sigma \sqrt{\pi a} \beta(a) \quad (4.4)$$

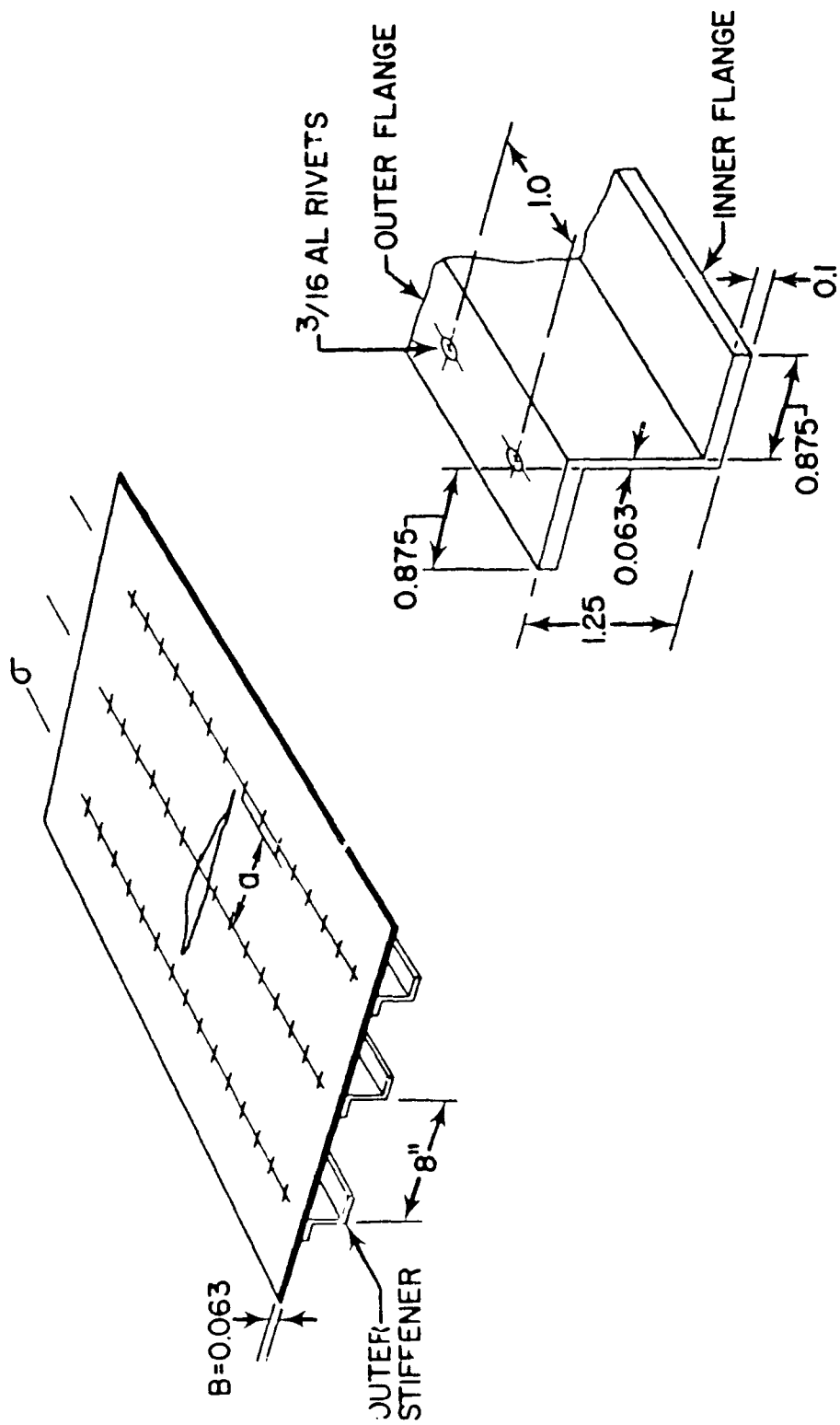


Figure 4.12 Geometry of the Stiffened Panel

where $\beta(a)$ is a correction factor due to all geometrical effects. It is a function of crack length and also includes the following geometrical size effects:

- * Stiffener spacing
- * Stiffener section properties - area, inertia, neutral axis location
- * Stiffener elastic or plastic material properties
- * Fastener displacement, either linear or nonlinear
- * Skin thickness.

Swift [68] calculated $\beta(a)$ using the displacement compatibility method. The values of crack length, "a", $\beta(a)$, and residual strength of the plate and stiffener for the eight inch stiffener spacing are presented in Table (4.5). The relationship between residual strength of the plate and crack length is illustrated in Figure (4.13) for the same geometry. The relationship between the residual strength of the plate and stiffener system and crack length in the plate is illustrated in Figure (4.14). Here, the initial damage assumptions are represented by a 0.05 inch surface flaw in the center of the plate, and a 0.05 inch through flaw in the outer stiffeners.

These figures are a typical part of a damage tolerance-residual strength diagram. The part relating flight hours to crack length is not shown here. These figures clearly show the effect of the presence of the stiffener on the residual strength of the skin, as the crack tip approaches the stiffener, thereby, lowering ΔK , the

Table 4.5

Crack Length, $\beta(a)$ and Residual Strength for an 8 Inch Stiffener Spacing and Stiffener Area of 0.4113 Inch².

Crack Length, a	$\beta(a)$	Residual Strength		
		Stiffened Plate	Unstiffened Plate	Stiffener
0.25	2.1827	62.03 ksi	156.35 ksi	78.76 ksi
0.50	2.0647	46.37	110.56	78.57
0.75	1.9363	40.37	90.27	78.34
1.00	1.8254	37.09	78.18	78.02
2.00	1.5560	30.97	55.28	76.23
3.00	1.4175	27.58	45.14	73.65
4.00	1.3252	25.54	39.09	70.22
5.00	1.2501	24.22	34.96	65.73
6.00	1.1763	23.50	31.92	59.89
7.00	1.0837	23.61	29.55	52.24
8.00	0.849	26.75	27.64	42.43
9.00	0.7102	31.78	26.06	35.18
10.00	0.6682	32.04	24.72	31.33
11.00	0.6571	31.07	23.56	28.84

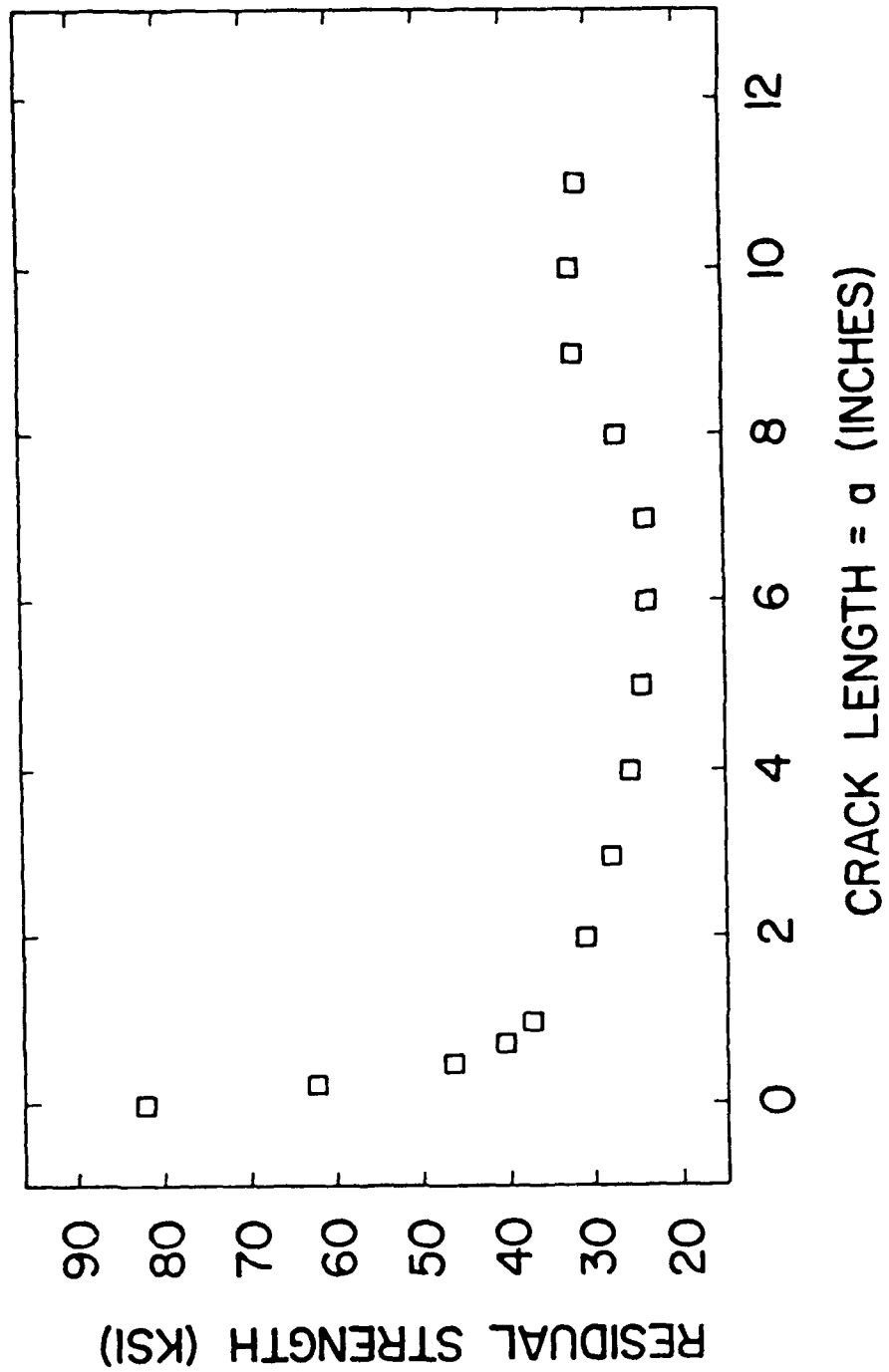


Figure 4.13 Residual Strength of a Plate as a Function of Crack Length for a Center Cracked Panel with Broken Center Stiffener

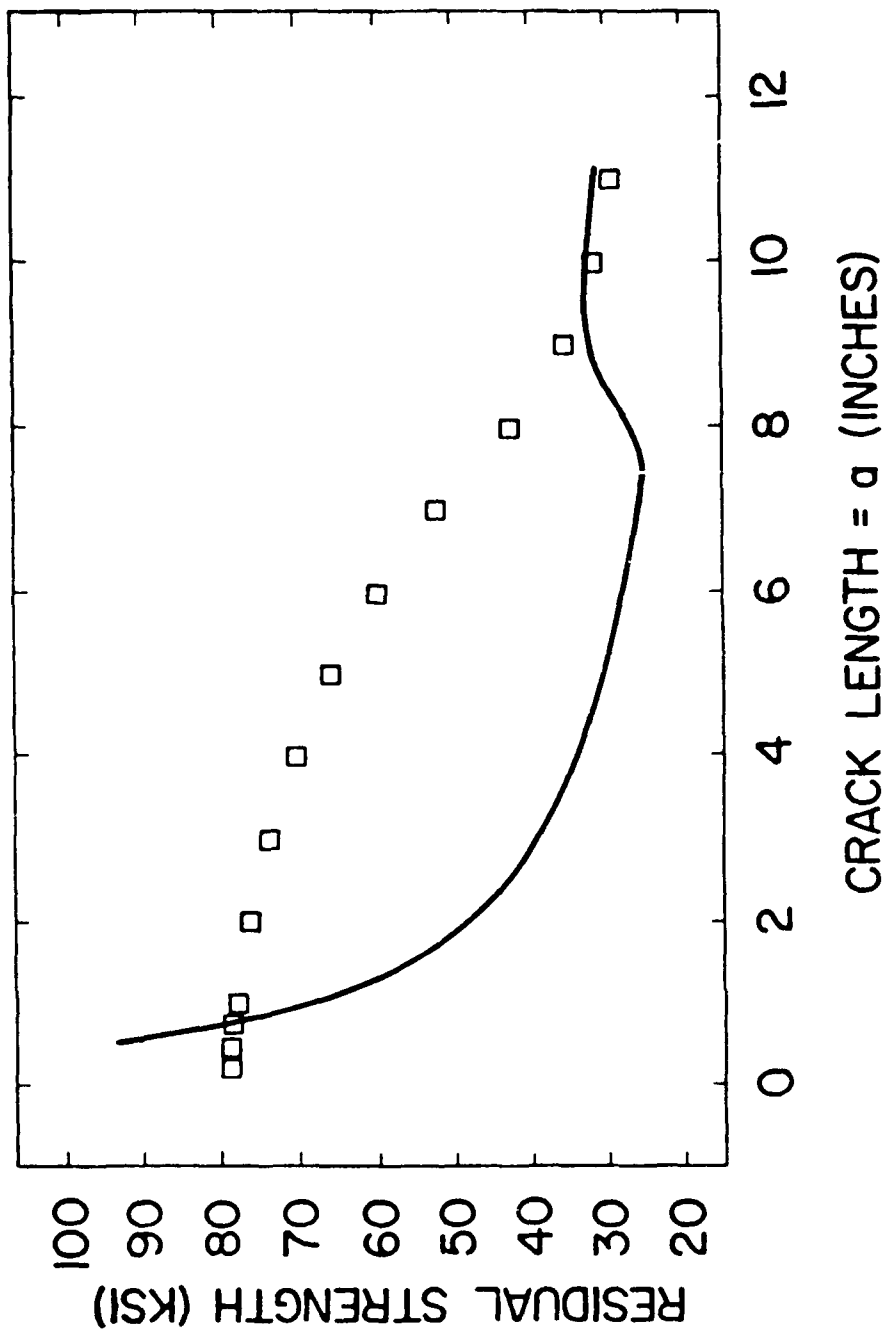


Figure 4.14 Residual strength of a stiffener and a plate as a function of crack length for a center cracked panel; stiffener spacing = 8 inches, $K_C=120$ ksi·in., $F_{tu}=82$ ksi

driving force of the crack. This phenomenon is reflected numerically in the values of the residual strength of the panel, as reported in Table (4.5), column 3. (after Ref. 68). As the crack tip approaches the stiffener, the residual strength actually increases in the panel.

Fast crack growth occurs when the stress exceeds the residual strength of the plate. The residual strength of the plate is represented by the solid line in Figure (4.14). The propagating crack will be arrested at the stiffener, if the applied stress is less than the residual strength of the plate and stiffener system.

Failure will occur when the residual strength of the plate-stiffener system is unable to resist the applied stress. This level of resistance is represented by the squares in Figure (4.14). The residual strength of the panel was calculated directly from Equation (4.5) for crack lengths significantly less than the stiffener spacing:

$$R(a) = \frac{K_C}{\sqrt{\pi a}} \quad (4.5)$$

where $R(a)$ is the residual strength of the plate, which is a function of the crack length a , K_C is the fracture toughness of the plate, and a is the crack length in the plate.

When the crack tip approaches the stiffener and $\beta(a)$ becomes less than one, Equation (4.5) was modified by $\beta(a)$ for the residual strength of the plate, R :

$$R(a) = \frac{K_c}{\sqrt{\pi a} \beta(a)} \quad (4.6)$$

The tabulated residual strength values at discrete values of crack length can be used to define failure. The probability of failure can be defined as the probability that the residual strength will fall below the required residual strength associated with resisting P_{xx} , the load calculated from the damage tolerant design requirements. The residual strength $R[a(t)]$ can be defined mathematically as a function of the crack size "a" as $R[a(t)] = g(a)$, where g is a monotonic function. Then crack size "a" can be expressed in terms of the residual strength as

$$a(t) = g^{-1}[R(a(t))] \quad (4.7)$$

where g^{-1} is the inverse of the g function. The function can be partitioned and evaluated in segments. Then, the probability of failure, P_f , can be defined as:

$$\begin{aligned} P_f &= P\{P_{xx} > R(a(t))\} \\ &= P\{P_{xx} > g[a(t)]\} \\ &= 1 - P\{a(t) < g^{-1}(P_{xx})\} \end{aligned} \quad (4.8)$$

or,

$$P_f = 1 - F_{a(t)}[g^{-1}(P_{xx})] \quad (4.9)$$

in which $g^{-1}(P_{xx})$ is nothing but the critical crack size associated with the load P_{xx} . If such a critical crack size is denoted by a_{xx} , i.e., $g^{-1}(P_{xx}) = a_{xx}$, then the probability of failure of a panel in the n th service

interval $[(n-\tau), n\tau]$ is given by the probability of failure of a panel in the n th service interval

$$P_f(n\tau) = \int_{a_{xx}}^{\infty} f_{a(n\tau)}(x) dx \quad (4.10)$$

An example for the calculation of the probability of repair and failure for a redundant lower wing skin of a transport aircraft will now be presented. The P_{xx} load must be used which reflects the maximum average internal member load that will occur once in M times the inspection interval according to Mil-A-87221 [1]. P_{xx} should be at least equal to the design limit load, but need not be greater than 1.2 times the maximum load in one lifetime, if P_{xx} is greater than the design limit load. The base level inspection is typically performed at 1/4 of the lifetime and $M=20$. The walk around visual inspection is performed once every ten flights and $M=100$.

P_{xx} can be found from exceedance curves, such as presented in Figure (4.15) for a component in the lower wing skin of a medium range transport aircraft. Both the plate and stiffener exceedance curves are shown in the same figure. Once P_{xx} has been selected, the critical crack length is found from the P_{xx} versus a relationship, either Equation (4.5) or (4.6).

The equation for the probability of detection, $F_D(x)$ (2.9), was modified to reflect a visual NDI system, which was useful for longer critical crack sizes. The parameters were adjusted to reflect a detection system, where cracks

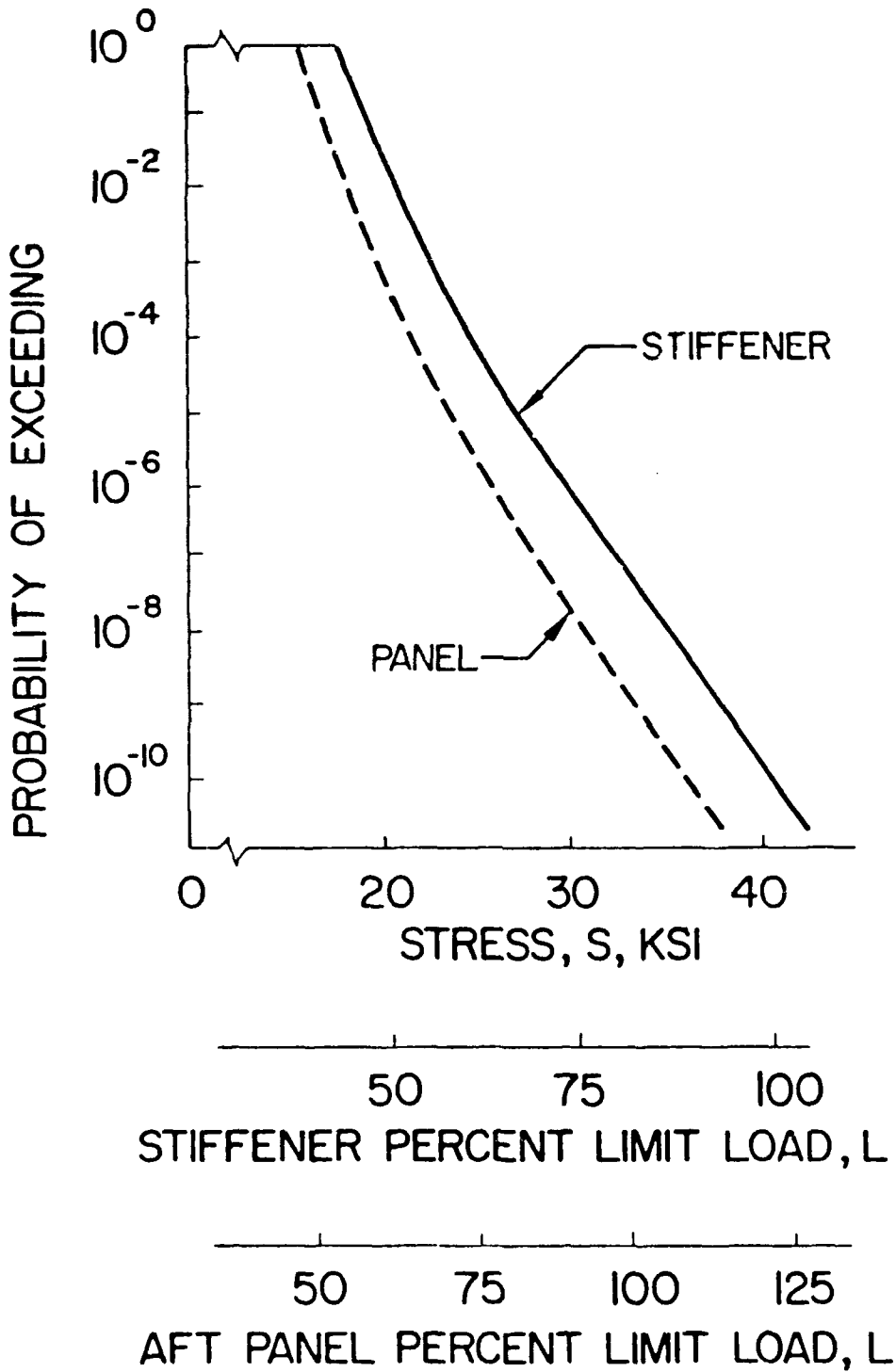


Figure 4.15

The Stress Exceedance Curve for a Lower Aft Panel and Stiffener

could be detected when they reached approximately two inches in length. The parameters, $\alpha^* = -9.159$, and $\beta^* = 16.4$ were used in Equation (2.9) to reflect this level of inspection. The function is plotted in Figure (4.16). The service life of such a stiffened panel system is 60,000 flight hours.

4.2.1 Slow Crack Growth Approach

Suppose the fail-safe design feature of the panel-stiffener system is disregarded. In other words, the stiffener's ability to pick up loads from the plate as the crack approaches the stiffener is neglected, so that the plate is considered to be unstiffened. Therefore, the slow crack growth approach should be used and the critical crack size, a_{xx} , was defined at the point where the residual strength in the plate fell below P_{xx} as calculated from Equation (4.5) and Figure (4.17). For this example, the critical crack size was equal to 6.061 inches, corresponding to a design limit stress of 27.5 ksi. The maximum expected stress in the plate, as given by the exceedance curve in Figure (4.15), was 22 ksi in 60,000 flight hours. Since this stress is less than the design limit stress, the design limit stress was used.

4.2.1.1 Deterministic Crack Growth Approach

The equivalent initial flaw size distribution parameters, NDI system parameters and critical flaw sizes are summarized in Table (4.6). The deterministic crack

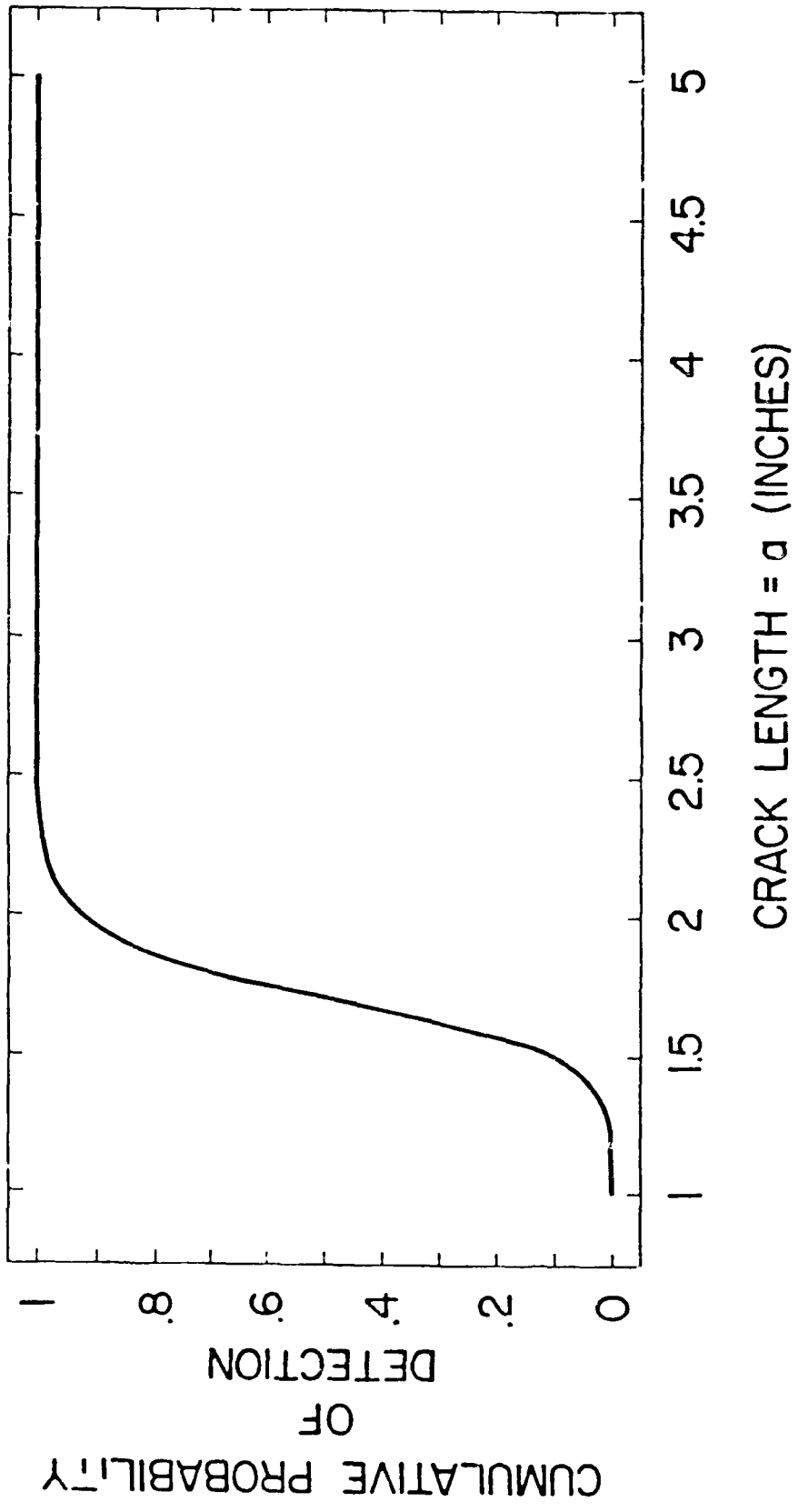


Figure 4.16 The Probability of Detection Curve for a Visual Inspection

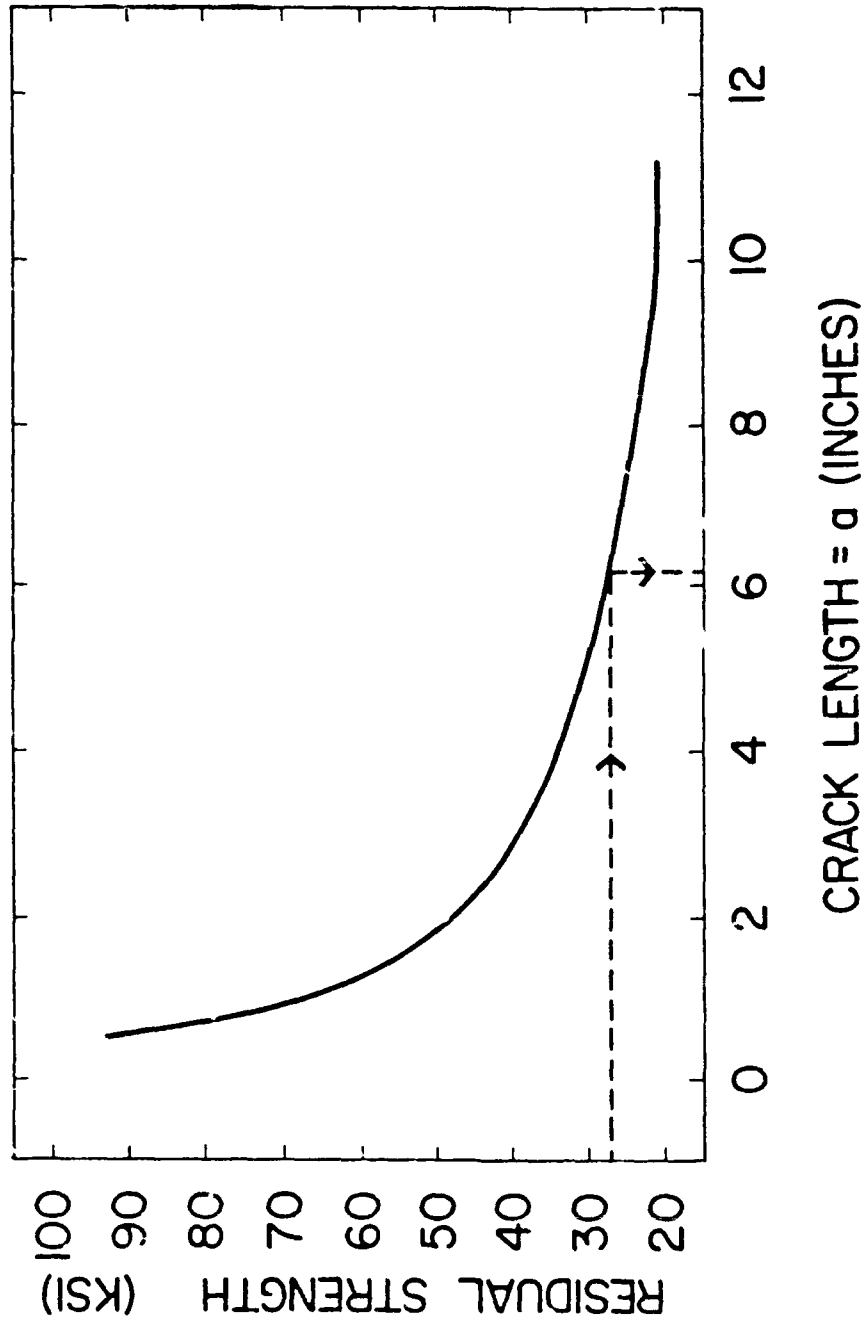


Figure 4.17 Residual Strength as a Function of Crack Length for an Unstiffened Panel, $K_C = 120 \text{ ksi}/\text{in.}$

Table 4.6

Parameters for the Stiffened Panel Example

$$Q = 1.504E-4$$

$$b = 1.10$$

$$\sigma_z = .1267$$

$$a_{cr} = 6.061 \text{ inches for slow crack growth approach}$$

$$a_{xx} = 8.142 \text{ inches for fail safe approach}$$

Initial Flaw Size Parameters

$$\alpha = 1.823$$

$$\phi = 1.928$$

$$x_u = 0.03$$

NDI Parameters

System #1

Visual

$$\alpha^* = 55.28$$

$$\beta^* = 16.4$$

$$\alpha^* = -9.159$$

$$\beta^* = 16.4$$

growth rate model presented in Eq. (4.1) was used and crack growth rate parameters, $Q=1.504E-4$ and $b=1.10$ were selected for the purpose of illustration.

The results of the deterministic crack growth analysis are presented in Figure (4.18). The solid curve at the top of the figure, as denoted by zero, represents the probability of failure without inspection maintenance. The critical crack size was 6.061 inches. The next curve down in Figure (4.18) represents the probability of failure for four isochronal visual inspections at 12,000 flight hour service intervals, as denoted by 4. The next curve represents the probability of failure for five isochronal visual inspections, occurring at 10,000 flight hour service intervals, and denoted by 5. The probability of failure for one, two and three isochronal visual inspections differed little from the no inspection case, and were therefore not included on the figure.

These probabilities of failure may be too high to be acceptable for a primary structure. A visual inspection alone will not ensure safety. A more reliable NDI system is necessary to bring the probabilities of failure down to an acceptable level. NDI system #1 was used and the results yielded a probability of failure of $2.378E-8$ at 60,000 flight hours for one inspection at 30,000 flight hours. More inspections resulted in no probability of failure, because of the upper bound of the Weibull compatible distribution for the equivalent initial flaw size, as well

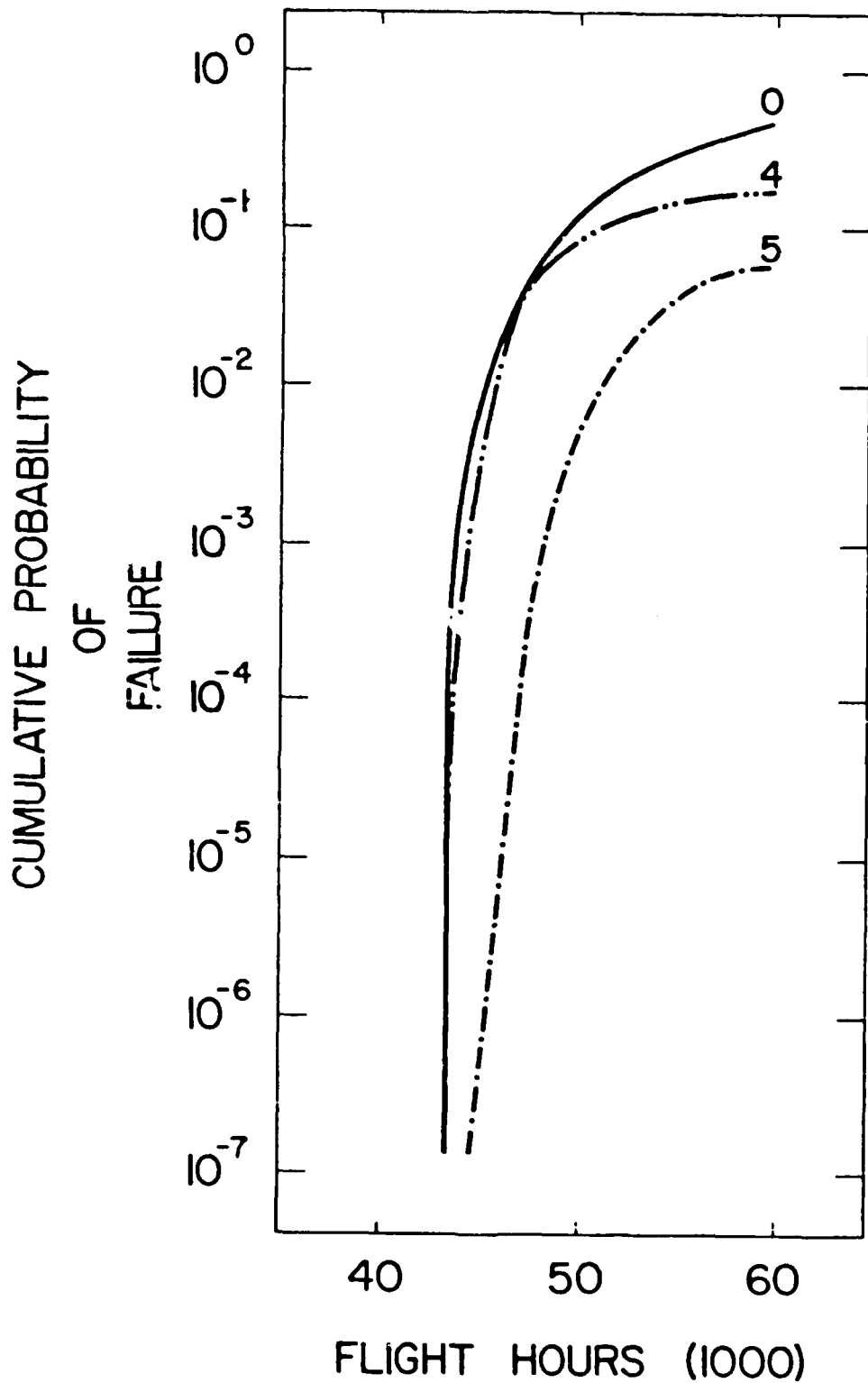


Figure 4.18 The Cumulative Probability of Failure for an Unstiffened Panel, with $a_{xx}=6.061$ inches, the Deterministic Crack Growth Method and 0, 4 and 5 Visual Inspections

as the nature of the deterministic crack growth. These examples illustrate the importance of using the proper NDI system for the force management plan.

The probabilities of detection and repair are shown in Tables (4.7a) and 4.7b) for the NDI system #1 and the visual inspections. The NDI system finds more flaws than the visual inspection, and the more often the inspection, the more total flaws are found.

4.2.1.2 Stochastic Crack Growth Approach

The slow crack growth example was rerun, using the stochastic crack growth approach as represented by Equation (4.5). The probability of failure for no inspections and five visual inspections is shown in Figure (4.19). The results for five visual inspections is very close to that for no inspections, indicating that very little gain in safety is seen by relying on a visual inspection. However, with the application of NDI system #1, the probability of failure reduces significantly as illustrated in Figure 4.20), which shows the results for one to five inspections. The difference between the two approaches presented above is that the stochastic crack growth approach results in higher probabilities of failure; as expected, because of the possibility of fast crack growth. The probabilities of repair are presented in Tables (4.8a) and (4.8b) for both visual and NDI system #1 inspections. As expected, the NDI

Table 4.7

Average Percentage of Repair for Stiffened Panel Example
 Using Deterministic Crack Growth Analysis
 and $a_{xx} = 6.061$ Inches

a. Visual Inspection

Service Interval	1	2	3	4	5	Total
30,000	1.60E-6					1.6E-6
20,000	2.55E-15	7.00				7.0
15,000	2.53E-19	1.60E-6	20.9			20.9
12,000	1.22E-21	1.18E-12	0.5	26.1		26.6
10,000	3.59E-23	2.55E-15	1.6E-6	7.0	27.8	34.8

b. NDI System #1

Service Interval	1	2	3	4	5	Total
30,000	77.4					77.5
20,000	51.9	56.0				117.9
15,000	35.0	54.7	51.0			140.7
12,000	24.4	45.2	43.7	26.1		156.8
10,000	17.7	37.3	38.2	37.4	37.4	168.8

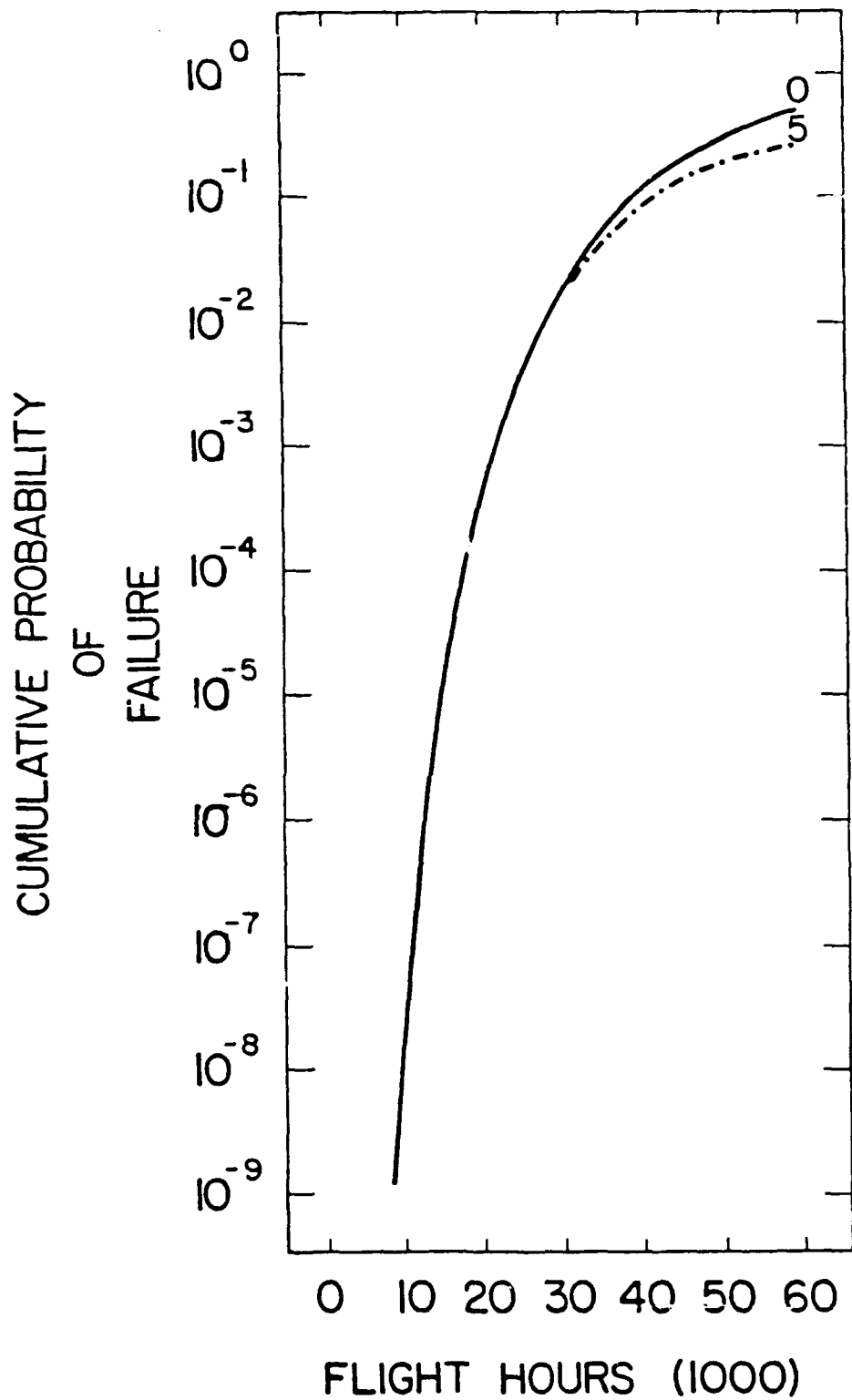


Figure 4.19

The Cumulative Probability of Failure for an Unstiffened Panel, with $a_{xx} = 6.061$ inches, the Stochastic Crack Growth Method and 0 and 5 Visual Inspections

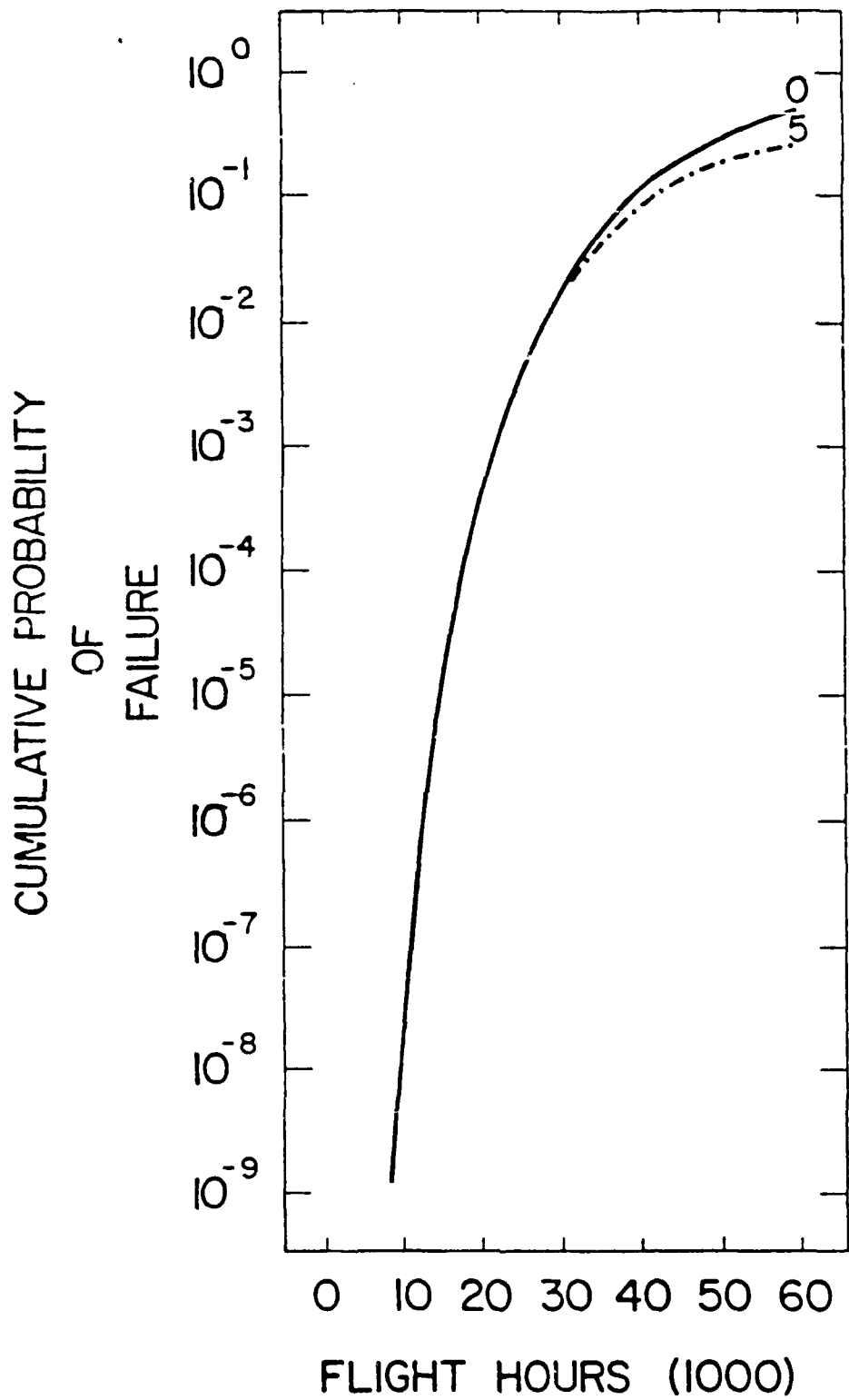


Figure 4.20

The Cumulative Probability of Failure for an Unstiffened Panel, with $a_{xx} = 6.061$ inches, the Stochastic Crack Growth Method, 0-5 Inspections with NDI System #1

Table 4.8

Average Percentage of Repair for the Stiffened Panel Example
Using Stochastic Crack Growth and $a_{xx} = 6.061$ Inches

a. Visual Inspection

Service Interval	1	2	3	4	5	Total
30,000	6.0					6.0
20,000	.32	18.9				19.2
15,000	.15E-1	6.0	24.7			30.7
12,000	.77E-3	1.4	13.5	27.5		52.4
10,000	.46E-4	.31	6.0	19.0	28.8	53.1

b. NDI System #1

Service Interval	1	2	3	4	5	Total
30,000	10.0					10.0
20,000	65.4	93.3				158.7
15,000	43.3	70.1	45.4			158.8
12,000	30.0	55.4	42.0	41.4		178.8
10,000	21.6	44.9	38.5	39.1	24.2	158.3

system #1 inspection finds more flaws than the visual inspection.

4.2.2 Crack Arrest Approach

Next, the stiffened panel example was rerun taking advantage of the presence of the stiffener. In this scenario, the crack will grow through the plate and arrest over the stiffener. The critical crack size, a_{xx} , in this case is approximately equal to, or larger than, the stiffener spacing, so the visual NDI system seemed appropriate to investigate. As the flaw in the plate grows, the residual strength of the stiffener degrades with flight hours and failure is dependent on the residual strength of the stiffener as its proportion of the load is increased. In other words, failure occurs when the crack grows throughout the plate and the residual strength of the stiffener is exceeded by the applied stress. Thus, the probability of failure is equal to the probability of the crack size exceeding 8.142 inches multiplied by the probability of the stress in the stiffener exceeding 41 KSI. The probability of stress exceedance for the stiffener was found to be 1.0×10^{-10} per flight from the stress exceedance curve of Fig. (4.15). This value was multiplied by the number of flights in the service interval to obtain the probability of stress exceedance for the stiffener in that service interval.

4 2.2.1 Deterministic Crack Growth Approach

4.2.2.1.1 General Master Curve Approach

The general master curve approach was considered for the crack arrest case because it could account for the decreasing crack growth rate as the crack approached the stiffener. The difference between the general master curve approach which accounts for arresting crack growth and the special case which does not, i.e., $\beta(a)=1$, are presented in Figure (4.21). The solid curve was calculated directly from Equation (3.7), whereas, the dotted curve represents the numerical integration of Equation (3.24) using the cubic spline interpolation of the crack length and β values from Table (4.5). Note that there is no difference in crack growth between the two models until the crack length reaches approximately eight inches, the stiffener spacing. As a result, the general master curve approach was not pursued in any detail, other than to check results of the special case in which $\beta(a)$ is set to be unity.

4.2.2.1.2 Special Case $\beta(a)=1$

The problem was formulated by considering that fatigue crack growth follows Eq. (3.7) until the crack size reaches 8.0 inches, at which point the crack was arrested. After that failure of the system occurred when the residual strength of the stiffener was exceeded.

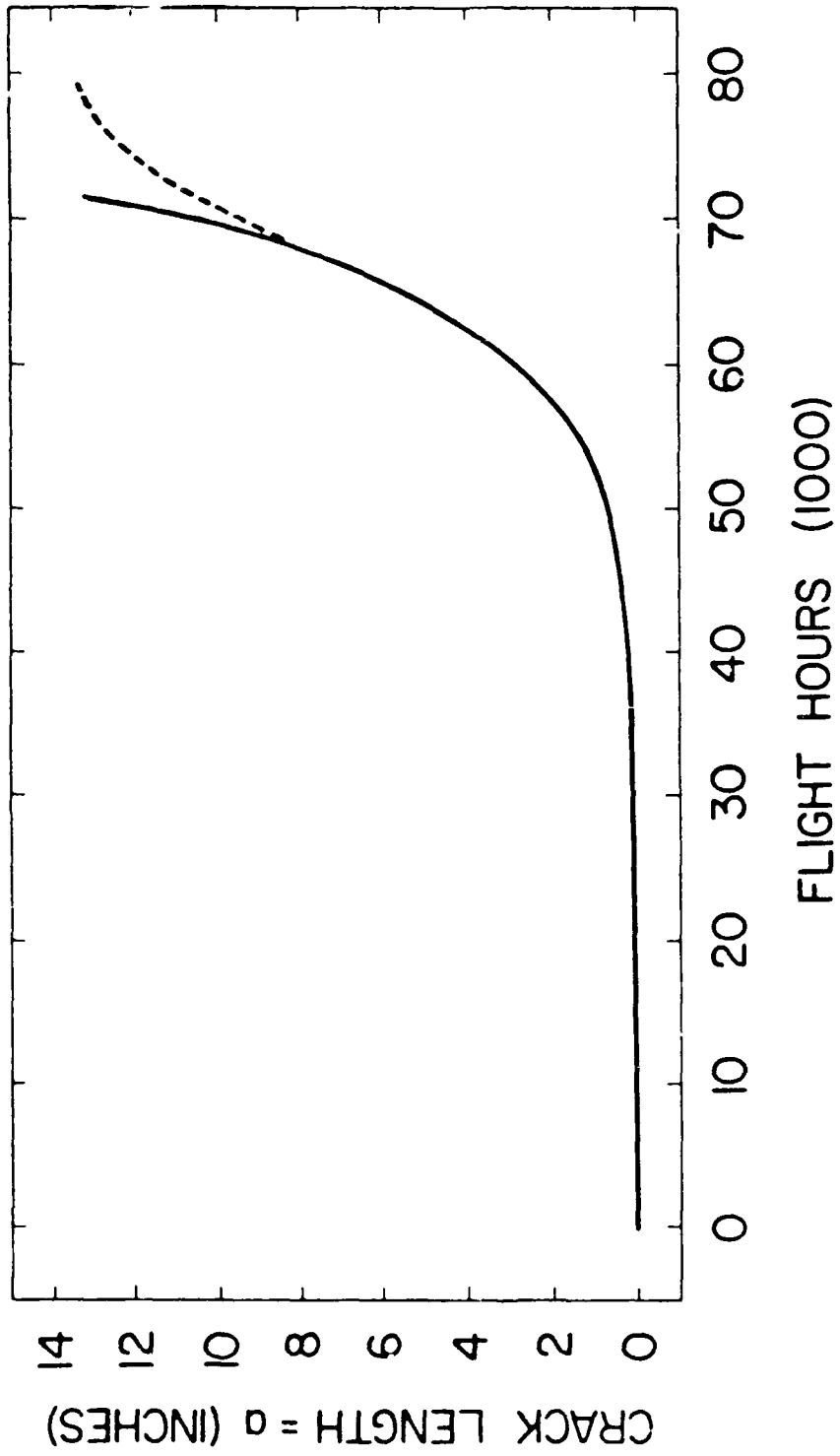


Figure 4.21 Two Master Curves, One with Crack Arrest, the Other Without

With the deterministic crack growth rate equation, the distribution of flaw sizes did not spread significantly as it grew forward. This is illustrated in Figure (4.22), where the growth of the median crack size of the initial distribution is represented by the solid curve, the growth of the 90th percentile flaw is represented by the dotted curve on the left, and the growth of the tenth percentile flaw is represented by the dotted curve on the right. It is observed from Fig. (4.22) that there are only 19,000 flight hours difference between the time it takes a large flaw, represented by the 90th percentile flaw, to reach 8.142 inches of the crack arrest structure. As a result, the probability of failure is negligible until such time as the 0.03 inch flaw (upper bound limit of the equivalent initial flaw size) has had time to grow to 8.142 inches. Then the probability of failure increases rapidly as the rest of the population reaches 8.142 inches. Another important characteristic of this panel stiffened system is that the probability of failure is negligible until a majority of the design service life had been expended. This feature is due to the closed upper end of the initial flaw size distribution in conjunction with a deterministic crack growth rate.

The effect of the visual inspections on the cumulative probability of failure is shown in Figure (4.23). In Figure (4.23) the solid curve at the top is the probability of failure for no inspection; beneath it, the probability of failure for one visual inspection, two isochronal visual

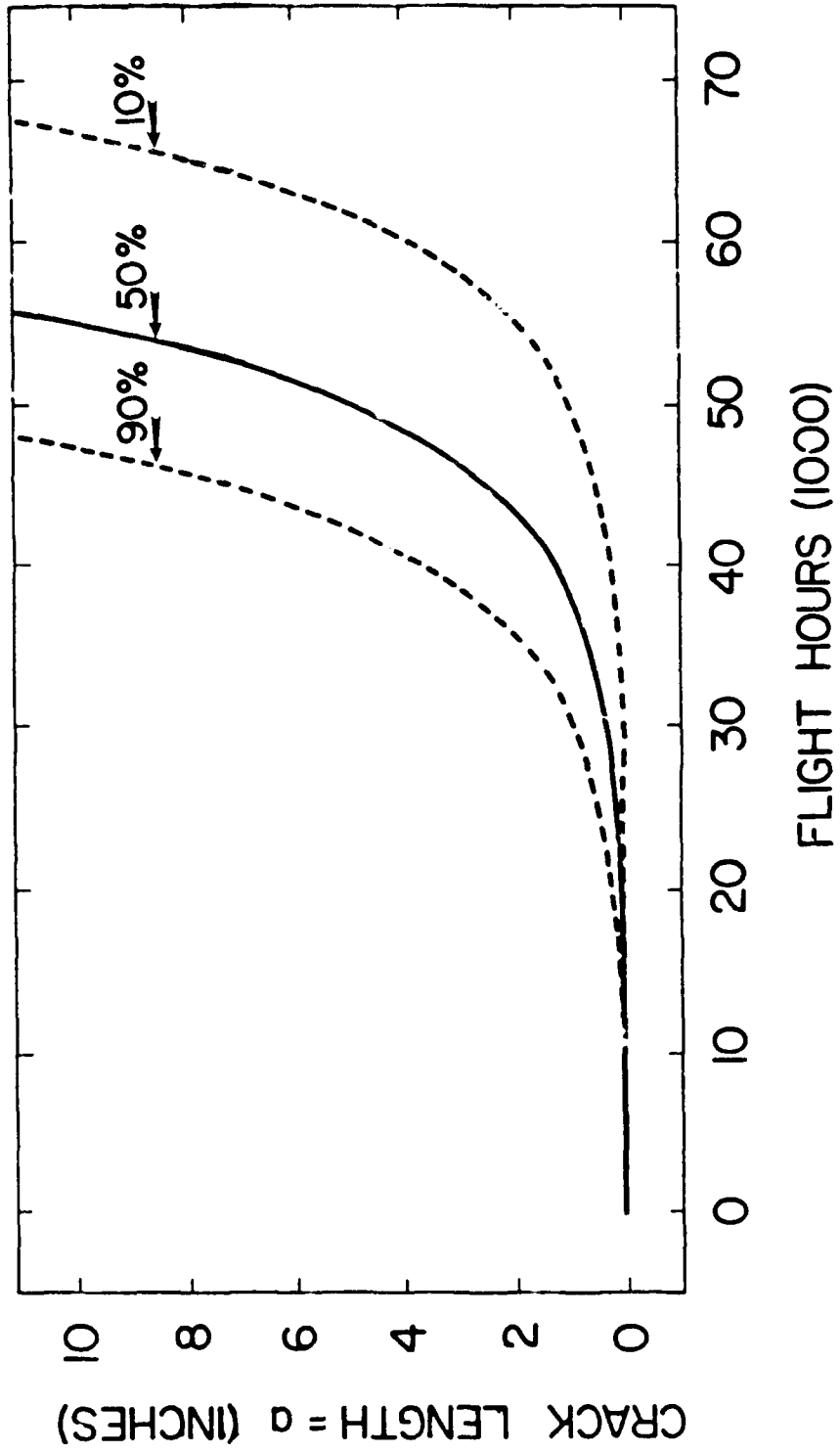


Figure 4.22 The Crack Growth Model Showing the Crack Growth of the Median Initial Flaw Size, the Tenth Percentile, and the 90th Percentile Initial Flaws

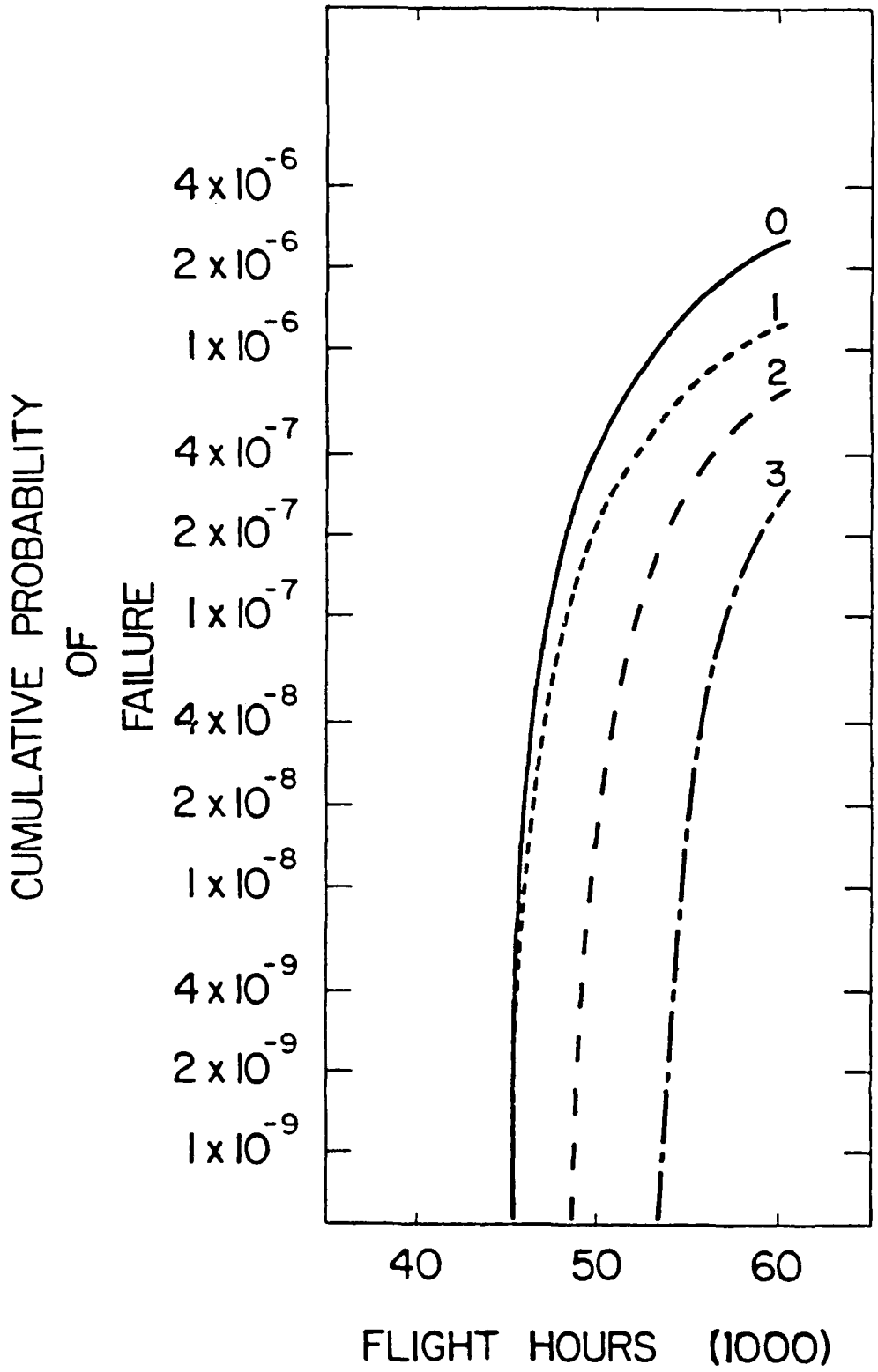


Figure 4.23 The Cumulative Probability of Failure for a Stiffened Panel with $a_{xx} = 8.142$ inches, the Deterministic Crack Growth Method, and 0-3 Visual Inspections

inspections, and at the bottom, three isochronal visual inspections over the service lifetime of 60,000 flight hours. Each additional inspection lowers the probability of failure. The case for no inspection resulted in probabilities of failure less than 10^{-5} throughout the design service life. The cases of two and three inspections lower the probability of failure to less than 10^{-6} . These results emphasize that designing with fail-safe features can be a great aid in service life management.

Table (4.9) contains the average percentage of repair for the stiffened panel which uses the master curve for the special case of $\beta(a) = 1$. This table highlights the fact that the probability of finding a flaw visually in the first 30,000 flight hours is extremely small. From 40,000 flight hours on, flaws have more chance of being found with a visual inspection. Consideration of the crack arrest feature of the design lowered the probability of failure at 60,000 flight hours by a factor of 10^{-6} for the no-inspection case.

4.2.2.2 Stochastic Crack Growth Rate

4.2.2.2.1 General Master Curve Approach

The general master curve approach was not considered for the stochastic crack growth approach because the effect of $\beta(a)$ on the fatigue crack growth damage accumulation is insignificant, as shown previously. Hence, the crack

Table 4.9

Average Percentage of Repair for the Stiffened Panel Example
Using Deterministic Crack Growth and $a_{xx} = 8.142$ Inches

a. Visual Inspection

Service Interval	1	2	3	4	5	Total
30,000	1.60E-6					1.6E-6
20,000	2.60E-15	7.0				7.0
15,000	2.37E-19	1.60E-6	22.0			22.0
12,000	1.74E-22	6.28E-12	5.0E-1	29.8		30.3
10,000	3.65E-23	2.60E-15	1.6E-6	7.0	27.8	34.8

retardation feature near the stiffener can be neglected and $\beta(a) = 1$ is reasonable. Thus, the analytical stochastic crack growth approach presented in Chapter III can be applied conveniently.

4.2.2.2.2 Special Case, $\beta(a) = 1$

The stochastic crack growth approach was considered for the special case $\beta(a) = 1$. The results of the probability of failure are presented in Figure (4.24) for no and five visual inspections. The visual inspections do not lower the probability of failure significantly over the non-inspection case. This result is true because the cracks accelerate as they grow longer, and this happens between inspections.

The results of the probability of failure are presented in Figure (4.25) which reflect no, one, two, three, four, and five inspections with NDI system #1. The probability of failure is kept below 10^{-10} for three or more inspections with repair. This level of safety is not necessary for a non-life threatening situation. The probability of failure is kept below 10^{-12} for four or more inspections. This level of safety is adequate for a situation involving loss of human life.

Table (4.10a,b) contains the average percentage of repair for the fail safe case with stochastic crack growth. Part a contains the results for one through four visual inspections. Part b contains the results for the same isochronal inspections using NDI system #1. As expected,

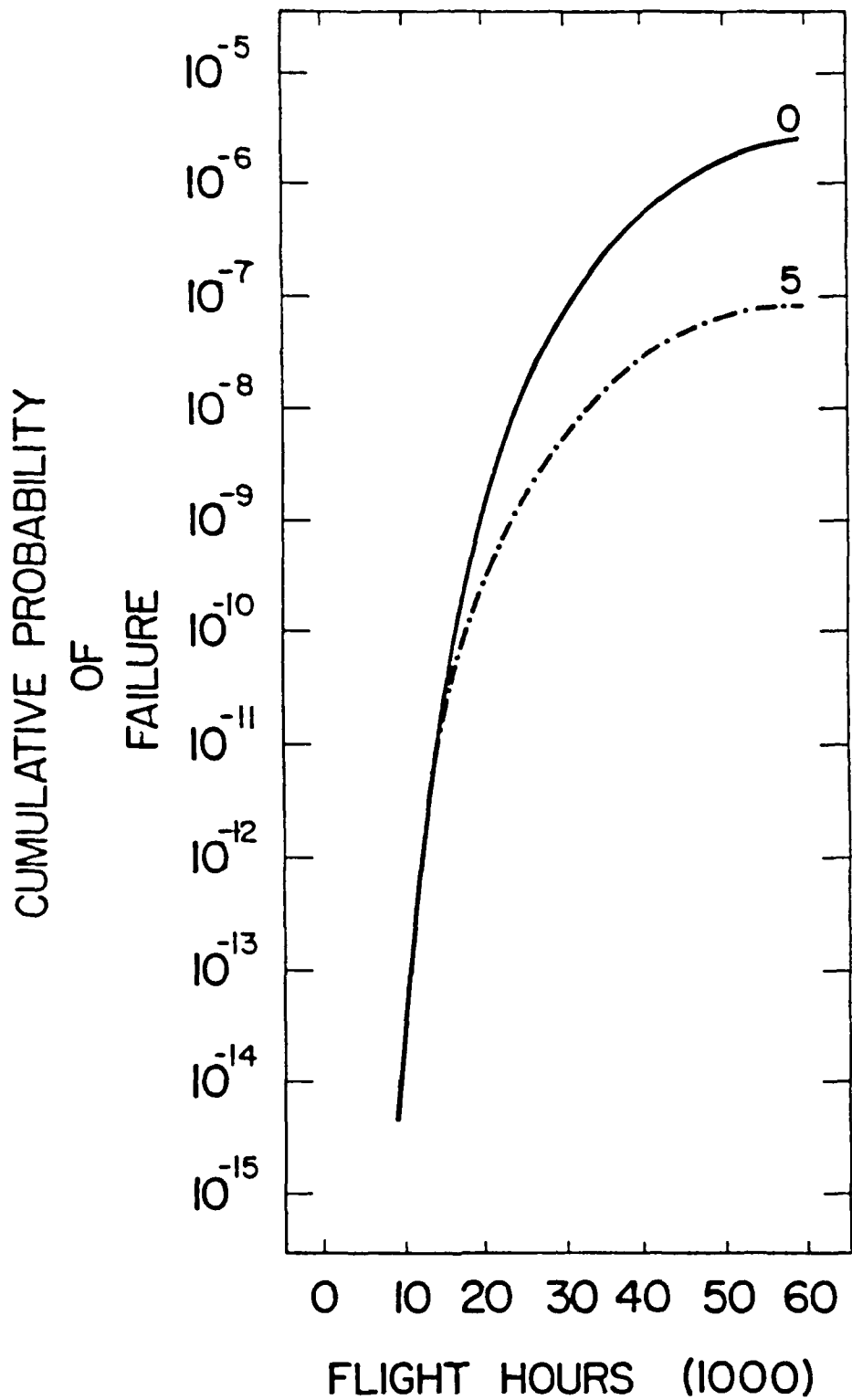


Figure 4.24 The Cumulative Probability of Failure for a Stiffened Panel, with $a_{xx} = 8.142$ inches, the Stochastic Crack Growth Method, and 0 and 5 Visual Inspections

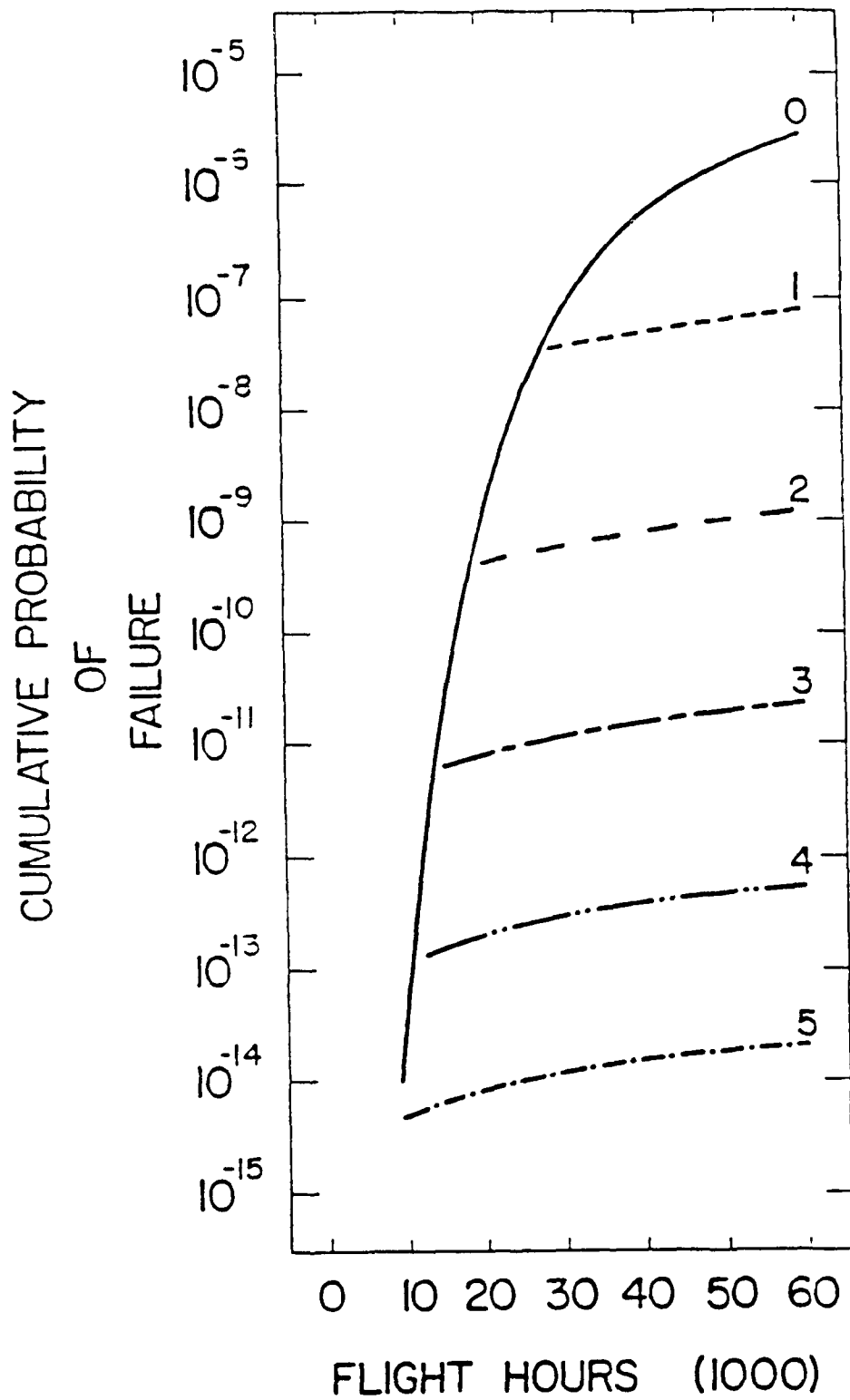


Figure 4.25

The Cumulative Probability of Failure for a Stiffened Panel, with $a_{xx} = 8.142$ inches, the Stochastic Crack Growth Method, and 0-5 Inspections using NDI System #1

Table 4.10

Average Percentage of Repair for Stiffened Panel Example
 With Stochastic Crack Growth and $a_{xx} = 8.142$ Inches

a. Visual Inspection

Service Interval	1	2	3	4	5	Total
30,000	6.8					6.8
20,000	0.35	23.0				23.4
15,000	1.61E-2	6.9	30.8			37.7
12,000	8.28E-4	1.6	16.3	34.8		52.7
10,000	5.01E-5	0.35	7.0	23.4	36.2	67.0

b. NDI System #1

Service Interval	1	2	3	4	5	Total
30,000	100.0					100.0
20,000	62.9	89.2				152.1
15,000	39.8	65.1	41.9			146.8
12,000	26.0	50.0	37.5	35.7		149.3
10,000	17.4	39.0	33.2	32.2	19.7	141.5

the NDI system #1 found many more flaws than the visual inspection.

Finally Figure (4.26) illustrates the effect of the effectiveness of the inspection system on the probability of failure for the stochastic crack growth analysis. The solid curve in Figure (4.26), denoted by "0", represents the probability of failure with no inspection, $a_{xx} = 8.142$ inches. The squares, denoted by "visual", represent the probability of failure for five visual inspections. The circles, at the bottom and denoted by "#1", represent the probability of failure for five inspections using NDI system #1. This figure emphasizes the significant effect that the type of inspection has on the probability of failure of the system.

4.3 Conclusions

The results of this analysis dictate that the safety of a structural system is very dependent on the sophistication of the NDI system used. The probabilities of failure were also dependent on the crack growth model that was used. The stochastic crack growth model gave higher probabilities of failure and hence it was more conservative.

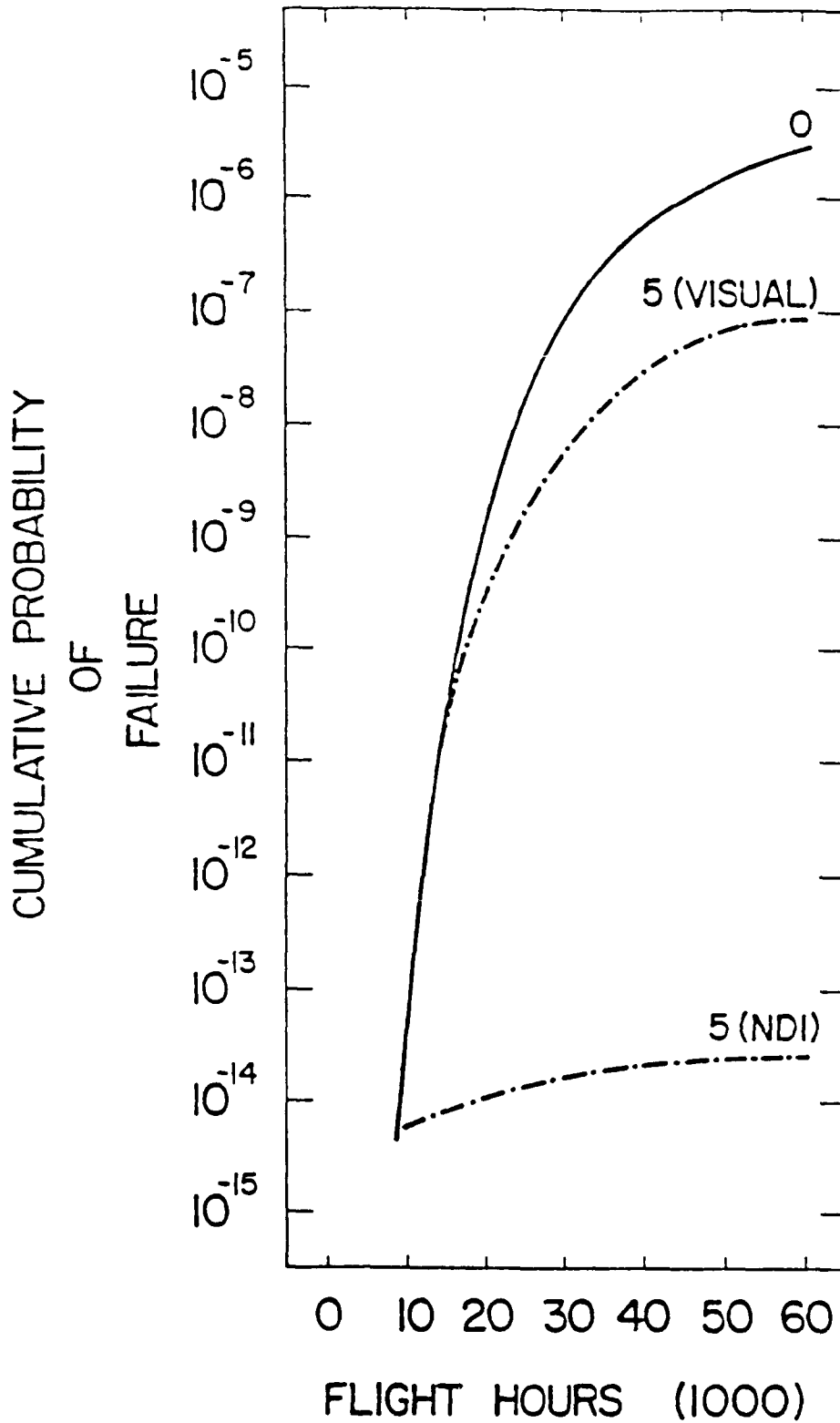


Figure 4.26

The Cumulative Probability of Failure for a Stiffened Panel, with $a_{xx} = 8.142$ inches, the Stochastic Crack Growth Method, 0 and 5 Visual and NDI System #1 Inspections

CHAPTER V

CONCLUSIONS AND RECOMMENDATIONS

5.1 Summary

Probabilistic damage tolerance methods were formulated for slow crack growth and fail-safe analyses of U.S. Air Force airframes. The two methods were applied to two components; a lug which represents a slow crack growth structure, and a stiffened panel which represents a fail-safe, crack arrest structure. The general master curve approach is very flexible because it can be used whenever the crack growth can be represented discretely. This is particularly helpful in a fail-safe structure because it can accommodate atypical crack, including crack-arrest. The stochastic crack growth approach is more conservative than the master curve approach because it considers the variability in the crack growth rate, and in these examples, did not handle crack arrest. The underlying assumptions of the models, as formulated here, will now be covered.

The master curve approach employs a Weibull compatible distribution to describe the initial flaw size distribution. A deterministic, discrete master curve was used to reflect the crack growth law. The variability of the crack growth rate was not considered in this method. For slow crack growth structures, the critical crack size was selected from the literature, for the lug example, or calculated from a power law, based on the residual strength of the plate, for

the stiffened panel example. For fail-safe structures, either a stress exceedance curve for the component in consideration, or the equation for turbulence from the military specification [1], can be used to select the maximum expected stress in the service interval, in accordance with the Damage Tolerance requirements for fail-safe structures. A crack length was then calculated which corresponded to the point at which the residual strength of the remaining structure was lower than that required for safety of flight until a return to base, maintenance depot, or other specified time interval. The residual strength versus crack length relationship was considered in a deterministic, discrete form. Interpolations were performed using a cubic spline method from IMSL [A1]. The derivatives needed for the transformation of variables were obtained directly from the cubic spline equations at the specified flight hours. This method could accommodate any arbitrary crack growth, and hence, component geometry. The probability of failure and repair involved numerically integrating single integrals, because the only random variable considered was the crack length. The log-odds function was used in these equations to represent the non-destructive inspection systems. Parameters were selected to reflect the attributes of either a narrow-banded or a wide-banded NDI system or a visual inspection.

The stochastic crack growth approach also used the Weibull compatible distribution as the initial flaw size distribution. A power law was used to describe the crack growth law. A lognormal random variable was used to account for the variability in crack growth rate. Thus, the crack growth rate was modelled as fully correlated. A deterministic value was chosen as the critical crack length. Because the probability of failure calculation included two random variables, a double integral resulted. This double integral was integrated numerically using Simpson's one-third rule. The non-destructive inspection (NDI) systems were represented by the log-odds function, with parameters selected to reflect a two automated and one visual NDI systems. These NDI systems are the same as used with the master curve approach. These functions were also incorporated into the calculation for the probability of failure, with no new introduction of variables.

The results for the selected slow crack growth example were presented in terms of the probability of failure for no inspection, one, two, three and four isochronal inspections, for the two different NDI systems and the visual inspection. The probability of repair was also calculated for the same NDI systems and intervals. Comparison of results was made on the effect of the inspection interval on the probability of failure and repair, and the type of inspection system. Both the special case of the master curve approach and the special case of the stochastic crack growth approach were

investigated. Field data from an Air Force technical report [73] were used to set input values.

The results for the selected fail safe example were presented in terms of the probability of failure for no inspection, and one to five isochronal visual and narrow-banded NDI system inspections, using both the stochastic crack growth approach and the master curve approach for comparison. The probability of repair was presented for the same NDI systems and intervals. Comparison of results was made on the effect of the inspection interval on the probability of failure and repair, and the type of crack growth model used.

5.2 Conclusions

The methodology formulated here can be used for a probabilistic damage tolerance analysis. In particular, the generalized master curve approach is extremely useful when analyzing structures designed to be fail safe. This approach can be a great asset when analyzing any component for which the crack growth law may not behave exponentially. The cubic spline interpolation scheme was used to transform crack lengths from one service time to another.

The methodology formulated in this dissertation can be used to wisely select inspection methods and inspection intervals for damage tolerant critical components. The advantage over deterministic methods is apparent; the force

management schedule can be designed to keep the probability of failure at an acceptable low level, and at the same time lower the cost of repair by omitting unnecessary inspections and repairs.

5.3 Recommendations for Future Research

The damage tolerance analyses performed in this investigation have been at the component level. The next important step is to perform the analysis at the systems level. It is extremely important to understand competing modes of failure, load distribution and sharing among members, especially for fail safe structures, and to guarantee that the level of safety among the damage tolerant critical components is at a consistent, or at least, identifiable level in a structure.

The analysis methods can be improved for the fail-safe structure by considering the time delay that takes place at the fastener holes, as the crack meets a hole, and initiates at the other side. The sensitivity of the initial flaw size assumptions need to be investigated so that the importance of material quality can be rightfully weighed in relationship to its impact on the reliability statement of the system.

The random nature of the crack growth rate needs to be understood at the material (micro-structure) level. This knowledge can be used to great advantage in improving the accuracy of the stochastic crack growth method. It should

also be incorporated in the master curve approach to reflect the possibility of a fast crack. With this in mind, experiments need to be performed on fail safe structures, so that the crack growth can be better modelled in terms of the mean trend, as well as the variability in crack growth and arrest.

Finally, a probabilistic risk analysis should be developed for airframes, in the context of the total weapon system. The probability of failure should be considered in the view of the consequence of failure. The failure of a component may not be catastrophic by itself, but may cause damage to critical hydraulic lines or aerodynamic surfaces, which yield catastrophic results. The consideration of the seriousness of the outcome is every bit as important as the ability to calculate the probability of occurrence; and the two concepts should be considered jointly.

This research represents a small step in the large process of making military and civilian flight as safe as possible. This process will continue as better quality control of material processing and fabrication progress and better inspection methods and practices emerge.

CHAPTER VI

REFERENCES

1. General Specifications for Aircraft Structures, MIL-A-87221 (USAF), 28 February 1985
2. Airplane Strength and Rigidity Reliability Requirements, Repeated Loads and Fatigue, MIL-A-08866B (USAF, 22 August 1975.
3. Aircraft Structural Integrity Program, Airplane Requirements, MIL-STD-1530A, 11 December 1975.
4. Gallagher, J.P., Giessler, F.G., and Berens, A.P., "USAF Damage Tolerant Design Handbook: Guidelines for the Analysis and Design of Damage Tolerant Aircraft Structures." Air Force Wright Aeronautical Laboratories, AFWAL-TR-82-3073, May 1984.
5. Rudd, J.L. and Gray, T.D., "Equivalent Initial Quality Method", U.S. Air Force Flight Dynamics Laboratory, AFFDL-TM-76-83, WPAFB, 1976.
6. Rudd, J.L. and Gray, T.D., "Quantification of Fastener Hole Quality", Proceedings, 18th AIAA/ASME/SAE Structures, Structural Dynamics and Materials Conference, 1977; also, Journal of Aircraft, Vol. 15, No. 3, March 1978. pp. 143-147.
7. Yang, J.N., "Statistical Estimation of Economic Life for Aircraft Structures", Proceedings, AIAA/ASME/ASCE/AHS 20th Structures, Structural Dynamics and Materials Conference, St. Louis, MO., April 1979, pp. 240-248, also; Journal of Aircraft, Vol. 17, No. 7, July 1980. pp. 528-535.
8. Yang, J.N., Manning, S.D. and Garver, W.R., "Durability Methods Development, Volume V, Durability Analysis Methodology Development." Air Force Flight Dynamics Laboratory, AFFDL-TR-79-3118, Vol. V, September 1979.
9. Yang, J.N. and Manning, S.D., "Distribution of Equivalent Initial Flaw Size", 1980 Proceedings, Annual Reliability and Maintainability Symposium, San Francisco, CA, 22-24 January 1980, pp. 112-120.
10. Manning, S.D. and Yang, J.N., "Advanced Durability Analysis - Vol. I - Analytical Methods", Air Force Wright Aeronautical Laboratories, AFWAL-TR-86-3017, Vol. I. November 1986.
11. Manning, S.D. and Yang, J.N., "USAF Durability Design Handbook: Guidelines for the Analysis and Design of Durable Aircraft Structures." Air Force Wright Aeronautical Laboratories, AFWAL-TR-83-3027, January 1984.

12. Manning, S.D. and Yang, J.N., "USAF Durability Design Handbook: Guidelines for the Analysis and Design of Durable Aircraft Structures." Air Force Wright Aeronautical Laboratories, AFWAL-TR-833027R (revised), November 1988.
13. Shinozuka, M., "Durability Methods Development - Vol. IV-Initial Quality Representation." Air Force Flight Dynamics Laboratory, AFFDL-TR-79-3118, Vol. IV, September 1979.
14. Garver, W.R., "Initial Quality of Advanced Joining Concepts", Air Force Wright Aeronautical Laboratories, AFWAL-TR-84-3066, December 1984.
15. Noronha, S.P., Henslee, D.E., Gordon, D.E., Wolanski, Z.R. and Yee, B.G.W., "Fastener Hole Quality." AFFDL-TR-78-206, Vol. I and II, December 1978.
16. Potter, J.M., "Advances in Fastener Hole Quality Through the Application of Solid Mechanics", Proceedings of the Army Symposium on Solid Mechanics, 1978 - Cast Studies on Structural Integrity and Reliability, AMMRC MS 78-3, September 1978, pp. 15-29.
17. Weibull, W. Fatigue Testing and Analysis of Results, Pergamon Press, 1961.
18. Clark, W.G., Jr. and Hudak, S.J., Jr., "Variability in Fatigue Crack Growth Rate Testing", Journal of Testing and Evaluation, JTEVA, Vol. 3, No. 6, 1975. pp. 454-476.
19. Wei, R.P., Wei, W. and Miller, G.A., "Effect of Measurement Precision and Data Processing Procedures on Variability in Fatigue Crack Growth Rate Data", Journal of Testing and Evaluation, JTEVA, Vol. 7, No. 2, March 1979, pp. 90-95.
20. Virkler, D.A., Hillberry, B.M. and Goel, P.K., "The Statistical Nature of Fatigue Crack Propagation." Air Force Flight Dynamics Laboratory, AFFDL-TR-78-43, April 1978.
21. Artley, M.E., Gallagher, J.P. and Stalnaker, H.D., "Variations in Crack Growth Rate Behavior." Fracture Mechanics, ASTM STP 677, C.W. Smith, ed., 1978. pp. 54-67.
22. Yang, J.N., Salivar, G.C., and Annis, C.G., Jr., "Statistical Modeling of Fatigue-Crack Growth in a Nickel-Base Superalloy." Engineering Fracture Mechanics, Vol. 18, No. 2, pp. 257-270.

23. Yang, J.N., Salivar, G.C., and Annis, C.G., Jr., "Statistics of Crack Growth in Engine Materials - Vol. 1: Constant Amplitude Fatigue Crack Growth at Elevated Temperatures." Air Force Wright Aeronautical Laboratories, AFWAL-TR-82-4040, Vol. 1, July 1982.
24. Yang, J.N., Salivar, G.C., and Annis, C.G., Jr., "Statistics of Crack Growth in Engine Materials - Vol. 2: Spectrum Loading and Advanced Techniques", Air Force Wright Aeronautical Laboratories, AFWAL-TR-82-4040, Vol. 2, June 1983.
25. Salivar, G.C., Yang, J.N., and Schartz, B., "Stochastic Crack Propagation of Engine Materials under Block-Type Spectrum Loading in High Temperature", to appear in Journal of Engineering Fracture Mechanics, July 1988.
26. Kozin, F. and Bogdanoff, J.L., "On the Probabilistic Modeling of Fatigue Crack Growth", Engineering Fracture Mechanics, Vol. 18, No. 3, 1983, pp. 623-632.
27. Kozin, F. and Bogdanoff, J.L., "A Critical Analysis of Some Probabilistic Models of Fatigue Crack Growth." Engineering Fracture Mechanics, Vol. 14, pp. 59-89, 1981.
28. Lin, Y.K. and Yang, J.N., "On the Statistical Moments of Fatigue Crack Propagation", Engineering Fracture Mechanics, Vol. 18, No. 2, 1983. pp. 243-256.
29. Lin, Y.K. and Yang, J.N., "A Stochastic Theory of Fatigue Crack Propagation", AIAA Journal of Aircraft, Vol. 23, No. 1, 1985, pp. 117-124.
30. Lin, Y.K., Wu, W.F. and Yang, J.N., "Stochastic Modeling of Fatigue Crack Propagation", Probabilistic Methods in the Mechanics of Solids and Structures, Proceedings, IUTAM Symposium, Stockholm, Sweden, 1984. Springer, 1985. pp. 103-110.
31. Yang, J.N., Hsi, W.H. and Manning, S.D., "Stochastic Crack Propagation with Applications to Durability and Damage Tolerance Analysis", Air Force Wright Aeronautical Laboratories, AFWAL-TR-3062, May 1985.
32. Yang, J.N., Hsi, W.H., Manning, S.D., and Rudd, J.L., "Stochastic Crack Growth Models for Applications to Aircraft Structures." Chapter 4 in Probabilistic Fracture Mechanics and Reliability, J.W. Provan, ed. Martinus Nijhoff Publishers, 1987, pp. 213-267.
33. Yang, J.N., Hsi, W.H., and Manning, S.D., "Stochastic Crack Propagation in Fastener Holes under Spectrum Loading", Journal of Aircraft, 1983.

34. Yang, J.N., Hsi, W.H., and Manning, S.D., "Stochastic Crack Propagation in Fastener Holes", Proceedings, 26th AIAA/ASME/ASCE/AHS Structures, Structural Dynamics and Materials Conference, Orlando, FL, 15-17 April 1985, pp. 225-233, American Institute of Aeronautics and Astronautics Paper No. 85-0666, also in Journal of Aircraft, Vol. 22, No. 9, Sept. 1985, pp. 810-817.
35. Yang, J.N., Manning, S.D., Rudd, J.L. and Artley, M.E., "Probabilistic Durability Analysis Methods for Metallic Airframes." Journal of Probabilistic Engineering Mechanics, Vol. 1, No. 4, December 1986.
36. Yang, J.N., Manning, S.D., Rudd, J.L., Artley, M.E. and Lincoln, J.W., "Stochastic Approach for Predicting Functional Impairment of Metallic Airframes." Proceedings, 28th AIAA/ASME/ASCE/AHS Structures, Structural Dynamics and Materials Conference, Monterey, CA, April 1987.
37. Yang, J.N., Manning, S.D., Akbarpour, A., and Artley, M.E., "Demonstration of Probabilistic-Based Durability Analysis Method for Metallic Airframes", Proceedings, 29th AIAA/ASME/ASCE/AHS/ASC Structures, Structural Dynamics and Materials Conference, Williamsburg, VA, April 1988.
38. Manning, S.D., Yang, J.N. and Rudd, J.L., "Durability of Aircraft Structures", Chapter 5 in Probabilistic Fracture Mechanics and Reliability, J.W. Provan, ed. Martinus Nijhoff Publishers, 1987, pp. 213-267.
39. Yang, J.N. and Chen, S., "Fatigue Reliability of Structural Components under Scheduled Inspection and Repair Maintenance", Proceedings, IUTAM Symposium, Stockholm 1984, Probabilistic Methods in Mechanics of Solids and Structures. eds: S. Eggwertz and N.C. Lind, Springer-Verlag, 1985, pp. 559-568.
40. Spencer, B.F., Jr. and Tang, J., "Markov Process Model for Fatigue Crack Growth." Journal of Engineering Mechanics, American Society of Civil Engineers, to appear, 1988.
41. Spencer, B.F., Jr., Tang, J., Artley, M.E., and Storr, H.J., Jr., "A Stochastic Approach to Modeling Fatigue Crack Growth", Proceedings, 29th AIAA/ASME/ASCE/AHS/ASC Structures, Structural Dynamics and Materials Conference, Williamsburg, VA, April 1988.
42. Ortiz, K., "On the Stochastic Modeling of Fatigue Crack Growth", Ph.D. Dissertation, Stanford University, February, 1985.

43. Ortiz, K. and Kerimidjian, A.S., "Time Series Analysis of Fatigue Crack Growth Data", Engineering Fracture Mechanics, Vol. 24, No. 5, 1986, pp. 657-675.
44. Yang, J.N. and Chen, S., "Fatigue Reliability of Gas Turbine Engine Components under Scheduled Inspection Maintenance", Journal of Aircraft, Vol. 22, No. 5, May 1985, pp. 415-422.
45. Yang, J.N. and Chen, S., "An Exploratory Study of Retirement for Cause for Gas Turbine Engine Components", Journal of Propulsion and Power, Vol. 2, No. 1, Jan-Feb 1986, pp. 38-49.
46. Larsen, J.M., Schwartz, B.J. and Annis, C.G. Jr., "Cumulative Fracture Mechanics Under Engine Spectra." Air Force Materials Laboratory, AFML-TR-79-4159, January 1980.
47. Bell, R.P., Campbell, D.D., Morcock, D.S., and Richmond, G., "C141 Aircraft Information Retrieval System - Final Engineering Report - Phase I", Lockheed-George Company internal report, LG83ER0158, Vol. I, December 1984.
48. Berens, A.P. and Hovey, P.W., "Evaluation of NDE Reliability Characterization." Air Force Wright Aeronautical Laboratories, AFWAL-TR-81-4160, November 1981.
49. Berens, A.P. and Hovey, P.W., "Flaw Detection Reliability Criteria - Vol. I - Methods and Results." Air Force Wright Aeronautical Laboratories, AFWAL-TR-84-4022, Vol. I, April 1984.
50. Berens, A.P. and Hovey, P.W., "The Sample Size and Flaw Size Effects in NDI Reliability Experiments." Proceedings, The Review of Progress in Quantitative Nondestructive Evaluation, at U.C. San Diego, July 1984.
51. Berens, A.P. and Hovey, P.E., "Quantifying NDI Capability for Damage Tolerance Analysis." Proceedings, The Review of Progress in Quantitative Nondestructive Evaluation, at U.C. Santa Cruz, August 1983.
52. Berens, A.P. and Hovey, P.W., "Statistical Methods for Estimating Crack Detection Probabilities", Probabilistic Fracture Mechanics and Fatigue Methods, ASTM STP 798, 1983. pp. 79-84.

53. Packman, P.F., Klima, S.F., Davies, R.L., Malpani, J., Moyzis, J., Walker, W., Yee, B.G.W., and Johnson, D.P., "Reliability of Flaw Detection by Nondestructive Inspection." ASM Metal Handbook, Vol. II, 8th Edition, Metals Park, OH 1976. pp. 214-224.
54. Yee, B.G.W., Chang, F.H., Coughman, J.C., Lemon, G.H., and Packman, P.F., "Assessment of NDE Reliability Data." NASA CR-134991, National Aeronautics and Space Administration, Lewis Research Center, Cleveland, OH 1976.
55. Sarphe, C.S. and Preston, M.B., "Evaluation of Reliability Analysis Approach to Fatigue Life Variability of Aircraft Structures using C-141 In-Service Data." Lockheed Quarterly Report No. 3, 1 Dec. 71 to 29 Feb. 72, Contract F33615-71-C-1529, Air Force Materials Laboratory, March 1972.
56. Yang, J.N., and Donath, R.C., "Improving NDE Capability through Multiple Inspection with Application to Gas Turbine Engine Disks", Air Force Wright Aeronautical Laboratories, AFWAL-TR-82-4111, June 1983.
57. Yang, J.N. and Donath, R.C., "Improving NDE Reliability through Multiple Inspections", Review of Progress in Quantitative NDE, edited by D.O. Thompson and D.E. Chimenti, Plenum Press, NY, Vol. 2A, April 1983, pp. 69-78.
58. Eggwertz, S., "Investigation of Fatigue Life and Residual Strength of Wing Panel for Reliability Purposes", Probabilistic Aspects of Fatigue, ASTM STP 511 1972, pp. 75-105.
59. Lincoln, J.W., "Method for Computation of Structural Failure Probability for an Aircraft", Aeronautical Systems Division, ASD-TR-80-5035, July 1980.
60. Lincoln, J.W., "Risk Assessment of Aging Military Aircraft", Journal of Aircraft, Vol. 22, No. 8, Aug. 1985, pp. 687-691.
61. Yang, J.N. and Trapp, W.J., "Reliability Analysis of Aircraft Structures under Random Loading and Periodic Inspection." AIAA Journal, Vol. 12, No. 12, December 1974, pp. 1623-1630.
62. Yang, J.N. and Trapp, W.J., "Reliability Analysis of Fatigue-Sensitive Aircraft Structures under Random Loading and Periodic Inspection." Air Force Materials Laboratory, AFML-TR-74-29, February 1974.

63. Shinozuka, M., "Development of Reliability-Based Aircraft Safety Criteria: An Impact Analysis, Vol. I." Air Force Flight Dynamics Laboratory, AFFDL-TR-76-36, April 1976.
64. Manning, S.D., Yang, J.N. and Rudd, J.L., "Durability of Aircraft Structures." Chapter 5 in Probabilistic Fracture Mechanics and Reliability, J.W. Provan, ed. Martinus Nijhoff Publishers, 1987, pp. 213-267.
65. Palmberg, B., Blom, A.F. and Effwertz, S., "Probabilistic Damage Tolerance Analysis of Aircraft Structures", Chapter 2 in Probabilistic Fracture Mechanics and Reliability, J.W. Provan, ed. Martinus Nijhoff Publishers, 1987, pp. 47-128.
66. Yang, J.N., "Reliability Analysis of Structures under Periodic Proof Test in Service", AIAA Journal, Vol. 14, No. 9, Sept. 1976, pp. 1225-1234.
67. Yang, J.N., "Optimal Periodic Proof Test Based on Cost-Effective and Reliability Criteria", AIAA Journal, Vol. 15, No. 3, March 1977, pp. 402-409.
68. Swift, T., "Damage Tolerance Analysis of Redundant Structures", Lecture 1, presented to Fracture Mechanics Design Methodology AGARD-NATO Lecture Series, Delft, Netherlands; Munich, Germany; and Lisbon, Portugal, 2-13 October 1978.
69. Harter, J.M., "MODGRO, Users Manual", Air Force Wright Aeronautical Laboratories, AFWAL-TR-87-157-FIBE, Feb. 1988.
70. Kathiresan, K., Hsu, T.M., Brussat, T.R., "Advanced Life Analysis Methods - Crack Growth Analysis Methods for Attachment Lugs", Air Force Wright Aeronautical Laboratories, AFWAL-TR-84-3080, Vol. II, Sept. 1984.
71. Schijve, J., "Fatigue of Aircraft Structures", Report LR-486, Delft University of Technology, Delft, The Netherlands, April 1986.
72. Kathiresan, K., and Brussat T.R., "Advanced Life Analysis Methods - Executive Summary", Air Force Wright Aeronautical Laboratories, AFWAL-TR-84-3080, Vol. V, September 1984.
73. Kathiresan, K., and Brussat T.R., "Advanced Life Analysis Methods - Tabulated Test Data for Attachment Lugs", Air Force Wright Aeronautical Laboratories, AFWAL-TR-84-3080, Vol. IV., Sept. 1984.

74. Annual Book of ASTM Standards, "Test Method for Constant-Load-Amplitude Fatigue Crack Growth Rates Above 10 m/cycle", E 647, American Society for Testing and Materials, Philadelphia, PA.

APPENDIX A

The Cubic Spline Method

The cubic spline method was used to interpolate values in the master curve. A subroutine called ICSCCU was selected from the IMSL library [A1]. ICSCCU computes the coefficients of $N-1$ cubic polynomials to be used to interpolate a set of N points from a single-valued function. The $N-1$ by 3 matrix provides the spline coefficients to a cubic spline produced is continuous and has continuous first and second derivatives.

The IMSL library subroutine ICSEVU was used to evaluate the value of the function at the required point of evaluation. The value of the spline approximation, S , at y is:

$$S(y) = C(I,3)D + C(I,2)D + C(I,1)D + t(I) \quad (A.1)$$

where $X(I)$ is less than or equal to y and y is less than $X(I+1)$, and $D = y - X(I)$. The $X(I)$ is less than $X(I+1)$.

The cubic spline method insures that the derivatives exist and are continuous. This property becomes useful when using the density functions to transform the variables discretely from one point in time to another. The derivative at a point can be found analytically by taking the derivative of the cubic equation given in (A.1) and substituting in the proper value for the argument. The chain rule is employed in the transformation in which $dy/dx = [dS(y)/dt]/dS(x)/dt$. The values for both the numerator and the denominator of this expression are found

analytically using the C(I,J) matrix coefficients from
ICSCCU.

Reference

- A1. IMSL, The International Math and Statistics Subroutine
Library, IMSL Inc., Houston, TX. 1984.